IDENTIFICATION AND CHARACTERIZATION OF P53 TARGET GENES

By

Kathryn G Eby

Dissertation

Submitted to the Faculty of the

Graduate School of Vanderbilt University

in partial fulfillment of the requirements

for the degree of

DOCTOR OF PHILOSOPHY

in

Biochemistry

August, 2010

Nashville, Tennessee

Approved:

Jennifer Pietenpol, Chair

Bruce Carter

Scott Hiebert

Larry Marnett

Sandra Zinkel

ACKNOWLEDGEMENTS

I truly believe my thesis work resulted in large part from a collaborative effort involving everyone in the laboratory including rotation students! To begin, I cannot fully express my gratitude to Dr. Jennifer Pietenpol for the opportunity to work in such a rich scientific environment on a topic of great interest to me, p53. Her patience and guidance have been instrumental to my progress from student to scientist. Most notably, her love and passion for research was infectious at times when results were not clear cut, and Dr. Pietenpol's drive and work ethic made the late night and early mornings more enjoyable to share. In addition to the science she taught me, I am honored to learn from a mentor that NEVER sways from a positive outlook. Dr. Pietenpol wastes no time or energy on negative attitudes and takes all challenges head-on with an affirmative philosophy. Graduate school challenged me in ways I had not considered and it was Dr. Pietenpol's support throughout that has brought to this final stage of writing and defending my work.

For all the helpful insight and guidance through my time as a graduate student I would like to thank Drs. Bruce Carter, Scott Hiebert, Larry Marnett, and Sandra Zinkel who comprised my thesis committee. Many thanks to the MSTP leadership including Drs. Terry Dermody, Susan Wente, Larry Swift, Michelle Grundy, and Jim Bills who make up the team that over the years guide and help students find our appropriate scientific niches. Additionally, thanks to the

administrators who helped with all the happenings behind the scenes so that I could continue to work including Peggy Fischer, Marlene Jayne, Jan Lotterer, Lindsay Meyers, and Cindy Sullivan. A special thanks to the department of Biochemistry, our department head Dr. Michael Waterman, and director of graduate studies Dr. David Cortez who have created our excellent curriculum.

Dr. Pietenpol has created a rich lab environment to conduct research by bringing in post-docs, graduate students, and senior leadership that run the lab smoothly and contribute actively to each other's projects. First to the wonderful women who run the lab like a well oiled machine: Lab Mama or Kim Johnson orders and receives reagents faster than we can think what to do with them to keep our projects going at break neck speed, she fills our tummies with amazing homemade cookies, and listens to our work and personal problems with a seasoned ear. Her technical skills in immunohistochemistry led to our initial success in staining detectable markers for autophagy. I plan to take Kim with me on job negotiations because no one gets a better deal anywhere. Lucy Tang has magical hands that make beautiful westerns and can accomplish even the toughest cloning project in under a week time. It was a great privilege to work with Lucy to further our understanding of the p53 family in autophagic signaling. Deb Mays was instrumental in my training from the beginning by taking me on as a rotation student and helping me with experimental design as I learned the ropes. Deb's skills in chromatin immunoprecipitation and numerous other methods directly led to publishable results and I am excited that she will be

continuing on the p53 loss-of-function screen along with Lucy even after I am gone! Along with the science it was great to share early mornings and late nights with Deb going over edits of manuscripts or just talking our mutual love of animals. As tissue culture consists of a large portion of our experiments I am very thankful to Qing for all her wonderful help in running our tissue culture core.

We have also been lucky in the laboratory to have a number of post-docs from diverse backgrounds bringing in their own expertise who have shared generously in teaching everyone. Thank you to Kim Dahlman during my first years in the lab for her help in experimental design, scientific writing, and friendship. Earle Burgess, a fellow in the laboratory, participated in teaching me during my rotation and sharing his perspective on the blending of clinical responsibilities with basic science research. Josh Bauer entered only a couple months after me and has been an extremely productive post-doc with three manuscripts published or under review. He has pioneered the siRNA technology in our lab, teaching others including myself how to optimize and use these methods to further our own research. He is an excellent and patient teacher with a serious mind. Our late night Vandy basketball games followed by lab experiments made it even more fun! Brian Lehmann joined during the middle of my graduate school bringing with him fresh perspectives and expertise in the field of autophagy for which our lab had not previously had experience. Chats going over the best model and methods for autophagy with Brian helped finish some of the necessary experiments for our paper and I am grateful. Brad Creamer is a

new lab member whom I affectionately call “my post-doc” as we were matched graduate student to post-doc for weekly meetings. We often commiserate together over the length of the scientific review process and then we shared congratulations when our respective manuscripts’ acceptance occurred within one week of each other. Last, and definitely not least is Chris Barton whom I have known for several years since our rotation together in another laboratory that neither of us joined and we both ended up in Dr. Pietenpol’s lab. Chris has always gone out of his way to teach and be helpful, offering his assistance, reagents, and editing skills for which I am forever grateful. He and Josh brainstormed with me early on about the advantages and disadvantages of different techniques and what would be the highest-yield without getting scooped in this competitive field. I am thankful to both of them for their immense help throughout the entire process and for their friendship.

Jennifer Rosenbluth was a great baymate and older MSTP who has always answered questions and helped me link the function of an unknown protein with the growing field of autophagy that she was concentrating on at the time. Chris Pendleton has been a great colleague in optimizing an initial screen that was not fulfilled. His sense of humor was always a pleasure to have for an afternoon break. I was also happy to have three wonderful rotation students during my third year of graduate school whom all reinvigorated me with their enthusiasm for the science and novel approaches/ techniques that they brought to the task. Clayton Marshall and Bojana Jovanovic have made wonderful

additions to the laboratory. Seema Sinha and Clayton Marshall came along during revisions on my publications and worked hard in helping me finish the manuscript.

We share and receive critical input during lab meetings from Dr. Cortez and Dr. Zinkel's laboratory members. In addition each of these labs have helped to teach me novel techniques. Dr. Zinkel's lab was instructive on options for apoptotic measures, and Courtney Lovejoy from Dr. Cortez's lab taught me how to perform immunofluorescence and certain flow cytometry analyses. Courtney was a great listening ear when I wanted to brainstorm as well as being an amazing friend outside the lab. Carmen Perez is also a close friend that I met as a graduate of Dr. Pietenpol's laboratory and great contributor to the p63 field. I miss these two women greatly as they have moved on to the next step in their careers.

Thank you to the mighty women of the MSTP entering year 2004 for your support, listening ears, and friendly reminders to get paperwork done. A special thanks to Aubrey Hunt in Scott Hiebert's lab who served with me on the faculty admissions committee, kept me going during long nights of qualifying exam studying, as well as teaching me the technical aspects of annexin V staining by flow cytometry. To Curt Gabriel, another MSTP student who has been a great listener especially when I have needed the shoulder to lean on.

I could not have made it to this point without my support system outside of school. Thanks to my riding instructor Wren Fraser and the horses who have

soothed my soul over the last several years. Much happiness has already come from a newer addition to my animal family, a golden retriever named Baylee, who makes me smile and take ten minute breaks to pet her all the time. Thanks to my extended family that stay in contact and cheer me on from afar. To my immediate family for giving me the encouragement to pursue an MD/PhD even when I thought I was crazy. Special thanks to my mother who is the strongest woman I know. Lastly, unending gratitude to my fiancé Tom Beckermann who has added a joy that I cannot explain to my life. For his encouragement, his comedy, his understanding and his amazing heart.

"Success is the ability to go from failure to failure without losing your enthusiasm." -- Winston Churchill

TABLE OF CONTENTS

LIST OF TABLES

LIST OF FIGURES

LIST OF ABBREVIATIONS

5-FU	5-fluorouracil
AA	amino acids
AP	apyrimidinic site
APAF1	apoptotic protease activating factor 1
ARF	alternative reading frame
ASPP	apoptotic specific regulator of p53
ATG	autophagy genes
ATM	ataxia telangiectasa mutated
ATR	ataxia telangiectasa and Rad3 related
BCL2	b-cell lymphoma protein 2
BCL6	b-cell lymphoma 6 protein
BCL-XL	b-cell lymphoma extra long
BER	base excision repair
BIK	bcl2 interacting killer
BOP1	block of proliferation 1
BP	basepairs
CDK1	cyclin dependent kinase 1
CHIP	chromatin immunoprecipitation
CHIP-seq	chromatin immunoprecipitation sequencing
CHR	chromosome

CK2	checkpoint kinase 2 homolog
COP1	constitutively photomorphogenic 1
DAPK1	death associated protein kinase family member 1
DDB2	DNA damage binding protein 2
DEC1	deleted in esophageal cancer
DMEM	dulbecco's modified eagle medium
DNA	deoxyribonucleic acid
DRAM	damage regulated autophagy modulator
EDN2	endothelin-2
EDTA	ethylenediamine tetracetic acid dehydrate
EGF	epidermal growth factor
FBS	fetal bovine serum
GADD45	growth arrest and DNA damage inducible gene 45
GFP	green fluorescent protein
GSK3b	glycogen synthase kinase 3b
H2AX	histone H2A family member X
HCAS	human cellular apoptosis susceptibility protein
HIF	hypoxia inducible factor
HKGS	human keratinocyte growth supplement
HMECs	human mammary epithelial cells
HOGG1	8-oxoguanine DNA glycosylase
HPREC	human prostate epithelial cells

ISG20L1	interferon stimulated gene 20-like family member 1
KAP1	krab-zfp-associated
KB	kilobases
KDA	kildalton
LIMK2b	LIM domain kinase 2
MAP1LC3	microtubule associated-protein 1 light chain 3
MDM2	murine double mutant 2
MEF	mouse embryonic fibroblast
MIRNA	micro ribonucleic acid
MLH1	mutL homolog 1
MMR	mismatch repair
MSH2	mutS homolog 2
MTOR	mammalian target of rapamycin
NCRNA	noncoding ribonucleic acid
NEDD8	neural precursor cell expressed, down-regulated 8
NER	nucleotide excision
NES	nuclear export sequence
NHEK	normal human epidermal keratinocytes
p53R2	p53-induced ribonucleotide reductase gene 2
PARP	poly adp ribose polymerase
PBS	phosphate buffered solution
pCAF	p300/ cbp-associated factor

PCNA	proliferating cell nuclear antigen
PERP	p53 apoptosis effector related to PMP22
PET	paired end-ditag
PEX14	peroxisomal membrane protein 14
PI3KI	class I phosphoinositide 3-kinase
PIG3	p53 inducible protein 3
Pirh2	p53-inducible gene that encodes a RING-H2 protein
PML	promyelocytic leukemia
PU	purine
PUMA	p53 upregulated modulator of apoptosis
PWM	position weight matrix
PY	pyrimidine
qRT-PCR	quantitative real-time polymerase chain reaction
RB	retinoblastoma protein
RFP	red fluorescent protein
RH30	rhabdomyosarcoma 30 cell line
RhoA	ras homolog gene family, member A
RITA	reactivation of p53 and induction of apooptosis
ROCK	Rho kinases
RPS27L	ribosomal protein 27-like
RRNA	ribosomal ribonucleic acid
S15	serine 15

S46	serine 46
SAM	sterile alpha motif
SESN1	sestrin1
SHRNA	short-hairpin rna
SIRNA	short-interfering rna
STK11	serine/threonine kinase 11
SUMO1	smt3 suppressor of mif two 3 homolog 1
T18	threonine 18
TA	transactivation domain
TSC2	tuberous sclerosis 2
UV	ultraviolet radiation
UVRAG	UV irradiation resistance-associated gene

CHAPTER I

OVERVIEW

Since the discovery of p53, more than 30 years of research has yielded numerous publications all aiming to better understand p53 signaling in normal and disease states. First discovered as a proto-oncogene, p53 has since been shown to act as a potent tumor suppressor through both transcription-dependent and –independent signaling mechanisms. The goal of my dissertation research was to perform genomic analyses that would identify a subset of novel p53 target genes and further elucidate their functional roles downstream of the p53 signaling network.

Introduction

Prior to the invention of genomic technologies, the identification of putative transcriptional targets consisted of a gene-by-gene approach using nuclease protection assays as well as *in vitro* DNA binding and reporter assays. As a result, identification of transcription factor signaling networks was challenging. The advent of genomic analyses such as gene expression microarrays, genome-wide chromatin immunoprecipitation (ChIP) methods, and novel computational algorithms has allowed for the high-throughput discovery of transcriptional networks. There are approximately 2600 proteins in the human

genome that are assumed to function as transcription factors based on identification of DNA binding domains (Sturzbecher *et al.*, 1992). As these genomic methods allow further identification of transcriptional targets for the numerous potential transcription factors, we are beginning to understand the vast signaling capability that a single transcription factor has, both uniquely and through crosstalk with other transcription factors and co-factors. Further, these signaling networks will likely have important clinical utility, given that sequence mutations in transcription factors are the cause of multiple disease states and can be exploited as potential therapeutic targets.

A sequence-specific transcription factor contains a DNA binding domain that recognizes a unique genomic sequence and may bind to thousands of locations in the genome. A variety of factors influence the activity of transcription factors including spatial localization, accessibility of the DNA-binding site, and sequence specific recognition of the consensus binding region (Mitchell and Tjian, 1989). Cellular localization itself is often regulated by protein-protein interactions or post-translational modifications. Protein interactions and post-translational modifications may activate a transcription factor by targeting it to the nucleus or alternatively inactivate the transcription factor by marking it for degradation (Ptashne and Gann, 1998). For example NF-kappaB is maintained in the cytoplasm due to a protein interaction with Inhibitor kappaB alpha by obscuring the nuclear import signal (Baeuerle and Baltimore, 1988). In addition, numerous stress events, such as DNA damage, can influence protein-protein

interactions and post-translational modification of a transcription factor to regulate its subcellular localization and, ultimately, its activity (Cheng *et al.*, 2009; Rathmell *et al.*, 1997).

In addition to localization, a transcription factor and the basal transcription machinery require accessibility to the DNA binding region. Chromatin is made up of DNA wrapped around histone proteins (nucleosomes) and can be found either condensed as heterochromatin or during interphase in a loose state known as euchromatin (Olins and Olins, 1974). Chromatin structure due to nucleosome placement can also create DNA-specific binding sequences from two half-sites that are not close in the coding region but by bringing the DNA loops together the two halves of a DNA binding sequence can achieve close spatial orientation (Rippe *et al.*, 1995).

For precise regulation of gene expression, another tier of specificity is observed at the genome level using the consensus binding site. Consensus sequences, also referred to as response elements, are commonly located in the promoter region, enhancer, or within one kB downstream of the transcriptional start site of a gene. A response element contains a unique sequence of DNA that can be specifically recognized by a transcription factor. The complexity of response element binding by transcription factors is augmented by the fact that response elements can be degenerate, variations of the consensus binding sequence that can confer different binding affinities. The p53 consensus binding site consists of two 10 bp half-sites (5'-PuPuPuC(A/T)(T/A)GPyPyPy-3', where

Pu=Purine and Py=Pyrimidine) separated by a 0-13 spacer (el-Deiry *et al.*, 1992). Since the initial definition of the consensus binding site, genomic screening has shown that the 20 bp palindrome without a spacer is preferentially bound by p53 tetramers (Ma and Levine, 2007; Wei *et al.*, 2006).

p53: Sequence-Specific Transcriptional Activator and Tumor Suppressor

p53 was first discovered in 1979 and described as a proto-oncogene (Lane and Crawford, 1979; Linzer and Levine, 1979). After three decades of work and greater than 53,000 published articles, we now understand this transcription factor is a potent tumor suppressor (Hinds *et al.*, 1989; Levine, 1989). One observation linking p53 to tumor suppressor activity was that ectopic wild-type p53 expression inhibited oncogene-mediated rat fibroblast transformation and colony forming ability (Eliyahu *et al.*, 1989). Moreover, rare clones that did undergo transformation in those studies expressed a mutant, inactive form of p53 (Finlay *et al.*, 1989). Another key observation defining p53 as a tumor suppressor was allelic deletions of the *p53* locus on chr 17 in 75% of colon cancers, and the remaining p53 allele showed mutated p53 in two tumors studied resulting in the classic Knudson two-hit hypothesis for a tumor suppressor gene (Baker *et al.*, 1989; Knudson, 1971).

Since its discovery, studies have characterized p53 as the most frequently mutated gene in all human tumors (Caron de Fromentel and Soussi, 1992; Hollstein *et al.*). In 2009, the International Agency for Research on Cancer

counted 26,597 published somatic mutations and 535 germline mutations in the *p53* gene (Petitjean *et al.*, 2007). Of these somatic mutations, the majority are comprised of missense mutations located in the DNA binding domain that alter the ability of p53 to bind to DNA (Flaman *et al.*, 1998). As point mutations in p53 continue to be studied, there is growing evidence that these alterations not only inhibit p53 binding to its consensus sites but also confer dominant-negative activity through dimerization of the mutant and wild-type p53 (Milner and Medcalf, 1991).

Germline p53 mutations are not infrequent, and genomic sequencing in larger patient populations suggest that alterations in p53 may be responsible for as much as 20% of all inherited cancers (Palmero *et al. 2010*). Li-Fraumeni syndrome is an autosomal dominant disorder most commonly associated with a germline mutation in p53 (Malkin *et al.*, 1990), but has also been attributed to mutations in CHK2 (Bell *et al.*, 1999). Patients with Li-Fraumeni are at risk for early onset of a wide range of cancer types including breast, brain, soft tissue sarcomas, bone sarcomas, and adrenal cortical carcinomas (Bell *et al.*, 1999; Birch *et al.*, 2001; Malkin *et al.*, 1990).

In tumors where mutations in p53 are not present, there are frequent alterations in other nodes of the p53 signaling pathway. For example, the 90 kDa protein murine double mutant 2 (MDM2) binds and negatively regulates p53 (Momand *et al.*, 2000), and is amplified in numerous cancers that retain wild-type p53 (Fakharzadeh *et al.*, 1991). In neuroblastoma tumors that rarely exhibit

mutations of p53, homozygous deletion of $p14^{ARF}$ allows escape from p53-mediated growth arrest (Thompson *et al.*, 2001). $p14^{ARF}$ in normal conditions serves to sequester MDM2 thus inhibiting the E3 ubiquitin ligase activity of MDM2 to degrade p53 (Honda and Yasuda, 1999).

Due to its ability to induce growth arrest and apoptosis in a majority of tumor types, p53 is commonly considered an anticancer therapeutic target. p53 is a challenging target, as it is frequently lost or mutated in human tumors. Therefore therapeutic approaches include activating wild-type p53, reactivating and selectively inhibiting mutant p53, or selectively inhibiting the wild-type p53 in normal cells to reduce side-effects during chemoradiation.

Currently several adenoviral vectors carrying wild-type p53 that require intratumoral injection (brand name Advexin) are in clinical trials and are being well tolerated and efficacious in late stage disease patients (Vazquez *et al.*, 2008). Another adenoviral vector, ONYX-015, selectively replicated in p53-deficient cancer cells (Bischoff *et al.*, 1996). Although only minor antitumor activity was seen with ONYX-015 alone, a significant antitumor effect was achieved when combined with chemotherapeutic agents (Heise *et al.*, 2000; Khuri *et al.*, 2000).

In addition to gene therapy, other approaches for modulation of p53 activity are being developed, including investigation of small molecules that either directly interact with p53 or disrupt normal interactions with negative regulators such as MDM2. For example, Nutlins are a class of small-molecule MDM2

inhibitors that have antitumor efficacy in mouse xenograft models (Vassilev *et al.*, 2004). Nutlin binds MDM2 at the p53-binding pocket, inhibiting the MDM2-p53 interaction and stabilizing p53. Additionally, RITA (reactivation of p53 and induction of apoptosis) was identified in a chemical screen of small molecules designed to bind to p53 and block its interaction with negative regulatory factors. In mouse models, RITA induced tumor cell apoptosis under conditions of normoxia and hypoxia (Issaeva *et al.*, 2004; Yang *et al.*, 2009).

p53 Structure and Regulation

p53 is a 393 amino acid (aa) protein containing an N-terminal transcriptional activation domain (1 - 63 aa), a proline rich domain (64 - 92 aa), a central DNA binding domain (93 - 300), a nuclear localization signal domain (316-325 aa), a homo-oligomerization domain (307 - 355 aa), and a C-terminal domain that is involved in regulation of the DNA binding domain (356 - 393aa) (Cho *et al.*, 1994; Muller-Tiemann *et al.*, 1998; Wang *et al.*, 1994) (Figure 1a). Each domain is crucial for the regulation and transcriptional activity of p53. As its name suggests, the N-terminal transcriptional activation domain is the binding region for cofactors that regulate the transcriptional activity of p53, such as MDM2. (Fields and Jang, 1990; Momand *et al.*, 1992). The proline-rich domain is thought to be necessary for the pro-apoptotic function of p53. Specifically,

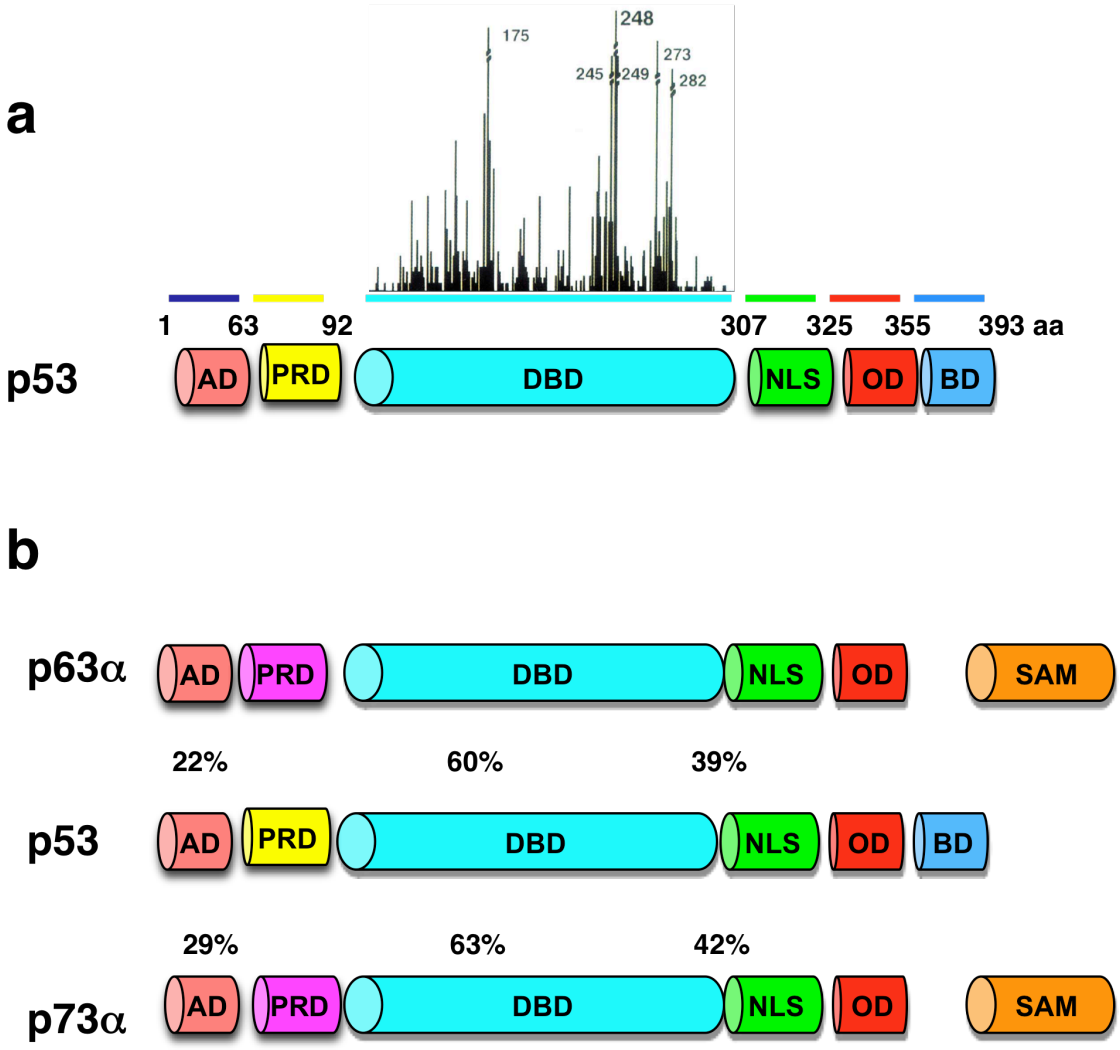

Figure 1. p53 Family Member Sequence Homology

(a) p53 is a 393 amino acid protein composed of a transactivation domain (AD), a proline rich domain (PRD), DNA-binding domain (DBD), nuclear localization signal domain (NLS), oligomerization domain (OD), and a C-terminal basic domain (BD). Histogram represents the frequency of mutations found in the DBD. Amino acids are shown for hot spot mutations. **(b)** The p53 family has a high sequence identity in the DNA binding domain where p53/p63α has a 60% and p53/ p73α has 63% identity. The transactivation domains (AD) and oligomerization domains (OD) also have significant homology. p63 and p73 are unique from p53 due to the presence of a sterile alpha motif (SAM). % denotes percent identity

binding of the apoptotic specific regulator of p53 (ASPP) family of proteins occurs in this proline rich domain, and this cofactor interaction has been reported to influence the ability of p53 to induce a subset of pro-apoptotic target genes (Samuels-Lev *et al.*, 2001). Additionally, p53 proteins lacking the proline-rich domain fail to activate specific target genes such as PIG3 and as a result are unable to induce apoptosis (Baptiste *et al.*, 2002 1998, Bergamaschi et al, 2006).

The DNA binding domain is comprised of an antiparellel β sandwich that is stabilized by a Zn^{++} ion to enable interaction with, and binding of, DNA (Duan and Nilsson, 2006; Pavletich *et al.*, 1993). Mutations occurring in the DNA domain may disrupt protein structure and alter the ability of p53 to bind DNA (Cho *et al.*, 1994). The oligomerization domain contains an amphipathic helix that allows for homodimerization and formation of transcriptionally active p53 tetramers (Sturzbecher *et al.*, 1992 1994). Lastly, post-translational modifications such as phosphorylation, glycosylation, ubiquitination, acetylation, and sumoylation occur frequently in both the N- and C-terminal region of p53. The C-terminal domain can negatively regulate p53 activity through its non-specific nucleic acid binding activity (Bayle *et al.*, 1995). Modifications at the C-terminus often inhibit the ability of this domain to negatively regulate sequence-specific DNA binding of p53 (Weinberg *et al.*, 2004). Additionally, these modifications can alter protein stability (Li *et al.*, 2003a), oligomerization state (Nicholls *et al.*, 2002), nuclear

export (Stommel *et al.*, 1999), and degree of ubiquitination of p53 (Nakamura *et al.*, 2000; Rodriguez *et al.*, 2000).

p53 stability is regulated at the protein level by post-translational modifications that either stabilize or mark the protein for degradation. MDM2 is a proto-oncogene that functions as a major negative regulator of p53 (Momand *et al.*, 2000). MDM2 is a transcriptional target of p53; this regulation creates an auto-regulatory feedback loop that acts to tightly regulate p53 activity. Upon stabilization, p53 transcriptionally induces expression of MDM2 that, in turn, functions as an E3 ubiquitin ligase to target p53 for nuclear export and proteasomal degradation (Honda *et al.*, 1997). The p53 nuclear export signal (NES) is structurally masked in its tetrameric complex. p53 ubiquitination by MDM2 disrupts the tetrameric state of p53 and exposes its NES, at which point p53 is translocated to the cytoplasm for degradation (Freedman *et al.*, 1997). Depending on tissue- or stress–specific contexts, p53 forms autoregulatory loops with other E3 ubiquitin ligases (Pirh2, COP1) (Dornan *et al.*, 2004; Leng *et al.*, 2003) and ubiquitin analogues (SUMO1, Nedd8) (Buschmann *et al.*, 2000 2004).

In addition, post-translational modifications of p53 occur at more than 40 different amino acid residues, where they act to influence p53 stability, localization, and co-factor interactions. These regulating modifications include, but are not limited to, acetylation by pCAF and p300 (Liu *et al.*, 1999), phosphorylation by ATM, ATR, and CK2 (Gu and Roeder, 1997; Jongmans *et al.*, 1996) and sumolation through PML nuclear bodies (Buschmann *et al.*, 2001).

One well-characterized event is the phosphorylation of p53 at serine-15 (S15) by DNA-protein kinase (Lees-Miller *et al.*, 1992). p53 S15 mutations abrogate the ability of p53 to induce cell cycle arrest. Microtubule-inhibitors increase phosphorylation at S15 and threonine-18 (T18) (Stewart *et al.*, 2001). Moreover phosphorylation of serine-46 (S46) is important for transcriptional induction of pro-apoptotic genes by p53 (Oda *et al.*, 2000b). Although much emphasis is placed on deciphering the "code" of p53 post-translational modifications and cell fate determination, the *in vivo* importance of these modifications in disease is still unclear. As mentioned above, the majority of missense mutations in human tumors occur in the DNA-binding domain and inhibit the ability of p53 to bind and transcriptionally activate its target genes. These hotspot mutations do not commonly coincide with amino acids that are post-translationally modified in p53, and the N- and C-terminal domains that are locations of modification are infrequently altered in tumors.

The p53 Family of Transcription Factors

Although the discovery of p53 preceded that of its family members, p63 and p73, p53 is evolutionarily the youngest of the family (Yang *et al.*, 1998 1997). Invertebrate species express a single p63-like protein, and the existence of all three family members did not occur until the evolution of vertebrate species (Derry *et al.*, 2001). While the three family members exhibit significant sequence and structural homology, they retain both overlapping and unique functions.

Each family member gene encodes an N-terminal transactivation domain, a central DNA binding domain, and C-terminal oligomerization domain (Figure 1b). Despite the common gene structures, p63 and p73 can exist as one of a number of protein isoforms resulting from usage of multiple transcriptional start sites (TA and ΔN), as well as numerous C-terminal splicing events. To date, at least six different p63 isoforms and 14 (of 35 theoretical) p73 isoform variants have been described (De Laurenzi *et al.*, 1998; Stiewe *et al.*, 2002; Yang *et al.*, 1998). Until recently, p53 was thought to exist as a single isoform, but recent studies suggest as many as nine possible p53 variants (Ghosh *et al.*, 2004). In addition to common protein regions within the family, p63 and p73 contain a C-terminal SAM domain that mediates protein-protein interactions (Figure 1b). The functional significance of the p63 SAM region became evident with the discovery that germline mutations in this domain result in developmental disorders such as ectodermal dysplasia and limb-mammary syndrome (Brunner *et al.*, 2002).

Unlike $p53^{-/-}$ mice that develop normally and succumb to spontaneous tumorigenesis (Donehower *et al.*, 1992), p63-deficient mice die shortly following birth due to the complete lack of stratified epithelia and all its derivatives (Mills *et al.*, 1999; Yang *et al.*, 1999). These murine phenotypes are recapitulated in human disease, as heterozygous germline p63 mutations result in ectodermal dysplasia, orofacial clefting, and limb malformation (Celli *et al.*, 1999; Ianakiev *et al.*, 2000; Perez *et al.*, 2007).

Global deletion of the *p73* gene in mice results in neurological, immunological, and pheromonal defects, evidence that p73, like its family member p63, is required for a number of developmental processes (Yang *et al.*, 2000). Recently, the studies of mouse models with isoform specific p73 deletions have shown that p73 regulation of distinct biological processes must be studied in the context of individual isoforms. The first isoform specific knockout generated was TAp73$^{-/-}$ mice (Tomasini *et al.*, 2008). These mice were similar to the p73$^{-/-}$ mice, in that they exhibited infertility and hippocampal dysgenesis. Unlike global p73-deficient mice, 73% of TAp73$^{-/-}$ mice died from the development of spontaneous tumors, most of which were comprised of lung adenocarcinomas. Global deletion of the ΔNp73 isoform resulted in mice that were fertile, yet displayed signs of neurodegeneration. Evidence also showed that ΔNp73 depletion resulted in an increased sensitivity to DNA damage, along with higher levels of p53-dependent apoptosis (Wilhelm *et al, 2010*).

As homozygous p63 deletions are incompatible with life, heterozygous mouse studies also suggest a role for p63 in tumor suppression, where 10% of p63$^{+/-}$ mice developed squamous cell carcinomas. These studies suggest that loss of a single p63 allele is sufficient for the development of tumors (Flores *et al.*, 2005). Additionally, compound heterozygote p53$^{+/-}$p63$^{+/-}$ mice displayed a striking difference in the rate of tumor metastasis compared to p53$^{+/-}$ supporting a role for p63 not only in tumor suppression but also in metastasis. Interestingly, p63 is rarely mutated in human tumors and is most often overexpressed in

squamous cell carcinomas, suggesting an oncogenic function of p63 in tumorigenesis (Sniezek *et al.*, 2004; Yamaguchi *et al.*, 2000). Like squamous cell carcinomas, a subset of breast cancers display a basal-like phenotype overexpressing ΔNp63α, consistent with numerous reports that this isoform can act in a dominant-negative manner towards the pro-apoptotic functions of its family members, p53 and p73 (Perou *et al.*, 2000; Yang *et al.*, 1998).

Despite their unique differences with regards to signaling, the p53 family members retain the ability to functionally cooperate, as evidenced by their ability to physically interact with each other. p73 and p63 can form homotetramers, as well as heterotypic interactions amongst themselves but not with wild-type p53 (Davison *et al.*, 1999). Mutated p53 is suggested to function in a dominant negative fashion by interacting with wild-type p53 and inhibiting its activity through the p53 oligomerization domain. Similarly, interactions between the core domain of mutant p53 and p73 can downregulate the growth suppressive pro-apoptotic anti-tumoral activity of p73 isoforms (Gaiddon *et al.*, 2001; Strano *et al.*, 2002).

With approximately 60% sequence identity in the DNA binding domain, the p53 family of transcription factors have both overlapping and unique binding motifs (Osada *et al.*, 2005; Perez *et al.*, 2007; Yang *et al.*, 2006). For example, selectivity in target gene expression can occur due to the preference of p63 for A/G at position 5 and C/T at position 16 in the consensus binding sequence (Perez *et al.*, 2007). ChIP analysis following ectopic expression of individual p53

family members showed that 72% of the p53-binding sites could be bound by p63 and/or p73 (Smeenk *et al.*, 2008). Work presented in Chapter III of this dissertation will describe subsets of genes both uniquely regulated by p53, as well as genes co-regulated by different p53 family members.

p53 family members can also functionally cooperate to regulate specific biological outcomes, such as apoptosis. $p63^{-/-}$ $p73^{-/-}$ MEFs are unable to undergo p53-dependent apoptosis after DNA damage, suggesting the necessity of p63 and p73 as co-factors during p53-dependent apoptosis (Flores *et al.*, 2002). In addition to cooperative protein interactions at select promoters, p53, p63, and p73 participate in cross-family feedback loops. For example, ΔNp73 expression is regulated by p53 to form a negative autoregulatory loop, whereby ΔNp73 competes at p53 consensus binding regions (Kartasheva *et al.*, 2002). Additionally, p73 activation after DNA damage induces MDM2, a negative regulator of both p53 and p73 activity (Wang *et al.*, 2001). MDM2 binds and sequesters p73, negatively regulating its transcriptional activity by inhibiting the ability of p73 to interact with its coactivator, p300 (Zeng *et al.*, 1999).

Methods for the Identification of Transcriptional Target Genes

Initially, the discovery of transcription factor target genes primarily occurred through a one-assay-one-gene approach, thus limiting the ability to rapidly discover large signaling networks regulated by a single transcription factor. Given the human genome consists of four unique DNA bases, a six bp

response element is predicted to occur >700,000 times in the genome (Georges *et al.*). With the release of the human genome sequence, algorithms using position weight matrices (PWM) were created to predict *in silico* transcription factor binding sites (Venter *et al.*, 2001). Though useful, *in silico* methods are unable to assess chromatin structure or account for the necessary activation of transcription factors, thus yielding numerous false positives.

While *in silico* methods often fail to address *in vivo* issues, chromatin immunoprecipitation (ChIP) methods enable the identification of response elements directly bound by a transcription factor under a given biological condition. It is important to note that this method identifies DNA binding sites and putative transcriptional targets in the biologically-relevant context of normal or cell stress conditions, as well as the state of chromatin structure. ChIP-sequencing (ChIP-seq) allows for the high-throughput identification of genomic transcription factor binding sites (Johnson *et al.*, 2007). ChIP-seq does not require large amounts of starting material and the sequencing platforms allow greater coverage than can be achieved with ChIP-library methods. Of course this method also has limitations including antibody availability, epitope access, and specificity for use in the immunoprecipitation step. Moreover, CHIP relies on chemical crosslinking that may unnecessarily include interactions of extraneous DNA-protein or protein-protein bonds. Lastly, the necessary starting material to perform large-scale ChIP assays is often prohibitive in primary cultures or clinical specimens (Kang *et al.*, 2002).

ChIP-based methodologies are useful tools to identify putative regulatory sites for a transcription factor; however, it does not yield data about regulation of a gene near the bound response element. To address the latter, an investigator can combine ChIP analysis with gene expression microarray technologies to correlate binding and regulation of a gene. Microarray experiments allow for analysis of gene expression under control and experimental conditions, one of which could be used to study transcription factors (Schena *et al.*, 1995). Gene expression microarrays allows comprehensive analyses of transcript level changes across samples but does not inform whether changes in gene expression are a direct result of the condition you are testing or rather a by-product of secondary signaling. The work presented in Chapter III of this thesis is based on the integrated analysis of multiple genome-wide ChIP and gene expression microarray analyses for the identification of direct p53 target genes.

Transcription-Dependent Functions of p53

Currently, 150 genes have been published and functionally characterized as p53 transcriptional targets. Genome-wide ChIP analyses have revealed that p53 has approximately 1600 binding sites in the genome (Cawley *et al.*, 2004; Smeenk *et al.*, 2008). Perhaps the most well-known transcription-dependent functions of p53 include transcriptional activation of target genes involved in cell cycle regulation, genomic stability, cellular senescence, and apoptosis with

growing evidence for target genes involved in angiogenesis, cell migration, and autophagy.

Role of p53 in Cell Cycle and Genomic Stability

p53 transcriptional activity is essential for proper G1 cell cycle checkpoint function (Pietenpol *et al.*, 1994). The first p53 target gene described was p21 (CDKN1a/WAF1/CIP1) (el-Deiry *et al.*, 1993). p21 is a cyclin-dependent kinase inhibitor that binds to and inactivates cyclin-CDK2 and –CDK4 complexes that are necessary for progression through the G1-phase of the cell cycle (Gu *et al.*, 1993). p21 is necessary for DNA damage induced, p53-dependent, G1 arrest (el-Deiry *et al.*, 1994). While p53 is most well-known for its ability to induce target gene expression, it also retains transcriptional repressor activity. Repression of c-Myc expression by p53 is necessary for G1-phase cell cycle arrest to occur (Ho *et al.*, 2005; Sachdeva *et al.*, 2009). This repression occurs through a mechanism of histone deacetylation, as well as through induction of miR-145 by p53 that itself downregulates c-Myc.

Entry into mitosis can also be blocked by p53 after DNA damage at the G2/M checkpoint, and this arrest is mediated by a number of genes and different mechanisms. One mechanism of p53-mediated G2/M arrest is through the inhibition of CDK1/cyclinB complexes by p21 (Harper *et al.*, 1995; Medema *et al.*, 1998). The growth arrest and DNA damage inducible gene 45 (GADD45) is another p53 transcriptional target that causes the G2/M arrest by dissociating the

cyclin B subunit from CDK1 (Zhan *et al.*, 1999). Our group showed that p53 prevents premature exit from G2 cell cycle arrest through a p21 and RB-dependent mechanism that inhibits and then decreases cyclin B1-CDK1 activity (Flatt *et al.*, 2000). p53 also transcriptionally activates 14-3-3σ, a gene that is necessary for maintenance of the G2/M checkpoint through its ability to sequester the cyclinB/CDK1 complex in the cytoplasm (Chan *et al.*, 1999).

p53 also alters G2/M arrest through mechanisms involving topoisomerase II. Topoisomerase II regulates chromatin structure by binding to DNA, creating double-stranded DNA breaks, and allowing torsional strain to be relieved by rotating one of the broken DNA strands prior to reannealing (Kingma and Osheroff, 1997). Topoisomerase II is active during the G2/M transition while chromosomes are becoming highly condensed. In response to cell stress, p53 is stabilized and can repress the promoter of topoisomerase II to initiate a G2/M arrest (Sandri *et al.*, 1996).

In addition to cell cycle regulatory genes, p53 also transcriptionally regulates genes involved in global genomic repair, as well as individual processes such as nucleotide excision repair (NER) and mismatch repair (MMR). The gene p53-induced ribonucleotide reductase 2 (p53R2) is a DNA repair protein that directly provides the substrates, deoxynucleotides, for DNA synthesis and repair (Tanaka *et al.*, 2000). Another well-known p53 target gene involved in DNA damage and repair, DNA damage binding protein 2 (DDB2), is responsible for the binding of DDB1 and the movement of repair complex to sites of lesions

(Hwang *et al.*, 1999). DDB2 is involved in the global genome repair pathway of NER (Stoyanova *et al.*, 2009). Nucleotide excision repair is a process that repairs pyrimidine dimers, a type of DNA damage resulting from UV radiation.

During normal cell replication, base mismatches left uncorrected by the proofreading capabilities of DNA polymerases are addressed by mismatch repair (MMR). p53 transcriptionally upregulates several key MMR genes including MLH1 (Chen and Sadowski, 2005), a gene that recruits enzymes to the site of repair; MSH2, which recognizes sites of damage (Scherer *et al.*, 2000); and PCNA, a gene needed to facilitate repair of the mismatched base (Xu and Morris, 1999).

Role of p53 in Cellular Senescence

Cellular senescence is a process by which cells lose their ability to divide. Cells undergoing senescence exhibit a round and flattened morphology and can be identified by their expression of senescence-associated β-galactosidase (β-gal). β-galactosidase is a lysosomal hydrolase typically active at the low pH of 4.0 but becomes active in senescent cells only at a pH of 6.0 (Dimri *et al.*, 1995). Cellular senescence is induced by two unique pathways, both of which are regulated by p53. The first mechanism, known as the telomere or aging pathway, occurs when cells undergo senescence as a result of critically shortened telomeres (Karlseder *et al.*, 2002). Alternatively, a second mechanism

of cellular senescence can be caused through a stress induced pathway such as oncogenic activation or DNA damage (Di Micco *et al.*, 2006).

In the telomere or aging model of senescence, cells undergo a limited number of cell divisions, at which time chromosomal telomeres reach a critically shortened length. At this point, cellular senescence is induced to prevent permanent chromosomal damage, and detection of markers occur that are typically associated with DNA double-strand breaks, such as phosphorylated H2AX and foci consisting of DNA repair proteins (Takai *et al.*, 2003). Additionally, senescent cells have activated Chk1 and Chk2 (d'Adda di Fagagna *et al.*, 2003). The Chk1 protein is necessary for telomere induced senescence as depletion of this kinase rescues cell cycle progression (d'Adda di Fagagna *et al.*, 2003). During senescence, p53 is stabilized and can be detected at response elements of growth arrest genes, such as p21 and GADD45 (Jackson and Pereira-Smith, 2006).

In the oncogenic model of senescence, cells permanently exit the cell cycle as a mechanism for protection against cellular transformation. Ectopic expression of oncogenes such as K-ras and c-Myc will activate p14ARF to sequester the p53 negative regulator MDM2 and allow activation of p53 (Shay *et al.*, 1991). Recently, DEC1 was identified as a p53 target gene required for K-ras induced senescence (Qian *et al.*, 2008). DNA damage induction of senescence, on the other hand, requires ATM/ATR activation and phosphorylation of p53 that activates senescence (Alcorta *et al.*, 1996).

Role of p53 in Regulation of Angiogenesis

Evidence suggests a tumor suppressive role for p53 through the inhibition of angiogenesis, or inhibiting creation of new blood vessels from pre-existing ones. p53 can inhibit production of proangiogenic factors, increase the levels of endogenous angiogenic inhibitors, and interfere with other upstream activators of angiogenesis. During tumor formation, angiogenesis is induced when tumor cells are exposed to hypoxic conditions. Hypoxia inducible factor (Reef *et al.*) recognizes hypoxic signals and transcriptionally upregulates vascular endothelial growth factors for tumor angiogenesis (Liu *et al.*, 1995). p53 directly binds HIF and targets it for degradation (Ravi *et al.*, 2000). p53 also specifically activates a number of secreted antiangiogenic factors including thrombospondin-1 that negatively regulates angiogenesis by inhibiting proliferation and migration of endothelial cells (Dameron *et al.*, 1994). Increased expression of antiangiogenic collagens present in the basement membrane of blood vessels is another way that p53 inhibits angiogenesis (Teodoro *et al.*, 2006). Furthermore, p53-mediated transcriptional repression of pro-angiogenic factors includes vascular endothelial growth factor (Pal *et al.*, 2001), basic growth factor (Ueba *et al.*, 1994), and basic growth factor binding protein (Sherif *et al.*, 2001; Subbaramaiah *et al.*, 1999).

Role of p53 in Cell Movement and Migration

As tumors progress, cells metastasize from the primary site to nearby or distant locations. During metastasis, tumor cells undergo cytoskeletal and morphological changes, as well as negotiate extracellular matrix barriers. Cells first become polarized before sending out filopodia extensions that recognize barriers and interact with the environment (Timpson *et al.*, 2001). Rho GTPases (Rac1, Cdc42, and RhoA) and Rho kinases (ROCK) are a few of the proteins implicated at different stages in tumor progression to control cell protrusions and sense spatial information (Sahai and Marshall, 2003).

p53 prevents cellular movement and migration by inhibiting filopodia formation and cell spreading downstream of the activity of Cdc42 (Gadea *et al.*, 2002; Gadea *et al.*, 2004). Cdc42 is activated at the extending front of a cell to form a complex that establishes cell polarity through a pathway that involves inactivation of glycogen synthase kinase 3b (GSK3b) (Etienne-Manneville and Hall, 2003). p53 activates GSK3b through nuclear binding and stabilization, effectively stopping cell polarization (Watcharasit *et al.*, 2002). The p53-dependent target gene LIM-kinase 2b (LIMK2b) is a known regulator of actin dynamics and further links p53 with cellular motility (Hsu *et al.*).

p53 and apoptosis

Apoptosis, or programmed cell death, is a normal physiological function essential for proper differentiation, development, and tumor suppression.

Apoptosis is characterized by morphology changes including plasma membrane blebbing, cell detachment, cell shrinkage, nuclear fragmentation, chromatin condensation, and chromosomal DNA fragmentation (Kerr *et al.*, 1972). Apoptosis differs from necrosis in that it does not typically elicit an immune response as in the case with necrotic cell death.

Induction of apoptosis occurs through two mechanisms. The first known as the intrinsic pathway, results when cellular stresses signal through the mitochondria to activate the caspase cascade (Lee and Bernstein, 1995). The second pathway, known as the extrinsic, or signal transduction pathway, is triggered by an interaction of extracellular ligands with transmembrane receptors that initiate activation of the caspase cascade and results in cell death (Bredesen, 2000). p53 regulates both pathways of apoptosis through transcriptionally-dependent mechanisms.

The p53-upregulated modulator of apoptosis (PUMA) was discovered as a direct target gene encoding two BH3 domains that allows binding to the Bcl-2 proteins and release of cytochrome C from the mitochondria (Nakano and Vousden, 2001). PUMA-deficient mice are unable to undergo p53-dependent apoptosis in response to ionizing radiation and cytokine withdrawal (Jeffers *et al.*, 2003). Another p53-regulated apoptotic target gene, Noxa, contains a BH3 domain that binds to Bcl-2, which is required for mitochondrial membrane permeabilization (Oda *et al.*, 2000a). A p53 target that plays a role in the intrinsic apoptotic pathway is the apoptotic protease activating factor 1 (APAF-1).

Following release of cytochrome C, APAF-1 oligomerizes to form the apoptosome and activates the caspase cascade through cleavage of procaspase-9 (Robles *et al.*, 2001). Evidence of p53-dependent apoptosis through activation of the extrinsic pathway occurs through transcriptional activation of Fas/CD95 and tumor necrosis factor family members (Fukazawa *et al.*, 1999). Tumor necrosis factors recruit adaptor molecules to bind and activate procaspase-8 cleavage, thus activating the caspase cascade (Burns *et al.*, 2001; Li *et al.*, 2003b). The above described transcriptional targets are only a few of the many identified players in p53-dependent apoptosis.

The biochemical signaling linking p53 to final cell fate is still not completely understood. Many factors are associated with cell fate including the cell of origin, type and extent of cell stress, p53-specific post-translational modifications, and the presence of p53 interacting cofactors. As mentioned previously, phosphorylation of p53 at serine-46 is associated with apoptosis. Specifically, some reports suggests this post-translational modification is required for upregulation of unique p53 target genes, including the p53-regulated Apoptosis-Inducing Protein 1 that functions to increase the mitochondrial membrane permeability and subsequent release of cytochrome C (Oda *et al.*, 2000b). The human cellular apoptosis susceptibility protein (hCAS) binds p53 apoptotic genes including p53AIP1 and PIG3, and hCAS suppression was sufficient to abrogate p53-dependent apoptosis (Tanaka *et al.*, 2007).

In addition to the well-known transcriptional role of p53 in apoptosis described above, p53 also regulates apoptosis in a transcription-independent manner. For example, DNA damage or hypoxic conditions can result in p53 translocation from the nucleus to the mitochondria where the tumor suppressor can increase mitochondrial membrane permeabilization by directly interacting with proapoptotic proteins Bax and Bak at the outer mitochondrial membrane (Chipuk *et al.*, 2004; Leu *et al.*, 2004). Additional support was provided by data showing that a transcription-independent role of p53 in apoptosis was observed when p53 mutants lacking the transcriptional activation domain still retained the ability to localize at mitochondria and induce apoptosis (Chipuk *et al.*, 2004). The transcription-independent role of p53 in apoptosis is controversial because it is difficult to fully separate the transcription-dependent and –independent mechanisms. Data showing that PUMA and Noxa-deficient mice are unable to undergo p53-mediated apoptosis would argue against a transcription-independent role of p53 during apoptosis. Proponents of the transcription-independent function of p53 suggest that only a basal level of the target genes Puma and Noxa is necessary in conjunction with the cytoplasmic functions of p53 to induce apoptosis.

Role of p53 in Autophagy

The term autophagy comes from the Greek roots ‘auto’, meaning self, and ‘phagy’, meaning to eat, thus making the appropriate reference to “eat oneself”.

Autophagy is most commonly studied as a response to cellular starvation; however, recent evidence shows that autophagy is also induced after cellular stresses, such as genotoxic damage. There are several types of autophagy such as macroautophagy, microautophagy, and selective autophagy. Macroautophagy is a vacuolar process of self-digesting portions of the cellular cytoplasm, including long-lived proteins and/or damaged organelles. This process begins with the formation of a double-membrane autophagosome that engulfs portions of the cytoplasm and later fuses with a lysosome containing degradative enzymes that breakdown larger macromolecules into monomeric components. These breakdown products are released into the cytoplasm and recycled by multiple cellular processes (Figure 2) (Berg *et al.*, 1998; De Duve and Wattiaux, 1966). Microautophagy refers to the direct uptake of cytoplasmic constituents for recycling through invagination of the lysosomal membrane. The third type of autophagy is selective-autophagy that encompasses several processes including chaperone-mediate autophagy and pexophagy (Beau *et al.*, 2008). Chaperone-mediated autophagy is a process whereby soluble

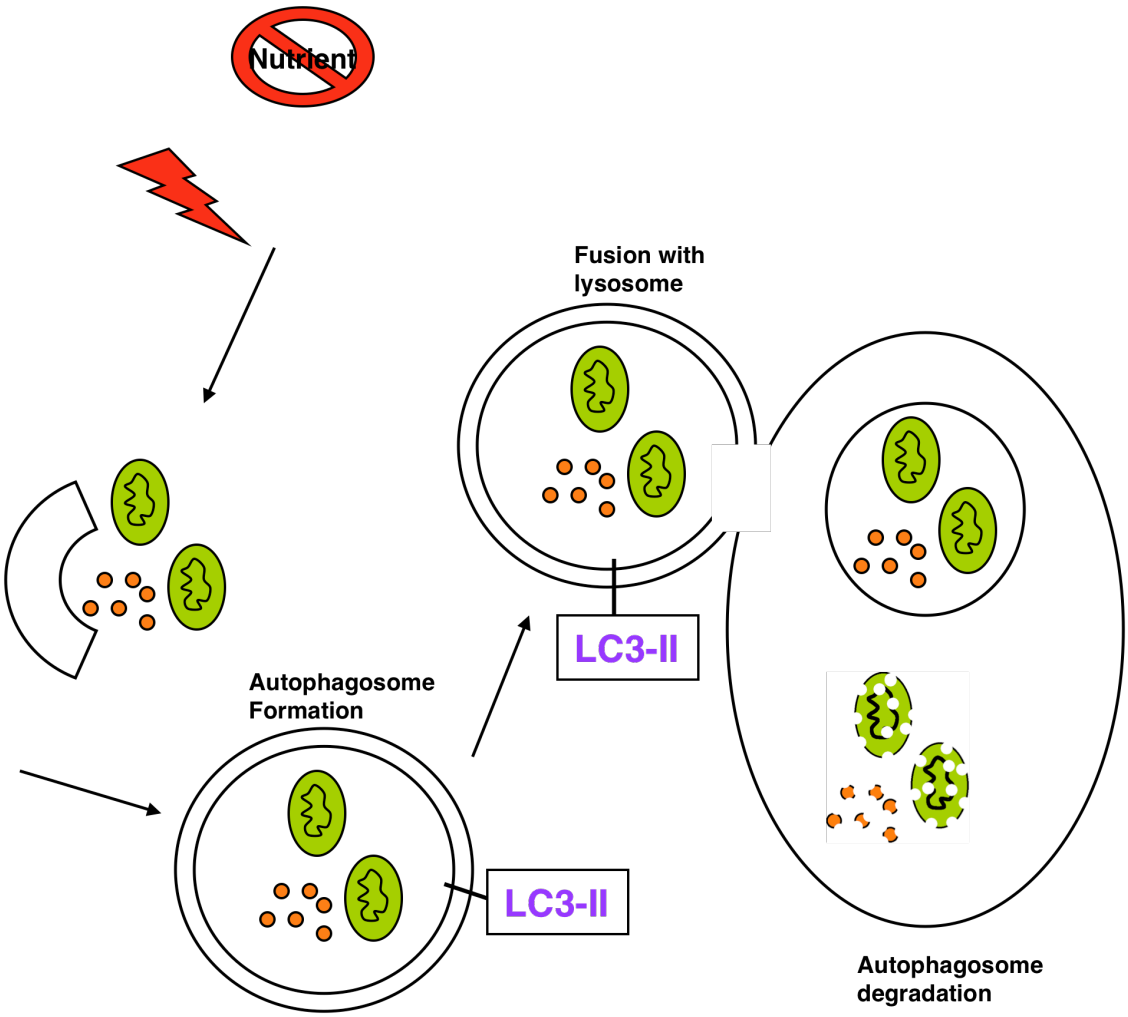

Figure 2. Autophagic Pathway
Autophagic induction occurs after nutrient withdrawal or genotoxic stress. Double membrane vesicles form that engulf cytoplasmic constituents including mitochondria and ribosomes. Final formation of the autophagosome involves inclusion of the microtubule-associated protein 1 light chain 3 (LC3-II) and is the gold standard method for detection of autophagy. The autophagosome then docks and fuses with a lysosome containing degradative enzymes that degrade autophagic constituents.

cytoplasmic proteins that contain a special targeting motif are transported to the lysosome using a chaperone complex. The chaperone complex consists of hsc70 and co-chaperones that relocate proteins to the lysosomal membrane where the Lamp-2A receptor recognizes and translocates the cargo into the lumen of the lysosome for degradation (Kaushik *et al.*, 2006). Other forms of selective autophagy have been recently discovered in *S. cerevisiae,* including organelle specific autophagy known as pexophagy where receptors such as Pex3 and Pex14 on peroxisomes are recognized by the Atg associated proteins involved in autophagosomal formation (Farre *et al.*, 2008).

Nutrient sensing is the signal for many of the pathways that control autophagy including the mammalian target of rapamycin (mTOR) pathway; Ras and c-AMP-dependent protein kinase A that monitor glucose levels; insulin receptors and Akt signaling; and the ATP-sensing AMPK pathway. In addition, various extra- and intracellular stresses can also activate the autophagy machinery including endoplasmic stress such as hypoxia (Yorimitsu *et al.*, 2006), the accumulation of unfolded proteins (Bernales *et al.*, 2006), pathogen infections (Gutierrez *et al.*, 2004), and genotoxic stress such as chemotherapeutics (Munoz-Gamez *et al.*, 2009). All of these signaling pathways converge to activate the AuTophaGy-related (ATG) genes that constitute the core machinery for the process of autophagy (Tsukada and Ohsumi, 1993). There are approximately 30 ATG genes involved in the different stages of autophagy that represent three major functional groups including i) the Atg9 and cycling

components, ii) vacuolar sorting proteins, and iii) the ubiquitin-like protein system (Xie and Klionsky, 2007).

The role of autophagy in cancer is paradoxical in that the process is known to provide energy and pro-survival mechanisms that can be oncogenic signals; however, downregulation of autophagy gene expression in human cancer, and knockdown of autophagy genes in mouse models, support a role for autophagy in tumor suppression. The first human gene discovered connecting autophagy and cancer was Beclin 1, that is monoallelically deleted in 50% of breast, ovarian, and prostate cancers (Shen *et al.*, 2008; Yue *et al.*, 2003). A mouse model with monoallelic loss of Beclin 1 is viable but shows a higher incidence of lymphomas, lung and liver carcinomas, hyperplastic mammary glands, and acceleration of premalignant lesions induced by hepatitis B virus (Qu *et al.*, 2003; Yue *et al.*, 2003). When Beclin 1 was ectopically expressed in the autophagy deficient MCF7 breast carcinoma cell line, that has minimal levels of Beclin 1 expression, functional autophagy was rescued and clonogenic survival decreased (Liang *et al.*, 1999). The UV irradiation resistance-associated gene (UVRAG) is a tumor suppressor mutated at high frequency in colon cancer and identified as a positive regulator of Beclin 1 as well as a promoter of autophagy (Liang *et al.*, 2007).

In addition to the direct role of these autophagic players in cancer, a number of upstream autophagy regulators are tumor suppressors and oncogenes. The class I phosphoinositide 3-kinase (PI3K-I) is a known oncogene

activated via receptor tyrosine kinases leading to cell growth and inhibition of autophagy by activating mTOR (mammalian target of rapamycin). PI3K is frequently activated in sporadic cancer where receptor tyrosine kinases are mutated, subsequently turning on mTOR and inhibiting autophagy (Petiot *et al.*, 2000). The tumor suppressor, STK11 (serine/threonine kinase 11) is mutated in patients with hereditary intestinal polyposis that increases the risk of cancer by 90% at age 70 (Rustgi, 2007). STK11 positively induces autophagy through activation of AMPK signaling (Liang *et al.*, 2007). Another well known tumor suppressor ARF (alternative reading frame of CDKN2A) sequesters MDM2, allowing accumulation of p53 levels and activation of p53 following oncogenic stress signals. ARF can induce autophagy in p53-dependent and –independent manners. The short mitochondrial ARF isoform induces autophagy and subsequent caspase-independent cell death that can be rescued with knockdown of ATG5 or Beclin 1 (Reef *et al.*, 2006). Additionally, ARF directly interacts with Bcl-xL that normally protects cells from autophagy by inhibiting Beclin 1 activity (Pimkina *et al.*, 2009).

p53 acts as a positive and negative regulator of autophagy. Furthermore, p53 can regulate autophagy in transcription-dependent and –independent manners. p53 acts in a transcription-independent function to negatively regulate autophagy. Expression of p53 in the p53-null HCT116 cell line rescued baseline autophagy to the same levels as p53-proficient HCT116 cells (Tasdemir *et al.*, 2008). Moreover, the role of p53 as an inhibitor of autophagy was confirmed

when ectopic expression of wild-type p53, a p53-DNA binding mutant, and a p53-cytoplasmic only variant all consistently showed repressive effects on autophagy (Morselli *et al.*, 2008; Tasdemir *et al.*, 2008).

The more widely described role of p53 in autophagy is through the transcription-dependent induction of autophagic activity following cellular stress. Autophagy is induced following numerous cellular stress signals that also activate p53 such as starvation, hypoxia (Levine and Abrams, 2008), endoplasmic reticulum stress, oxidative stress (Feng *et al.*, 2005), and DNA-damage (Katayama *et al.*, 2007). p53 upregulates the β1 and β2 subunits of AMP-activated protein kinase that act as a sensor of intracellular energy stores and stimulates autophagy by phosphorylating the TSC1/TSC2 complex that directly inhibits mTOR (Feng *et al.*, 2007). In addition, p53 regulates the upstream activators of AMPK, Sestrin1 and Sestrin2, after genotoxic and oxidative stress conditions, to induce autophagy (Budanov and Karin, 2008). p53 can also bind and directly regulate TSC2 after genotoxic stress further linking p53 to the mTOR pathway through induction of this mTOR inhibitor (Feng *et al.*, 2007).

DAPK-1 and DRAM1 are two additional novel connections between p53 and autophagy. DAPK-1 is regulated in a p53-dependent manner in numerous cell lines in response to adriamycin and ionizing radiation and is epigenetically silenced during tumorigenesis (Gozuacik and Kimchi, 2006; Martoriati *et al.*, 2005). Since its discovery as a p53 transcriptional target, publications have described the role of DAPK-1 in autophagy induction, including its ability to

phosphorylate Beclin 1, resulting in its disassociation from Bcl-xL (Harrison *et al.*, 2008; Zalckvar *et al.*, 2009). The damage-regulated autophagy modulator (DRAM) is regulated by p53 and its family member p73 but is only necessary for p53-mediated autophagy induction (Crighton *et al.*, 2007). DRAM is lysosomal in location, induces markers of autophagy, and decreases cell survival but the exact mechanism by which it functions in autophagy has not been deciphered (Crighton *et al.*, 2006). Through work completed in our laboratory, p73 binds and regulates a number of transcriptional targets involved in autophagy and metabolism including ATG5 and ATG7 (Rosenbluth *et al.*, 2009). In Chapter IV of this dissertation, I described the ISG20L1 gene and its functional characterization as a direct target of p53 and the family members, p63 and p73. Further, ISG20L1 induces autophagy in response to multiple genotoxic stresses, providing further evidence that p53 acts to promote DNA damage-induced autophagy.

Overall Goals of Dissertation Research

One focus of research in the Pietenpol laboratory is deciphering unique and overlapping functions of the p53 family of transcription factors. Multiple findings from our laboratory have contributed to the current understanding of how p53 and p63 coordinate cell fate decisions in response to stress and differentiation cues (Perez *et al.*, 2007). Further, we recently defined the p73 cistrome and used this dataset to gain mechanistic insight to the role of p73 in differentiation and tumorigenesis (Rosenbluth et al., under review). p53, p63,

and p73 have approximately 1600, 5800, and 7600 binding sites in the genome, respectively (Rosenbluth *et al.*, 2008; Smeenk *et al.*, 2008; Yang *et al.*, 2006). To date approximately 150 genes are documented as direct p53 target genes. The goal of this dissertation is to identify novel p53 family transcriptional target genes and mechanistically characterize their functions in biologically-relevant processes downstream of the p53 family signaling axis.

In Chapter III of this dissertation, I describe the use of statistical and bioinformatic tools to perform genomic analyses and identify a subset of novel p53 transcriptional targets. Further, I describe current and future plans to analyze these target genes, in a high-throughput manner, and identify the contribution of each to p53-regulated processes such as cell cycle arrest, apoptosis, and autophagy, among others.

In Chapter IV of this dissertation, I describe the identification of ISG20L1 as a target gene of the p53, as well as its family members p63 and p73. Further, I show that ISG20L1 acts downstream of p53 as a modulator of autophagy.

Lastly, in Chapter V of this work I will summarize the findings and significance of my completed research. I will further describe the questions that arise from this work and remain unanswered in the fields of p53 and autophagy.

CHAPTER II

MATERIALS AND METHODS

Cell Culture

The RKO, U2OS, H460, 293FT, HCT116, and H1299 cell lines were obtained from ATCC and cultured in DMEM medium with 10% fetal bovine serum supplement and 1% penicillin-streptomycin. The MDA-MB-231 were obtained from ATCC and cultured in McCoy's 5A-Dulbecco's modified Eagle's medium (Invitrogen). The $ATG5^{+/+}$ and $ATG5^{-/-}$ MEFs were a kind gift from Dr. Mizushima (Tokyo Medical and Dental University) and cultured in DMEM medium with 10% fetal bovine serum (Kuma *et al.*, 2004). The MDA-MB-231 was also obtained from ATCC and cultured in McCoy's 5A medium. The Rh30 cell line was kindly given by Peter Houghton (St. Jude Children's Research Hospital) and cultured in RPMI medium with 10% fetal bovine serum.

The ecdysone-inducible expression system (Invitrogen, Carlsbad, Ca) was used to generate cell lines that conditionally express p53. A human hemaglutinin-tagged p53 cDNA was ligated into the pIND vector. The resulting vector pIND-p53 was cotransfected with the pVgRXR vector into the human large cell lung carcinoma H1299, which is null for p53 family member expression. Stable clones were selected by limiting dilution of G418 (Mediatech) and Zeocin (Cayla) and the resulting cell lines were named H1299-inducible p53 (Hip53). The Hip53 ponasterone A-inducible p53 cell lines were cultured in DMEM

supplemented with 10% fetal bovine serum, 1% penicillin-streptomycin, 600 μg/mL G418 (Mediatech, Herndon, VA), and 400 μg/mL zeocin (Cayla, Toulouse, France). All cells were grown at 37°C with 5% CO2.

Primary human foreskin epidermal keratinocytes (NHEKs) were obtained from the Vanderbilt Skin Disease Research Core. NHEKs were isolated by collecting human foreskins in a 1:1 mixture of Dulbecco's modified eagle medium (DMEM) and nutrient mixture F-12 HAM (DMEM-F12) (Gibco, Gaithersburg, MD) supplemented with 5% fetal bovine serum (FBS) (dialyzed to remove calcium ions), and 50 μg/mL gentamicin (Gibco) and stored at 4°C. Foreskins were washed 3 times for 15 min each time in DMEM-F12 supplemented with gentamycin and 1% penicillin-streptomycin. Excess dermis was trimmed away and the dermal side of each foreskin was lightly scored with a sterile scalpel. The foreskins were placed dermis-side down on sterile filter paper and incubated in DMEM-F12 containing 0.25% bovine pancreas trypsin (Sigma Chemical Company, St. Louis, MO), 0.04% disodium ethylenediamine tetracetic acid dehydrate (EDTA), 50 μg/mL gentamycin, and 1% penicillin-streptomycin overnight at 4°C. After trypsinization, the epidermis was separated from the dermis, rinsed in DMEM-F12, minced, and then incubated in EpiLife keratinocyte growth medium (Cascade Biologics, Portland, OR) supplemented with human keratinocyte growth supplement (HKGS) (Cascade Biologics) and 50 μg/mL gentamicin fro 20 minutes at 37°C. The epidermis was triturated with a pipet, and any remaining trypsin was inactivated with excess media containing 5%

dialyzed FBS (Sigma). Cells were centrifuged at 500 rpm for 10 min, resuspended in keratinocyte growth medium, and palted. For all experiments, NHEKs were cultured in EpiLife keratinocyte growth medium (Cascade Biologics).

Primary human mammary epithelial cells (HMECs) were purified from normal breast tissue obtained by the Vanderbilt- Ingram Cancer Center Human Tissue Acquisition and Pathology Shared Resource Core and grown in DMEM serum supplemented with 10% fetal bovine serum, 0.2% gentamicin, 1% fungizone, and 1% penicillin-streptomycin, and stored for no more than 48 h prior to epithelial cell preparation. The exterior of the tissue was trimmed off with a sterile scalpel and weighed. Tissue is washed three times with sterile PBS and 0.2% gentamicin, 1% fungizone, and 1% penicillin-streptomycin and then minced with sterile scissors and placed in a sterile 500 mL flask. For every 10 g of tissue, 35 mL of Digestion Media were added. The Digestion Media is composed of Human Mammary Fibroblast Medium supplemented with 1 mg/Ml of collagenase (Sigma) and 0.2 mg/mL hyaluronidase (Sigma). The tissue was incubated with shaking at 37°C for 12 h. The cell mixture was transferred to sterile 50 mL conical tubes, spun at 1000 rpm for 10 min, resuspended in Human Mammary Fibroblast Medium, and plated. The plated cell mixture was placed at 37°C with 5% CO2 in a humidified incubator for 2 h, allowing the fibroblasts to attach to the tissue culture dish. The media containing non-adherent cells was collected and spun at 1000 rpm for 10 min. The cell pellet was resuspended and

cultured in growth media. The HMEC growth media is composed of DMEM/F12 medium 1:1 supplemented with 1.0 μg/mL insulin (Humulin R, Eli Lilly and Co.), 1.0 μg/mL hydrocortisone (Sigma), 10 μg/mL ascorbic acid (Sigma), 12.5 ng/mL human recombinant EGF (Gibco), 10 μg/mL apotransferrin (Sigma), 0.1 mM phosphoethanolamine (Sigma), 2.0 nM beta-estradiol (Sigma), 10 nM 3,3'5-triiodo-L-thyronine sodium salt (Sigma), 15 nM sodium selenite (Sigma), 2.0 mM L-glutamine, 1% penicillin-streptomycin, 1 ng/mL cholera enterotoxin (ICN Biomedicals, Inc.), 1% fetal bovine serum, and 35 μg/mL bovine pituitary extract (Gibco). Experiments and protocols involving HMECs were approved and considered to meet the criteria for Exempt Review by an Institutional Review Board Health Sciences Committee at Vanderbilt University.

Cell Treatment

The following chemotherapeutics were used in treatment of cell lines mentioned above as described in results 8 Gy ^{137}Cs ionizing radiation, 0.13 mM 5-FU (APP Pharmaceuticals), 20 μM etoposide (Bedford Laboratories), 5 μg/mL cisplatin (APP Pharmaceuticals), 5 nM paclitaxel (Sigma), 40 nM rapamycin (Calbiochem). Lysosomal inhibitors were used at final concentration of 10 μg/ mL of E64d (Calbiochem 330005) and pepstatin A (MP Biomedical 195368). The Hip53 cells were treated with 10 μM ponasterone A.

Cell Transfection and Small Interfering RNA

The following targeting sense strand sequences were used for siRNA: Dharmacon siControl (Non-Targeting siRNA #1) UAGCGACUAAACACUCAA; Dharmacon siISG20L1-1 CAGCAAGGUUCACGGAUAUUU; siISG20L1-2, AUACUAAGCAAGCGAGGGAUU; siISG20L-3, CUCAAUUGGAAACGUGAAAUU. Dharmacon siRNA ISG20L1 pools consisted of the above targeting vectors plus siISG20L1-4 CAGCAGGGCCACUCGUCUA. Dharmacon siRNAs were reverse transfected into H460, U2OS, and RKO cells (4.5×10^5) with Lipofectamine2000 (Invitrogen) according to the manufacturer's protocol.

To knockdown p53 in NHEK cells, a 19-bp short hairpin RNA, corresponding to nucleotides 611 to 629 of p53 RNA (GenBank NM000546), was annealed and cloned into the self-inactivating lentiviral vector (H1-LV) that contains a GFP reporter gene under control of human ubiquitin C promoter for monitoring infection efficiency. A scrambled oligonucleotide was designed as a negative control and also cloned in the H1-LV vector. These lentiviral vectors were transfected using $CaPO_4$ methods into 293FT cells. After 48 h viral medium was harvested and with the addition of 8 μg/mL polybrene used to infect NHEK cells.

293FT cells were transfected using Fugene 6 (Roche) to make pSico lentivirus. To knockdown p73 in MDA-MB-231 and Rh30, cells were infected with the pSico lentivirus system that expresses shRNA targeting all isoforms of p73.

Forty-eight h later, cells were treated with rapamycin (40 nM) and RNA harvested 24 h later. The shRNA targeting p73 sequence used in the pSico lentivirus is 5'-TCAAGGAGGAGTTCACGGA-3'.

293FT cells were transfected using Lipofectamine2000 with either pCEP4 empty control or cDNAs encoding p53, TAp63γ, TAp73β, or ΔNp63α and harvested 24 h later for RT-PCR or Western analysis.

Clonogenic Survival Assays were performed in HCT116, RKO, H1299 cells, as well as $ATG5^{+/+}$ and $ATG5^{-/-}$ MEFs transformed with SV40 large T antigen obtained from Dr. Mizushima (Kuma *et al.*, 2004). For all cell lines, Lipofectamine2000 was used to transfect either pCEP4 empty vector control or ISG20L1 in 60 mm dishes. Twenty-four h after transfection, cells were selected for 10 days under the appropriate hygromycin B concentration determined per cell line. Colonies were Wright stained and analyzed using the Biorad Quantity One software.

Protein Lysate Preparation

Cells were washed with ice-cold PBS and harvested in lysis buffer (50 mM Tris-HCL [pH 7.4], 100 mM NaCl, 0.5% Nonidet P-40, 4 mM EDTA, 1 mM dithiothreitol) supplemented with 50 mM NaF, 0.2 mM Na Vanadate, and the protease inhibitors antipain (10 μg/mL) (Sigma), and 4-(2-aminoethyl)-benzenesulfonylfluoride (200 μg/mL) (Calbiochem, San Diego, CA). Cells were incubated on ice for 1 h, and the protein supernatant was clarified by

centrifugation at 13,000 g for 15 min at 4°C. Protein concentration was determined by the Bio-Rad Protein Quantification Kit (Bio-Rad Laboratories, Hercules, CA).

Western Analysis and Antibodies

Protein lysates were boiled in 1x Laemmli sample buffer, separated by SDS-Page, and transferred them to Immobilon-P membranes (Millipore, Billerica, MA) for Western analysis. Membranes were blocked with 5% non-fat dry milk in TTBS (100 mM Tris-HCL [pH 7.5], 150 mM NaCl, 0.1% Tween-20) and then incubated in the antibodies mentioned below prepared in 1% non-fat dry milk. Fourteen percent SDS-polyacrylamide gels were used for analysis of LC3 using anti-MAP1LC3-II (Abgent AP1802a). Additional antibodies used for protein detection: anti-p53 (Santa Cruz Biotechnology, PAb1801), anti- β–Actin (Sigma-Aldrich, A5441- 0.2 mL), anti-PARP (Cell Signaling, #9542), anti- Caspase-3 (Cell Signaling, #9662), anti-p73 (Bethyl A300), p63 (4A4) (Santa Cruz, sc-8431), and anti-ISG20L1 (Bethyl Laboratories, rabbit affinity purified antibody). A peptide for ISG20L1 antibody production was designed at the C-terminus of ISG20L1, outside of the functional exonuclease domain found from amino acids 111-275, with the intent to increase antigenicity and accessibility of the antibody while decreasing possible cross-reactivity. The peptide product sequence "HGSRGGAREAQDRRN" targets amino acids 311-325 of ISG20L1 and these 15 amino acids are unique to the ISG20L1 sequence.

RNA Isolation and Real-Time Analysis

Total RNA was purified, reverse transcribed and quantitative real-time PCR was performed by the following: RNA isolation was done using the Aurum Total RNA Mini kit (Bio-Rad), and reverse transcription of 500 ng of mRNA was performed using the TaqMan Reverse Trasncription Reagents kit (Applied Biosystems, Carlsbad, Ca) to generate cDNA. The cDNA samples were diluted 1:4 and 2 *μ*l were used for qRT-PCR. Reactions were performed using the iQ SYPBR-Green Supermix (Bio-Rad). All primer sequences were obtained using the Primer3 resource at (http://frodo.wi.mit.edu/primer3/) (Rozen and Skaletsky, 2000). All primer sets were run under the following cycling conditions: 95°C for 3 minutes followed by 40 cycles of: 95°C for 10 sec and annealing at 60°C for 45 sec, with data acquisition during each cycle on an iCycler Thermal Cycler (Bio-Rad). Melting curve analysis following PCR cycling was used to determine purity and quality of PCR product.

RNA isolation and microarray experiments

The Hip53 cell model was used with treatment of ponasterone A to induce p53 activity for 24 h and the control vector alone cell line was also used. Experiment was performed in duplicate. RNA was isolated using the Aurum Total RNA Mini Kit (Bio-Rad) without addition of β-mercaptoethanol and submitted to the VMSR for quality control. The RNA was processed and microarray was hybridized by the VMSR. Microarray data analyses was

performed using the ArrayAssist software platform (Stratagene). A list of probes was created with fold-change in gene expression for p53 induced samples versus pVgRXR control.

Immunofluorescence, Immunohistochemistry, and Electron Microscopy

For immunofluorescence analysis, cells were grown on glass coverslips and fixed in a 4% paraformaldehyde solution for 10 min at room temperature. After rinsing with PBS, the cells were permeabilized with 0.5% Triton X-100 for 10 mins. Following another rinse with PBS, cells were blocked for 15 min at room temperature with 5% BSA-PBS solution. The ISG20L1 (Bethyl) and FLAG antibodies (Sigma, F3165 anti-FLAG M2) were diluted in 1% BSA-PBS and incubated on cells at 37°C with 5% CO_2 for 1 h. The coverslips were washed 3x with PBS and placed in 2° rabbit anti- Alexa Flour 546 and mouse anti- Alexa Flour 488, respectively for 1 h at room temperature, in the dark. The cells were washed 3x with PBS and counterstained with DAPI. All images were obtained using 1000x magnification on a Zeiss Axioplan microscope equipped with a Zeiss camera and software.

Direct immunofluorescence was performed on U2OS cells stably expressing mRFP-GFP-LC3. The mRFP-GFP-LC3 expression vector was kindly provided by Dr. Yoshimori (Osaka University) (Kimura *et al.*, 2007) and Dr. Mizushima (Tokyo Medical and Dental University). U2OS stably expressing the tagged LC3 protein were generated by transfecting the cells with the mRFP-GFP-

LC3 expression vector using FuGENE 6 (Roche, Indianapolis, IN) and selecting in geneticin (Cellgro, Manassas, VA). Engineered U2OS cells were then transfected with either pCEP4 control or ISG20L1 expression plasmids and treated for 24 h with 5-FU. The cells were fixed and analyzed as above using a Zeiss Axioplan. Fifty cells were counted, without knowledge of the plasmids expressed, and RFP-only foci are reported as a percentage of total foci.

For immunohistochemistry analysis, cells were grown on glass coverslips. The cells were fixed, and permeabilized as indicated above for IF analysis. Washes were done in 1x TBS/0.1% Tween- 20 (1x TBST), and cells were blocked overnight rocking at 4°C in 5% normal goat serum diluted in TBST. The coverslips were stained specifically for the cleaved LC3 using the Abgent LC3 specific 1° antibody (Abgent AP1806a) for 30 mins at room temperature. The coverslips were then washed 3 times in TBST. The secondary used was the Dako Cytomation LSAb2 system HRP kit (K0673) according to manufacturer's protocol. Cells were analyzed for LC3 staining and counted at 200x magnification.

U2OS cells were reverse transfected using Lipofectamine2000 with Dharmacon Nonsilencing control or siRNA targeting ISG20L1. Three days after reverse transfection, cells were treated or not for 24 h with 5-FU to induce autophagy. Cells were harvested, washed with PBS, and exposed to 2% glutaraldehyde for fixation. Sample were rinsed in buffer, postfixed in 1% OsO_4 for 1 h, dehydrated through an ethanol series and transferred into Epon resin.

Ultrathin sections (60–70 nm, silver-gray) were obtained using a Reichert Ultracut E microtome with a diamond knife, transferred to formvar-coated grids, and examined on a Phillips CM-10 transmission electron microscope (FEI, Hillsboro, OR), operating at 80 kV, and images were captured with an AMT 2 mega pixel camera (Advanced Microscopy Techniques, Danvers, MA).

Two replicates were performed and each time 25 micrographs were counted blindly for each control and ISG20L1 knockdown. Additionally, cells were photographed in an un-biased fashion according to their placement on the grid. Images were quantified using ImageJ software and taking into account various acceptable methods (Klionsky *et al.*, 2008; Swanlund *et al.*). We set to scale the pixel ratio to microns and used measurement analysis to quantify the area occupied by autophagosome and autolysosomes as compared to the total cytoplasmic area excluding the nucleus. Autophagosomes were defined as double or multiple membrane structures surrounding cytoplasmic material, and autolysosomes were defined as single membrane structures surrounding cytoplasmic constituents and various levels of degradation (Mizushima *et al.*, 2001).

Flow Cytometric Analyses

Flow cytometry was performed by incubating 1 x 10^6 cells in 20 μg/mL propridium iodide (Sigma-Aldrich) and measuring DNA content for 15,000 events using a FACSCaliber instrument (Becton- Dickinson) (Stewart and Pietenpol,

1999). Flow cytometry data were plotted using CellQuest software (Becton, Dickinson & Co). Annexin V-FITC staining detected by flow cytometry was performed using the Annexin V-FITC apoptosis detection kit (BD Pharmingen, 556547).

Chromatin Immunoprecipitation Analyses

HMECs were treated or not with 10 ug/mL cisplatin for 24 h and chromatin was prepared(Szak *et al.*, 2001). Growth media was aspirated from cells and replaced with 1.6% formaldehyde (EM Science, Gibbstown, NJ) solution in PBS. Cells were incubated in formaldehyde for 10 min at room temperature, followed by inhibition of the crosslinking reaction by the addition of glycine for a final concentration of 0.125 M. After 2 min incubation, cells were washed twice with PBS. Extracts were prepared by scraping cells in 1 mL of lyses buffer as above. Sonication of the cell lysates was performed to yield chromatin fragments of approximately 500-1000 bp, and debris was pelleted by centrifugation for 10 min at 13,000 x g, and 1- 1.5 mg of total protein extracts was pre-cleared with 10 μg of isotype matched antibody (Pierce, Rockford, IL) bound to PAS for 1 h with rocking at 4°C. The extracts were immunoprecipitated with 1 μg of the respective antibodies by rocking overnight at 4°C. Immunocomplexes were washed twice with buffer, four times with wash buffer (100 mM Tris [pH 8.5], 500 mM LiCl, 1% Noniodet P-40, 1% deoxycholic acid), followed by two more washes in lyses buffer. The protein was degraded in digestion buffer (120 μg/mL

Proteinase K, 10 mM Tris [pH 7.5], 5 mM EDTA, and 0.5% SDS) at 56°C overnight, and then incubated at 65°C for 30 min. The DNA was resuspended in 40 μ water, and 2 μl of each sample were used for PCR amplification.

PCR amplification was performed using primers ISG20L1 forward CAGCCTGTCCAACATGGC and ISG20L1 reverse GCTGAGGCCATAACTTGGAAA, GAPDH forward CACCAGCCATCCTGTCCTCC and GAPDH reverse GTTCCTTCCCAGCCCCCACT, and p21 forward GCTTGGGCAGCAGGCTG and p21 reverse AGCCCTGTCGCAAGGATC as previously described (Schavolt and Pietenpol, 2007). PCR was performed using one cycle of 5 min at 95°C; followed by different number of cycles as indicated below of: 95° for 30 s, annealing temperature as indicated below for 45 s, and 30 sec of 72°C; to be finished with 10 min at 72°C. AEN 40 Cycles Anneal 54°C, GAPDH 35 Cycles Anneal 62°C, and p21 35 Cycles Anneal 57°C. Amplified DNA was resolved on a 6% polyacrylamide gel and stained after with ethidium bromide.

To attain sufficient levels of p73 for ChIP analysis, ~1.7 x 10^7 rapidly growing Rh30 cells were treated for 24 h using vehicle control or 40 nM rapamycin. The samples were prepared and Genpathway analysis performed using the p73 antibody (Bethyl Laboratories, A300) for immunoprecipitation.

DNA Laddering

Cells were counted and 2 x 10^6 cells were removed and washed in PBS for DNA laddering analysis. Procedure was followed according to the Roche Apoptotic DNA-Ladder Kit (11 835 246 001). In brief, cells were lysed in an equal volume of proprietary lysis buffer, incubated for 10 min at room temperature, 100 μl of isopropanol was added and vortexed prior to loading the sample onto filter tubes. Filter tubes were spun 2x 1 min at 8000 rpm and washed after each spin with 500 μl washing buffer. After discarding flow through, filter tube samples were placed in collection tubes and 100 μl elution buffer was added and then spun for 1 min at 8000 rpm. DNA obtained from samples was run on a 1% agarose gel next to 1 kb DNA ladder and positive control DNA (U937 cells treated with camptothecin) supplied from Roche.

CHAPTER III

IDENTIFICATION OF NOVEL P53 FAMILY TRANSCRIPTIONAL TARGETS

Introduction

The tumor suppressor p53 functions as a sequence-specific DNA binding protein that regulates the expression of genes involved in cell-cycle arrest, apoptosis, DNA repair, senescence, cell growth, and anti-angiogenesis (Pietenpol *et al.*, 1994). Stress signals including DNA damage, oncogenic activation, metabolic changes, and hypoxia activate p53 (Debbas and White, 1993; Graeber *et al.*, 1994; Imamura *et al.*, 2001; Kastan *et al.*, 1991; Reisman *et al.*, 1993; Zhan *et al.*, 1993). As a transcription factor, p53 binds a degenerate DNA sequence consisting of 2- 10 bp decamers with palindromic sequences 5'-PuPuPuC(A/T)(T/A)GPyPyPy-3' separated by a 0- 13 bp spacer (pu= purine and py= pyrimidine) (el-Deiry *et al.*, 1992). In addition to variations within the consensus binding sequence, p53 binding at specific target genes is affected by p53 protein levels and post-translational modifications; co-factors; and accessibility of the binding site as determined by chromatin structure. Many of the p53 transcriptional targets that are well characterized and often used as positive controls were discovered in a one-gene-at-a-time approach, including p21 and MDM2 (el-Deiry *et al.*, 1993; Honda *et al.*, 1997). The first attempt to estimate p53 binding sites across the genome was based on data derived from a

yeast-based one-hybrid (Tokino *et al.*, 1994). Based on the fifty-seven p53 sites identified, results were extrapolated to suggest that there were between 200 to 300 total p53 binding sites in the genome (Tokino *et al.*, 1994). Several years later, the advent of oligonucleotide arrays allowed identification of putatively all p53 binding sites on chromosomes 21 and 22. From this data, the authors suggested that 1,600 binding sites existed in the entire genome (Cawley *et al.*, 2004). For comparison, c-Myc was estimated to have 25,000 binding sites from the same study (Cawley *et al.*, 2004). To date, only 150 of the approximate 1,600 putative transcriptional targets (assuming each binding site corresponds to regulation of one gene or one non-coding RNA 'gene') have been functionally characterized downstream of p53 signaling.

The p53 family members, p63 and p73, share an approximately 60% sequence identity with p53 in the DNA binding domain (Yang *et al.*, 2006). Work performed in our laboratory and others have suggested that each family member has unique binding specificity. For example, p63 selectively binds A/G at position 5 and C/T at position 16 of the 20 bp response element (Perez *et al.*, 2007)(Rosenbluth et al, not yet published). The family members have both unique and overlapping functions through their control of transcriptional targets. p63 and p73 can bind and regulate a number of well-characterized p53 transcriptional targets including p21, GADD45, PERP, and MDM2 (Barbieri and Pietenpol, 2005; Zhu *et al.*, 1998). Similar to p53, its family members are known to be modulated after exposure of cells to DNA-damage. For example, cisplatin-

elevates p73 activity (Agami *et al.*, 1999; Gong *et al.*, 1999; Yuan *et al.*, 1999) and UV radiation, paclitaxel, actinomycin D, bleomycin, and etoposide induce endogenous TAp63 activity (Gressner *et al.*, 2005; Katoh *et al.*, 2000; Okada *et al.*, 2002).

In addition to the large number of possible overlapping targets amongst the p53 family members, each has target genes it uniquely regulates as demonstrated best in the distinct phenotypes of the respective p53 family knock-out mice. Unlike the *p53*-null mouse model, that develops normally, for the most part, but has an increased incidence of tumorigenesis, the *p63*- and *p73*-null mouse models show defects in epithelial and neuronal development, respectively (Donehower *et al.*, 1992; Yang *et al.*, 1999; Yang *et al.*, 2000) These mouse models suggest that p63 and p73 play unique roles in development and differentiation. p63 and p73 transcriptionally regulate target genes not regulated by p53, such as Wnt4 that is necessary for the development of several organs including ovarian follicles (Osada *et al.*, 2005). Recently, microarray gene expression analysis was performed on RNA harvested from *p53-, p63-, or p73*-null MEFs after DNA damage. From this dataset each p53 family member uniquely regulated approximately 100 genes (Lin *et al.*, 2009). Data from these studies also suggest that p63 and p73 play a role in tumor suppression as they regulate a number of target genes involved in the DNA damage response and DNA repair.

Utilizing genomic technology our laboratory and others have identified numerous candidate target genes, both unique and overlapping for p53, p63, and p73-dependent regulation. We used a number of criteria to select p53 target genes to further characterize including: 1) identification of a p53 binding site within 20 kB of a select gene as determined by ChIP analyses, 2) differential regulation of a given gene by p53 as assayed by gene expression microarray, and 3) rank of a putative transcriptional target as determined by mathematical algorithms. To date, I have identified approximately 150 genes as putative p53 targets using the criteria listed above. My dissertation research was focused on functionally characterizing a select number of these genes and linking these genes to biologically relevant pathways downstream of p53 signaling.

Results

In order to increase the probability of identifying genes directly regulated by p53 and functionally significant in tumor suppression, I applied a panel of selection criteria to a number of datasets generated in our laboratory and available *in silico.* These selection criteria included: presence of a p53 binding site identified by ChIP analysis within 20 kB of a select gene and differential regulation of a gene by p53 as determined by gene expression microarray analyses. By using datasets generated from several different cell lines and conditions, we sought to eliminate cell type- or DNA damage- specific bias. After creation of a subset of putative target genes that are bound and regulated by

p53, we further analyzed the placement of these genes in the ranking predicted by the mathematical modeling algorithms applied to p53 gene expression analysis. Lastly, we compared the putative p53 targets with previously identified p63 and p73 transcriptional targets to determine unique and coordinate regulation (Figure 3).

ChIP-Based Datasets

To compile a comprehensive set of genomic p53 binding sites, we used ChIP-based datasets from several sources. The first was from our laboratory. Dr. Jamie Hearnes, a previous graduate student in the Pietenpol laboratory, identified p53-regulated target genes by combining ChIP with a yeast one-hybrid selection system (Hearnes *et al.*, 2005). Libraries were generated from primary human mammary epithelial cells (HMECs) and an immortal non-transformed breast cell line MCF-10A, both of which had been treated with adriamycin, a DNA intercalating agent that induced cell cycle arrest under these conditions (Hearnes *et al.*, 2005). From these cells p53-bound fragments were purified and cloned into a yeast expression system upstream of the HIS3 gene and transformed into an auxotrophic histidine-deficient yeast-strain with a galactose-inducible expression vector containing the p53 gene. This allowed for selection of yeast transformants, the growth of which was dependent on p53-mediated transcription from select human genomic fragments. The ChIP-yeast screen identified

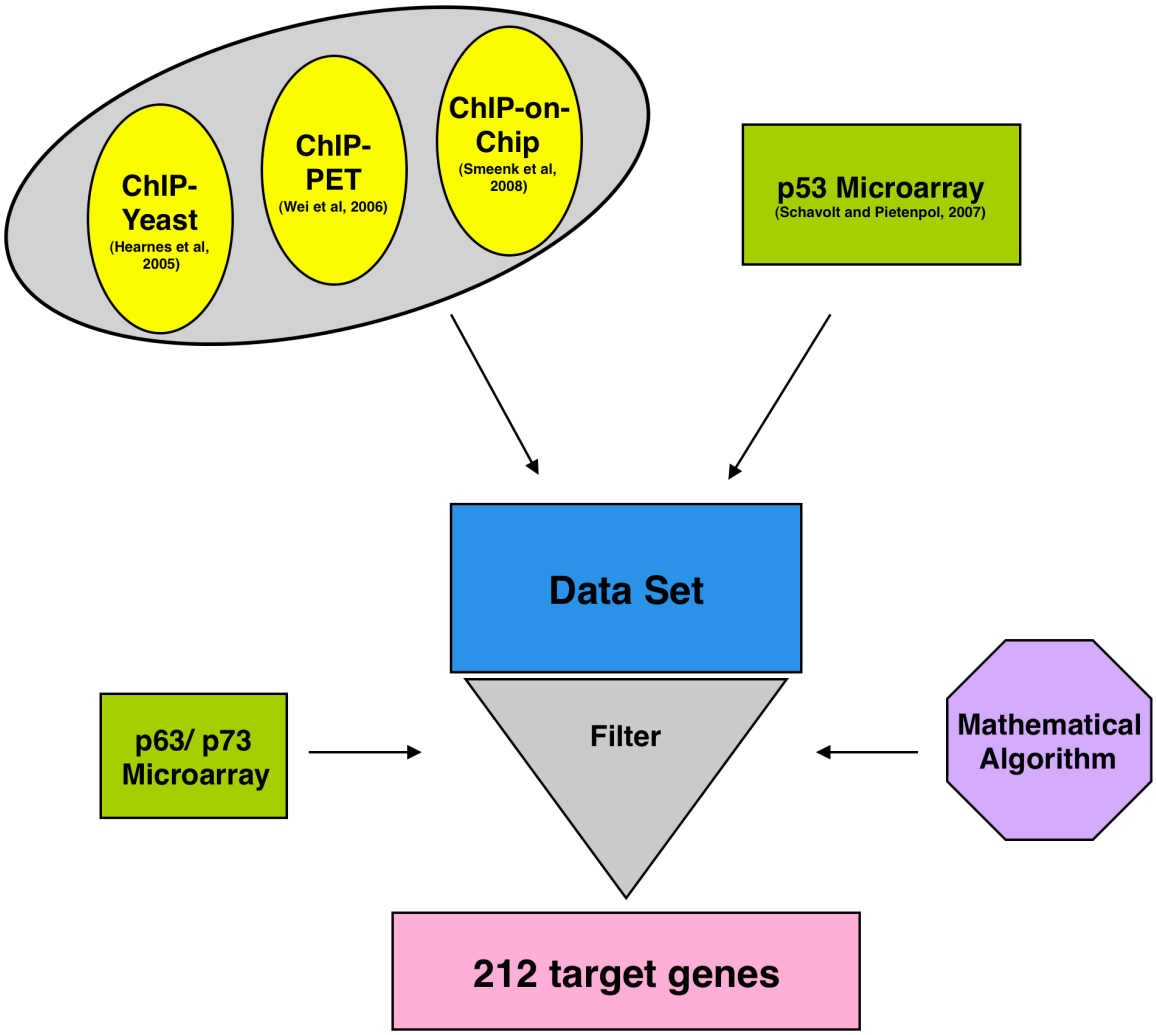

Figure 3. Genomic analyses to identify novel p53 targets A number of selection criteria were used to identify putative p53 transcriptional targets. We began by overlaying chromatin immunoprecipiation datasets with p53-dependent gene analysis. These genes were then further analyzed and filtered by comparing the p53-centric data set to transcriptional targets identified downstream of p63 and p73. We also used a novel hidden dynamic variable modeling algorithm that allows for statistical ranking of predicted targets as a filter.

genomic binding sites upstream of previously known p53 target genes including MDM2, p21, and DDB2. An additional 100 novel genomic binding sites were identified upstream of putative p53 target genes such as RPS27L (ribosomal protein 27-like) that was recently validated as part of the p53-dependent apoptotic pathway (He and Sun, 2007) as well as FLJ12484/ ISG20L1 that will be further discussed in Chapter IV of this dissertation.

In 2006, the first genome-wide ChIP analysis was performed using p53 binding sites by combining ChIP with paired-end ditag sequencing (ChIP-PET) (Wei *et al.*, 2006). The novelty of this technique not only allowed for genome-wide discovery of transcription factor binding sites but also capitalized on the efficiency of sequencing short tags (PET) to reduce background DNA without having to undergo further molecular validation. The DNA fragments that generated this dataset were from the colon cancer cell line HCT116 after treatment with 5-fluorouracail (5-FU), an antimetabolite. There were 1,766 PET-clusters defining genomic loci that represent potential sites of p53 interaction. Further analysis established a PET-cluster curve to estimate the level of nonspecific versus specific PET clustering events. Those regions containing three or more PETs to a cluster were identified as highly specific for p53 ChIP enrichment. A total of 323 genomic loci had PET-3 clusters and were identified as true p53 binding sites. The ChIP-PET analysis identified binding sites upstream of 61% of the previously known p53 target genes (Wei *et al.*, 2006). The p53 target gene p21 was found to have a high number of PETs (13)

clustered at the known p53 response element. Of the approximately 100 putative target genes associated with the 323 genomic loci, gene ontology analysis suggested many novel functions of p53 signaling through these target genes including cell adhesion and mobility, ion channel activity, and metabolism.

In 2008, the first p53 sequential ChIP-on-chip dataset was made available. This dataset was generated on a genomic ChIP with probe spacing of 100 bp. The DNA used in the hybridization was generated from U2OS cells growth arrested after treatment with actinomycin D. The study identified 1,546 genomic binding sites occupied by p53 with a 4% false positive rate (Smeenk *et al.*, 2008). In comparison to the previous ChIP-PET dataset discussed, this ChIP-on-chip genome-wide study has a similar 69% overlap of p53 genomic binding sites. The ChIP-on-chip screen contained 50% of the same genomic sequences identified by the ChIP-yeast screen described above.

When comparing these three ChIP-derived datasets, only eight genes were common to all including p21 and DDB2 (Table 1). All three of the ChIP datasets were performed in unique cells lines after different types of DNA-damage, and the methods used to identify p53 sites varied as described above. These differences amongst the ChIP datasets explain why only a small subset of similar p53 genes was found in common. Additionally, p53 selectively binds regions of the genome dependent on the genotoxic stress encountered that may also explain why so few genes were similar to all ChIP datasets. Overlaying of the two genome-wide ChIPs created a shared list of 103 genes (Table 2).

Table I. p53 transcriptional target genes common to ChIP-PET, ChIP-yeast, and ChIP-on-chip datasets

Symbol	Entrez Gene Name
CDKN1A *	**cyclin-dependent kinase inhibitor 1A (p21, Cip1)**
DDB2	**damage-specific DNA binding protein 2, 48kDa**
KPNA1	karyopherin alpha 1
MICA	MHC class I polypeptide-related sequence A
PDGFC	platelet derived growth factor C
PTPN14	protein tyrosine phosphatase, non-receptor type 14
RPS27L	**ribosomal protein S27-like**
TMEM30A	transmembrane protein 30A

* Bold font indicates genes previously identified at p53 targets

Table II. (part 1) p53 transcriptional target genes common to ChIP-PET and ChIP-on-chip datasets

Symbol	Entrez Gene Name
ACTN1	actinin, alpha 1
ADCY9	adenylate cyclase 9
ADORA2B	adenosine A2b receptor
ADRB1	adrenergic beta-1- receptor
ALDH3A1	aldehyde dehydrogenase 3 family, member A1
ALOX5	arachidonate 5-lipoxygenase
ANKRD10	ankyrin repeat domain 10
AVPR1A	arginine vasopressin receptor 1A
BAX *	**BCL2-associated X protein**
BIRC8	baculoviral IAP repeat-containing 8
BNC2	basonuclin 2
BTG4	B-cell translocation gene 4
C2ORF29	chromosome 2 open reading frame 29
C6ORF204	chromosome 6 open reading frame 204
C9ORF27	chromosome 9 open reading frame 27
CALD1	caldesmon 1
CCNG2	cyclin G2
CDC42EP3	CDC42 effector protein (Rho GTPase binding) 3
CDKN1A	**cyclin-dependent kinase inhibitor 1A (p21, Cip1)**
CHD2	chromodomain helicase DNA binding protein 2
CHN2	chimerin (chimaerin) 2
CYP3A7	cytochrome P450, family 3, subfamily A, polypeptide 7
CYP4F2	cytochrome P450, family 4, subfamily F, polypeptide 2
CYP4F3	cytochrome P450, family 4, subfamily F, polypeptide 3
DDB2	**damage-specific DNA binding protein 2, 48kDa**
DDIT4	DNA-damage-inducible transcript 4
DHRS2	dehydrogenase/reductase (SDR family) member 2
DYRK3	dual-specificity tyrosine-(Y)-phosphorylation regulated kinase 3
EDN2	endothelin 2
EHF	ets homologous factor
FAM12A	family with sequence similarity 12, member A
FAM20A	family with sequence similarity 20, member A
FAT1	FAT tumor suppressor homolog 1 (Drosophila)
FBLN1	fibulin 1
FGF2	**fibroblast growth factor 2**
FST	follistatin
GADD45A	**growth arrest and DNA-damage-inducible, alpha**
GDNF	glial cell derived neurotrophic factor
GNAI1	guanine nucleotide binding protein (G protein), alpha inhibiting activity polypeptide 1
GPC3	glypican 3
HAAO	3-hydroxyanthranilate 3,4-dioxygenase
HDAC9	histone deacetylase 9
HGF	hepatocyte growth factor
HS6ST2	heparan sulfate 6-O-sulfotransferase 2
ICOS	inducible T-cell co-stimulator
IER5	immediate early response 5
INSIG2	insulin induced gene 2
IRF2BP2	interferon regulatory factor 2 binding protein 2
KCNC2	potassium voltage-gated channel, Shaw-related subfamily, member 2
KCNK1	potassium channel, subfamily K, member 1
KCNMA1	potassium large conductance calcium-activated channel, subfamily M, alpha member 1

*** Genes listed in bold are known p53 transcriptional targets.**

Table II. (part 2) p53 transcriptional target genes common to ChIP-PET and ChIP-on-chip datasets

Symbol	Entrez Gene Name
KCNN3	potassium small conductance calcium-activated channel, subfamily N, member 3
KITLG	KIT ligand
KPNA1	karyopherin alpha 1 (importin alpha 5)
LAMA2	laminin, alpha 2
LTBP1	latent transforming growth factor beta binding protein 1
LZTS1	leucine zipper, putative tumor suppressor 1
MAP2K6	mitogen-activated protein kinase kinase 6
MAPK9	mitogen-activated protein kinase 9
MDM4	**Mdm4 p53 binding protein homolog**
MICA	MHC class I polypeptide-related sequence A
MYC	**v-myc myelocytomatosis viral oncogene homolog**
MYO3B	myosin IIIB
NHS	Nance-Horan syndrome
NLGN1	neuroligin 1
NOTCH1	**Notch homolog 1**
PCDH7	protocadherin 7
PCNA	**proliferating cell nuclear antigen**
PCNX	pecanex homolog
PDGFC	platelet derived growth factor C
PDP1	pyruvate dehyrogenase phosphatase catalytic subunit 1
PHF14	PHD finger protein 14
PPFIBP1	PTPRF interacting protein, binding protein 1
PRDM1	PR domain containing 1, with ZNF domain
PRIM2	primase, DNA, polypeptide 2
PRKCE	protein kinase C, epsilon
PSTPIP2	proline-serine-threonine phosphatase interacting protein 2
PTGFRN	prostaglandin F2 receptor negative regulator
PTPN14	protein tyrosine phosphatase, non-receptor type 14
PTPRM	protein tyrosine phosphatase, receptor type, M
PVRL1	poliovirus receptor-related 1
RPS19	ribosomal protein S19
RPS27L	**ribosomal protein S27-like**
RRAD	Ras-related associated with diabetes
RRM2B	**ribonucleotide reductase M2 B**
S100A2	**S100 calcium binding protein A2**
SFRS3	splicing factor, arginine/serine-rich 3
SLC12A4	solute carrier family 12 (potassium/chloride transporters), member 4
SNX16	sorting nexin 16
SNX5	sorting nexin 5
SORCS3	sortilin-related VPS10 domain containing receptor 3
STARD4	StAR-related lipid transfer (START) domain containing 4
SYNE1	spectrin repeat containing, nuclear envelope 1
SYT8	synaptotagmin VIII
TBX18	T-box 18
TGFA	transforming growth factor, alpha
TLE1	transducin-like enhancer of split 1 (E(sp1) homolog, Drosophila)
TLR3	toll-like receptor 3
TMEM30A	transmembrane protein 30A
TP53TG1	**TP53 target 1 (non-protein coding)**
TPO	thyroid peroxidase
TRIM22	**tripartite motif-containing 22**
TRIM29	tripartite motif-containing 29
WISP3	WNT1 inducible signaling pathway protein 3
ZCCHC2	zinc finger, CCHC domain containing 2

Gene Expression Datasets

To create an extensive collection of gene expression datasets, we used microarray datasets from several sources. The first dataset analyzed was from work performed in our laboratory by a previous graduate student, Dr. Kristy Schavolt. By ectopically expressing p53 using adenovirus in normal human epidermal keratinocytes as compared to GFP vector control adenovirus, she generated a list of approximately 2,000 genes upregulated at least 1.5-fold (Schavolt and Pietenpol, 2007).

Additionally, I analyzed differential gene expression in a p53-inducible cell model system that was generated in the laboratory by a previous graduate student, Dr. Patty Flatt (Flatt *et al.*, 2000). The inducible system was generated by transfection of pIND and pVgRXR vectors into the H1299 lung carcinoma cell line, which lacks detectable, endogenous expression of all p53 family members. The addition of ponasterone A caused induction of ectopic p53 and G1 and G2 cell cycle arrest (Flatt *et al.*, 2000).

We treated both the parental (p53-null) and HIp53 cell lines with ponasterone A for 24 h to induce p53. The experiment was performed in duplicate. At 24 h, cells were harvested and total RNA was isolated using the BioRad Aurum kit. Samples were submitted to the Vanderbilt Microarray core for quality control testing and gene expression analysis using the Affymetrix Expression (3') platform. The microarray dataset generated was robust given that the expression of a number of previously identified target genes (CDKN1A,

MDM2, BCLXL, and RPS27L) was increased after p53 induction as compared to the control *p53*-null parental cell line. Overall, the expression of 624 genes was increased 2-fold or greater in a p53-dependent manner after 24 h of ponasterone A treatment (Table 3).

Gene ontology analysis and qRT-PCR confirmation of p53-dependent regulation of putative target genes

The ChIP and gene expression microarray datasets described above were overlaid to create a list of potential p53 transcriptional targets. To investigate functional groupings of these genes based on protein domains and previous literature we used Ingenuity Software to perform gene ontology analyses. As would be expected, functional groupings of cell cycle, DNA repair, and cell death were found as well as functional categories not well linked to p53 signaling including cell-to-cell signaling, cell movement, and cellular metabolism (Figure 4).

Quantitative real-time PCR analysis was performed in paired sets of RKO or HCT116 colorectal cancer cell lines to determine p53-dependent regulation of 40 putative transcriptional targets identified using the p53 selection criteria. The RKO set includes RKOs expressing a CMV-neo empty vector or RKOs expressing the human papilloma virus E6 that binds and degrades p53 with the cellular E6a protein (Kessis *et al.*, 1993). These cells were treated with Nutlin (10 μM) for 24 h. This drug disrupts p53:MDM2 binding and causes stabilization of p53 (Vassilev *et al.*, 2004). The set of HCT116 cells includes HCT116 p53 (+/+) and (-/-), the latter generated by somatic cell recombination (Bunz *et al.*, 1998).

Table III. (part 1) Genes upregulated greater than 2-fold after p53 induction

Fold Change	Symbol	Entrez Gene Name
8.343	ABCA1	ATP-binding cassette, sub-family A, member 1
2.040	ABCB6	ATP-binding cassette, sub-family B, member 6
3.282	ABCG2	ATP-binding cassette, sub-family G, member 2
4.093	ABHD4	abhydrolase domain containing 4
2.117	ABI1	abl-interactor 1
4.971	ACOX1	acyl-Coenzyme A oxidase 1
11.750	ACTA2	actin, alpha 2, smooth muscle
2.182	ADARB1	adenosine deaminase, RNA-specific, B1
2.059	AFF4	AF4/FMR2 family, member 4
2.433	AGBL5	ATP/GTP binding protein-like 5
3.674	AGRN	agrin
2.338	AHNAK2	AHNAK nucleoprotein 2
2.407	AIFM2	apoptosis-inducing factor, mitochondrion-associated, 2
2.320	AK1	adenylate kinase 1
2.110	AK3L1	adenylate kinase 3-like 1
6.625	AKR1B10	aldo-keto reductase family 1, member B10
8.146	AKR1C3	aldo-keto reductase family 1, member C3
2.364	ALCAM	activated leukocyte cell adhesion molecule
2.371	ALDH1A3	aldehyde dehydrogenase 1 family, member A3
7.127	ALDH3A2	aldehyde dehydrogenase 3 family, member A2
2.951	ALDH4A1	aldehyde dehydrogenase 4 family, member A1
4.922	ALPK2	alpha-kinase 2
4.633	ALS2CL	ALS2 C-terminal like
2.320	STRADB	STE20-related kinase adaptor beta
3.803	AMN1	antagonist of mitotic exit network 1 homolog
6.519	ANKRA2	ankyrin repeat, family A, 2
2.302	ANKRD42	ankyrin repeat domain 42
2.196	KANK3	KN motif and ankyrin repeat domains 3
5.302	ANXA3	annexin A3
3.544	ANXA4	annexin A4
3.589	ANXA8	annexin A8
8.433	APAF1	apoptotic peptidase activating factor 1
4.185	APOBEC3C	apolipoprotein B mRNA editing catalytic polypeptide-like 3C
2.756	APOOL	apolipoprotein O-like
2.698	ARFGEF1	ADP-ribosylation factor guanine nucleotide-exchange factor 1
3.126	ARHGAP10	Rho GTPase activating protein 10
2.029	ARHGAP23	Rho GTPase activating protein 23
2.213	ARRDC1	arrestin domain containing 1
2.571	ARVCF	armadillo repeat gene deletes in velocardiofacial syndrome
2.444	ASCC3	activating signal cointegrator 1 complex subunit 3
2.780	ASS1	argininosuccinate synthetase 1
15.530	ASTN2	astrotactin 2
9.590	ATF3	activating transcription factor 3
2.095	ATP7A	ATPase, Cu++ transporting, alpha polypeptide
2.626	ATP7B	ATPase, Cu++ transporting, beta polypeptide
3.481	ATRX	alpha thalassemia/mental retardation syndrome X-linked
5.458	BAMBI	BMP and activin membrane-bound inhibitor homolog
3.901	BAX	BCL2-associated X protein
3.438	BCL10	B-cell CLL/lymphoma 10
2.228	BCL11A	B-cell CLL/lymphoma 11A
3.775	BCL2L1	BCL2-like 1
3.993	BCL6	B-cell CLL/lymphoma 6

Table III. (part 2) Genes upregulated greater than 2-fold after p53 induction

Fold Change	Symbol	Entrez Gene Name
6.201	BHLHE40	basic helix-loop-helix family, member e40
9.359	BIK	BCL2-interacting killer
2.506	BIRC3	baculoviral IAP repeat-containing 3
2.693	BLCAP	bladder cancer associated protein
2.410	BLOC1S2	biogenesis of lysosomal organelles complex-1, subunit 2
2.481	BMP1	bone morphogenetic protein 1
2.587	BNC1	basonuclin 1
2.535	BRMS1L	breast cancer metastasis-suppressor 1-like
2.801	BRWD3	bromodomain and WD repeat domain containing 3
3.830	NACC2	NACC family member 2
82.400	BTG2	BTG family, member 2
2.357	BTN3A1	butyrophilin, subfamily 3, member A1
2.844	BTN3A3	butyrophilin, subfamily 3, member A3
5.182	C10ORF10	chromosome 10 open reading frame 10
2.182	C10ORF47	chromosome 10 open reading frame 47
2.253	C10ORF54	chromosome 10 open reading frame 54
5.642	C12ORF5	chromosome 12 open reading frame 5
4.780	C13ORF31	chromosome 13 open reading frame 31
2.158	C14ORF28	chromosome 14 open reading frame 28
2.385	C16ORF5	chromosome 16 open reading frame 5
3.105	C18ORF1	chromosome 18 open reading frame 1
3.941	C18ORF25	chromosome 18 open reading frame 25
3.204	C18ORF56	chromosome 18 open reading frame 56
2.974	C19ORF33	chromosome 19 open reading frame 33
41.750	C1ORF187	chromosome 1 open reading frame 187
3.002	C1ORF57	chromosome 1 open reading frame 57
2.716	C1ORF63	chromosome 1 open reading frame 63
2.152	C20ORF108	chromosome 20 open reading frame 108
2.481	C20ORF112	chromosome 20 open reading frame 112
2.038	C20ORF117	chromosome 20 open reading frame 117
2.901	DNAJC28	DnaJ (Hsp40) homolog, subfamily C, member 28
2.130	C2ORF63	chromosome 2 open reading frame 63
5.195	C4ORF10	chromosome 4 open reading frame 10
3.014	C5ORF41	chromosome 5 open reading frame 41
3.448	C7ORF10	chromosome 7 open reading frame 10
2.640	C7ORF41	chromosome 7 open reading frame 41
3.583	C8ORF38	chromosome 8 open reading frame 38
3.118	FAM189A2	family with sequence similarity 189, member A2
20.390	C9ORF66	chromosome 9 open reading frame 66
2.069	C9ORF85	chromosome 9 open reading frame 85
2.592	CABC1	chaperone, ABC1 activity of bc1 complex homolog
2.221	CACNB2	calcium channel, voltage-dependent, beta 2 subunit
4.320	CASP1	caspase 1, apoptosis-related cysteine peptidase
3.557	CAV1	caveolin 1, caveolae protein, 22kDa
2.402	CBLB	Cas-Br-M ecotropic retroviral transforming sequence b
2.075	CCDC146	coiled-coil domain containing 146
2.048	CCDC43	coiled-coil domain containing 43
2.143	CCDC45	coiled-coil domain containing 45
2.293	CCDC69	coiled-coil domain containing 69
2.472	CCDC90B	coiled-coil domain containing 90B
2.252	CCNG1	cyclin G1
2.245	CCNG2	cyclin G2

Table III. (part 3) Genes upregulated greater than 2-fold after p53 induction

Fold Change	Symbol	Entrez Gene Name
2.279	CD55	CD55 molecule, decay accelerating factor for complement
4.528	CD82	CD82 molecule
2.017	CD83	CD83 molecule
2.412	CDC42EP4	CDC42 effector protein 4
2.462	CDC73	cell division cycle 73, Paf1/RNA polymerase II complex
3.592	CDH12	cadherin 12, type 2 (N-cadherin 2)
18.280	CDKN1A	cyclin-dependent kinase inhibitor 1A (p21, Cip1)
2.420	CDO1	cysteine dioxygenase, type I
7.108	CEACAM1	carcinoembryonic antigen-related cell adhesion molecule 1
2.210	CEL	carboxyl ester lipase (bile salt-stimulated lipase)
2.393	AGAP1	ArfGAP with GTPase domain, ankyrin repeat and PH domain 1
2.151	CES2	carboxylesterase 2
2.540	CFLAR	CASP8 and FADD-like apoptosis regulator
2.399	CGGBP1	CGG triplet repeat binding protein 1
2.904	CHST2	carbohydrate (N-acetylglucosamine-6-O) sulfotransferase 2
4.737	CITED4	Cbp/p300-interacting transactivator
3.394	CLIC4	chloride intracellular channel 4
8.166	CLMN	calmin (calponin-like, transmembrane)
2.594	CLN8	ceroid-lipofuscinosis, neuronal 8
2.338	CLP1	CLP1, cleavage and polyadenylation factor I subunit
3.300	CMBL	carboxymethylenebutenolidase homolog
4.365	COL27A1	collagen, type XXVII, alpha 1
2.496	COL4A5	collagen, type IV, alpha 5
3.506	COL9A3	collagen, type IX, alpha 3
2.154	CARD16	caspase recruitment domain family, member 16
2.791	CORO2A	coronin, actin binding protein, 2A
5.208	CORO6	coronin 6
2.458	CPEB2	cytoplasmic polyadenylation element binding protein 2
120.400	CPM	carboxypeptidase M
2.007	CREG1	cellular repressor of E1A-stimulated genes 1
2.673	CRIM1	cysteine rich transmembrane BMP regulator 1
2.627	CRYZL1	crystallin, zeta -like 1
2.077	CSDA	cold shock domain protein A
2.343	CTDSPL	CTD small phosphatase-like
4.451	CTNND1	catenin, delta 1
2.303	CTSO	cathepsin O
2.477	CUEDC1	CUE domain containing 1
138.700	CYFIP2	cytoplasmic FMR1 interacting protein 2
3.182	CYP24A1	cytochrome P450, family 24, subfamily A, polypeptide 1
24.370	D4S234E	DNA segment on chromosome 4
16.870	DCLK1	doublecortin-like kinase 1
2.127	DCTN5	dynactin 5 (p25)
2.917	DDAH1	dimethylarginine dimethylaminohydrolase 1
9.104	DDB2	damage-specific DNA binding protein 2, 48kDa
3.321	ASAP2	ArfGAP with SH3 domain, ankyrin repeat and PH domain 2
2.628	DDX58	DEAD box polypeptide 58
3.590	DENND1A	DENN/MADD domain containing 1A
2.326	DFNA5	deafness, autosomal dominant 5
15.480	DGKA	diacylglycerol kinase, alpha 80kDa
18.610	DHRS3	dehydrogenase/reductase member 3
2.189	DKK1	dickkopf homolog 1
3.045	DLG5	discs, large homolog 5

Table III. (part 4) Genes upregulated greater than 2-fold after p53 induction

Fold Change	Symbol	Entrez Gene Name
36.070	DOCK8	dedicator of cytokinesis 8
2.390	DPYSL4	dihydropyrimidinase-like 4
9.987	DRAM1	DNA-damage regulated autophagy modulator 1
3.435	DSP	desmoplakin
2.911	DTX2	deltex homolog 2
2.550	DUSP14	dual specificity phosphatase 14
2.012	DYNC1I1	dynein, cytoplasmic 1, intermediate chain 1
3.774	DYRK3	dual-specificity tyrosine-(Y)-phosphorylation regulated kinase 3
3.616	E2F7	E2F transcription factor 7
5.400	LPAR1	lysophosphatidic acid receptor 1
2.691	EDNRA	endothelin receptor type A
8.987	EFEMP1	EGF-containing fibulin-like extracellular matrix protein 1
3.265	EI24	etoposide induced 2.4 mRNA
2.689	EIF4G3	eukaryotic translation initiation factor 4 gamma, 3
2.998	ELL3	elongation factor RNA polymerase II-like 3
4.450	ENC1	ectodermal-neural cortex
4.442	EPAS1	endothelial PAS domain protein 1
2.338	EPB41	erythrocyte membrane protein band 4.1
2.301	EPHA2	EPH receptor A2
15.220	EPS8L2	EPS8-like 2
2.162	ERC1	ELKS/RAB6-interacting/CAST family member 1
3.595	ERCC6	excision repair cross-complementing group 6
2.240	ERO1LB	ERO1-like beta
3.208	ETNK1	ethanolamine kinase 1
2.048	EXT1	exostoses (multiple) 1
2.019	F11R	F11 receptor
5.109	F2RL2	coagulation factor II (thrombin) receptor-like 2
5.193	FADS3	fatty acid desaturase 3
2.736	FAM101A	family with sequence similarity 101, member A
5.568	FAM102A	family with sequence similarity 102, member A
2.208	FAM117A	family with sequence similarity 117, member A
22.350	FAM13C	family with sequence similarity 13, member C
2.962	FAM43A	family with sequence similarity 43, member A
2.141	ESYT2	extended synaptotagmin-like protein 2
2.391	FAM82A1	family with sequence similarity 82, member A1
3.043	FAM83H	family with sequence similarity 83, member H
12.090	FAM84B	family with sequence similarity 84, member B
4.885	FAS	Fas (TNF receptor superfamily, member 6)
3.485	FBN2	fibrillin 2
2.745	FBXL18	F-box and leucine-rich repeat protein 18
3.028	FBXL21	F-box and leucine-rich repeat protein 21 (gene/pseudogene)
2.740	FBXO22	F-box protein 22
5.664	FBXO44	F-box protein 44
2.047	FBXW7	F-box and WD repeat domain containing 7
3.282	FCHSD2	FCH and double SH3 domains 2
54.640	FDXR	ferredoxin reductase
2.059	FECH	ferrochelatase (protoporphyria)
5.524	FEZ1	fasciculation and elongation protein zeta 1 (zygin I)
2.738	FGD6	FYVE, RhoGEF and PH domain containing 6
2.590	FGF12	fibroblast growth factor 12
2.277	FGF2	fibroblast growth factor 2 (basic)
7.543	FGFR3	fibroblast growth factor receptor 3

Table III. (part 5) Genes upregulated greater than 2-fold after p53 induction

Fold Change	Symbol	Entrez Gene Name
2.637	FHL2	four and a half LIM domains 2
2.370	CPPED1	calcineurin-like phosphoesterase domain containing 1
4.573	C1ORF226	chromosome 1 open reading frame 226
3.476	SLC48A1	solute carrier family 48 (heme transporter), member 1
3.051	FLJ35776	hypothetical LOC649446
4.294	LVRN	laeverin
3.676	FLNC	filamin C, gamma
3.336	FLYWCH1	FLYWCH-type zinc finger 1
2.660	FNBP1	formin binding protein 1
3.514	FOXN3	forkhead box N3
2.737	FREQ	frequenin homolog (Drosophila)
6.665	FRMD8	FERM domain containing 8
2.178	FSCN1	fascin homolog 1, actin-bundling protein
2.064	FUCA1	fucosidase, alpha-L- 1, tissue
4.202	GABBR2	gamma-aminobutyric acid (GABA) B receptor, 2
2.498	GADD45A	growth arrest and DNA-damage-inducible, alpha
3.079	GAMT	guanidinoacetate N-methyltransferase
22.880	GAS6	growth arrest-specific 6
2.165	GATA3	GATA binding protein 3
4.204	GATS	GATS, stromal antigen 3 opposite strand
2.410	GBP1	guanylate binding protein 1, interferon-inducible, 67kDa
2.404	GCNT2	glucosaminyl (N-acetyl) transferase 2, I-branching enzyme
3.280	GDA	guanine deaminase
119.900	GDF15	growth differentiation factor 15
2.579	GJA3	gap junction protein, alpha 3, 46kDa
5.429	GJD3	gap junction protein, delta 3, 31.9kDa
3.336	GLS2	glutaminase 2 (liver, mitochondrial)
2.259	GNA12	guanine nucleotide binding protein (G protein) alpha 12
2.698	GNA15	guanine nucleotide binding protein, alpha 15
8.418	GPC1	glypican 1
4.103	GPHN	gephyrin
2.619	GPR126	G protein-coupled receptor 126
2.470	GPR155	G protein-coupled receptor 155
4.251	GPR172B	G protein-coupled receptor 172B
2.077	GPR75	G protein-coupled receptor 75
15.120	GPR87	G protein-coupled receptor 87
2.172	GREB1	growth regulation by estrogen in breast cancer 1
2.774	GRM3	glutamate receptor, metabotropic 3
2.705	GSDMD	gasdermin D
8.464	GTPBP2	GTP binding protein 2
2.394	H2AFB1	H2A histone family, member B1
2.362	HDX	highly divergent homeobox
3.518	HEG1	HEG homolog 1 (zebrafish)
2.902	HES2	hairy and enhancer of split 2
3.627	HHAT	hedgehog acyltransferase
2.857	HHAT	hedgehog acyltransferase
4.059	HIC2	hypermethylated in cancer 2
5.254	HMOX1	heme oxygenase (decycling) 1
5.512	NTM	neurotrimin
13.430	HOXC13	homeobox C13
2.282	HSD17B7	hydroxysteroid (17-beta) dehydrogenase 7
3.898	HSDL2	hydroxysteroid dehydrogenase like 2

Table III. (part 6) Genes upregulated greater than 2-fold after p53 induction

Fold Change	Symbol	Entrez Gene Name
3.773	HSP90B1	heat shock protein 90kDa beta (Grp94), member 1
2.373	HSPA6	heat shock 70kDa protein 6 (HSP70B')
4.014	HSPG2	heparan sulfate proteoglycan 2
3.385	ICOSLG	inducible T-cell co-stimulator ligand
4.804	ID2	inhibitor of DNA binding 2
2.541	ID3	inhibitor of DNA binding 3
4.510	IDUA	iduronidase, alpha-L-
13.950	IFI16	interferon, gamma-inducible protein 16
11.890	IFI44	interferon-induced protein 44
4.187	IGFBP4	insulin-like growth factor binding protein 4
4.182	IGFBP7	insulin-like growth factor binding protein 7
3.486	IKBIP	IKBKB interacting protein
2.464	IL10RB	interleukin 10 receptor, beta
4.205	IL1RAP	interleukin 1 receptor accessory protein
2.195	IL32	interleukin 32
2.527	IL7	interleukin 7
2.308	INPP1	inositol polyphosphate-1-phosphatase
2.897	IQCG	IQ motif containing G
3.381	IRF1	interferon regulatory factor 1
2.396	ISCU	iron-sulfur cluster scaffold homolog (E. coli)
3.313	ITGA3	integrin, alpha 3
3.488	ITGAV	integrin, alpha V
2.669	ITGB4	integrin, beta 4
3.720	ITGBL1	integrin, beta-like 1
4.816	ITIH5	inter-alpha inhibitor H5
2.846	ITPKC	inositol 1,4,5-trisphosphate 3-kinase C
2.031	ITSN2	intersectin 2
2.162	JAG2	jagged 2
4.360	KDM4B	lysine (K)-specific demethylase 4B
2.429	JUNB	jun B proto-oncogene
17.640	KCNB1	potassium voltage-gated channel
3.247	KCNMA1	potassium large conductance calcium-activated channel
4.229	KIAA0247	KIAA0247
2.898	KIAA0284	KIAA0284
2.760	SEL1L3	sel-1 suppressor of lin-12-like 3
3.605	RALGAPB	Ral GTPase activating protein, beta subunit
2.457	KIAA1267	KIAA1267
5.063	KIAA1324	KIAA1324
4.480	KIAA1462	KIAA1462
2.085	KIAA1671	KIAA1671
3.896	TNRC18	trinucleotide repeat containing 18
3.258	KIF1B	kinesin family member 1B
3.478	KIRREL	kin of IRRE like
4.585	KLF4	Kruppel-like factor 4
2.503	KLHL21	kelch-like 21
2.183	KLRC4	killer cell lectin-like receptor subfamily C, member 4
4.290	KRT15	keratin 15
2.276	KRT7	keratin 7
3.075	KSR1	kinase suppressor of ras 1
3.191	LAMA5	laminin, alpha 5
3.008	LAMP3	lysosomal-associated membrane protein 3
3.943	LAPTM5	lysosomal protein transmembrane 5

Table III. (part 7) Genes upregulated greater than 2-fold after p53 induction

Fold Change	Symbol	Entrez Gene Name
2.091	LFNG	O-fucosylpeptide 3-beta-N-acetylglucosaminyltransferase
4.366	LGALS3BP	lectin, galactoside-binding, soluble, 3 binding protein
2.161	LIMA1	LIM domain and actin binding 1
13.750	LIMCH1	LIM and calponin homology domains 1
2.314	LMNA	lamin A/C
2.572	LMNA	lamin A/C
2.822	LMNA	lamin A/C
19.690	BTBD19	BTB (POZ) domain containing 19
7.138	LOC158160	hydroxysteroid (17-beta) dehydrogenase 7 pseudogene 2
2.232	LOC158863	hypothetical protein LOC158863
2.770	SPATS2L	spermatogenesis associated, serine-rich 2-like
4.264	C14ORF182	chromosome 14 open reading frame 182
7.006	LOC284080	hypothetical protein LOC284080
2.046	LOC284804	hypothetical protein LOC284804
4.031	LOC389906	similar to Serine/threonine-protein kinase PRKX
2.485	LOC439949	hypothetical protein LOC439949
2.628	LOC497257	hypothetical LOC497257
3.722	LOC643650	hypothetical protein LOC643650
2.258	LOC646626	hypothetical LOC646626
3.664	LOC728449	hypothetical protein LOC728449
3.822	LOC90784	hypothetical protein LOC90784
3.476	LRDD	leucine-rich repeats and death domain containing
4.094	LRP1	low density lipoprotein-related protein 1
3.659	LRRK1	leucine-rich repeat kinase 1
2.407	LTBP2	latent transforming growth factor beta binding protein 2
7.577	MAMDC4	MAM domain containing 4
2.282	MAN2B1	mannosidase, alpha, class 2B, member 1
3.203	MAP2K5	mitogen-activated protein kinase kinase 5
2.301	MAP3K14	mitogen-activated protein kinase kinase kinase 14
5.891	MAP3K9	mitogen-activated protein kinase kinase kinase 9
2.053	MAP4K4	mitogen-activated protein kinase kinase kinase kinase 4
5.352	MAPKBP1	mitogen-activated protein kinase binding protein 1
2.689	MARCH8	membrane-associated ring finger (C3HC4) 8
3.975	MAZ	MYC-associated zinc finger protein
2.097	MBD6	methyl-CpG binding domain protein 6
2.871	MBNL2	muscleblind-like 2 (Drosophila)
2.716	LPCAT3	lysophosphatidylcholine acyltransferase 3
5.052	MCC	mutated in colorectal cancers
50.540	MDM2	Mdm2 p53 binding protein homolog (mouse)
2.107	MED13L	mediator complex subunit 13-like
3.032	MED15	mediator complex subunit 15
3.890	MED23	mediator complex subunit 23
2.666	MEF2A	myocyte enhancer factor 2A
25.200	MEGF6	multiple EGF-like-domains 6
3.984	C17ORF103	chromosome 17 open reading frame 103
2.474	FAM185A	family with sequence similarity 185, member A
2.596	LOC284440	hypothetical LOC284440
2.478	MIB2	mindbomb homolog 2
2.217	MICALL1	MICAL-like 1
2.204	MICALL2	MICAL-like 2
2.633	MINK1	misshapen-like kinase 1
2.405	MKX	mohawk homeobox

Table III. (part 8) Genes upregulated greater than 2-fold after p53 induction

Fold Change	Symbol	Entrez Gene Name
2.041	MLL	myeloid/lymphoid or mixed-lineage leukemia
2.157	MLLT10	myeloid/lymphoid or mixed-lineage leukemia
2.685	MMP28	matrix metallopeptidase 28
2.997	MON2	MON2 homolog
2.503	MPP7	membrane protein, palmitoylated 7
3.441	MR1	major histocompatibility complex, class I-related
2.189	MRPL49	mitochondrial ribosomal protein L49
3.131	MSRB2	methionine sulfoxide reductase B2
2.276	MYLK	myosin light chain kinase
2.634	MYO10	myosin X
2.678	MYO18A	myosin XVIIIA
3.481	MYO6	myosin VI
4.897	NADSYN1	NAD synthetase 1
6.324	NAP1L2	nucleosome assembly protein 1-like 2
2.980	NDST1	N-deacetylase/N-sulfotransferase (heparan glucosaminyl) 1
2.169	NDUFV3	NADH dehydrogenase (ubiquinone) flavoprotein 3, 10kDa
2.979	NEBL	nebulette
4.813	NFKBIA	nuclear factor of kappa light polypeptide gene enhancer
2.147	NINJ1	ninjurin 1
2.942	IGDCC4	immunoglobulin superfamily, DCC subclass, member 4
3.785	NOTCH1	Notch homolog 1, translocation-associated (Drosophila)
2.460	NOTCH3	Notch homolog 3 (Drosophila)
2.622	NR3C1	nuclear receptor subfamily 3, group C, member 1
3.954	NRCAM	neuronal cell adhesion molecule
2.673	HMGN5	high-mobility group nucleosome binding domain 5
9.709	NTN1	netrin 1
3.405	NUMB	numb homolog (Drosophila)
2.458	OBSL1	obscurin-like 1
2.343	OLIG2	oligodendrocyte lineage transcription factor 2
2.418	ORAI3	ORAI calcium release-activated calcium modulator 3
2.317	OSBPL9	oxysterol binding protein-like 9
2.277	P2RX4	purinergic receptor P2X, ligand-gated ion channel, 4
2.083	P4HA2	prolyl 4-hydroxylase, alpha polypeptide II
10.780	PANK1	pantothenate kinase 1
5.831	PAPLN	papilin, proteoglycan-like sulfated glycoprotein
6.141	PAPPA	pregnancy-associated plasma protein A, pappalysin 1
2.767	PARD3	par-3 partitioning defective 3 homolog (C. elegans)
2.079	PARP14	poly (ADP-ribose) polymerase family, member 14
2.212	PCDHGA4	protocadherin gamma subfamily A, 4
2.011	PCGF3	polycomb group ring finger 3
2.012	PCNX	pecanex homolog (Drosophila)
2.211	PCNXL2	pecanex-like 2 (Drosophila)
2.447	PCTK2	PCTAIRE protein kinase 2
4.668	PDE3A	phosphodiesterase 3A, cGMP-inhibited
2.348	PDGFC	platelet derived growth factor C
2.029	PDLIM1	PDZ and LIM domain 1
2.695	PGAP1	post-GPI attachment to proteins 1
3.259	PGBD3	piggyBac transposable element derived 3
5.861	PGPEP1	pyroglutamyl-peptidase I
2.359	PHACTR1	phosphatase and actin regulator 1
2.791	PHLDB3	pleckstrin homology-like domain, family B, member 3
2.168	PHPT1	phosphohistidine phosphatase 1

Table III. (part 9) Genes upregulated greater than 2-fold after p53 induction

Fold Change	Symbol	Entrez Gene Name
2.058	PHYH	phytanoyl-CoA 2-hydroxylase
2.018	PI4KB	phosphatidylinositol 4-kinase, catalytic, beta
2.731	PIK3C2A	phosphoinositide-3-kinase, class 2, alpha polypeptide
2.296	PIK3CD	phosphoinositide-3-kinase, catalytic, delta polypeptide
2.015	PIK3R1	phosphoinositide-3-kinase, regulatory subunit 1 (alpha)
2.034	PIK3R3	phosphoinositide-3-kinase, regulatory subunit 3 (gamma)
4.702	PISD	phosphatidylserine decarboxylase
4.294	PLCD3	phospholipase C, delta 3
15.990	PLCXD2	PSP C, X domain containing 2
2.269	PLEKHA8	pleckstrin homology domain containing, family A
3.595	PLEKHF1	pleckstrin homology domain containing, family F
4.643	PLEKHG1	pleckstrin homology domain containing, family G
2.689	PLK2	polo-like kinase 2 (Drosophila)
18.500	PLK3	polo-like kinase 3 (Drosophila)
4.434	PLXNB2	plexin B2
2.111	PML	promyelocytic leukemia
5.080	PODXL	podocalyxin-like
3.528	POLH	polymerase (DNA directed), eta
2.393	PPM1A	protein phosphatase 1A (formerly 2C)
4.892	PPM1D	protein phosphatase 1D magnesium-dependent, delta isoform
2.204	PPME1	protein phosphatase methylesterase 1
2.644	PPME1	protein phosphatase methylesterase 1
5.688	PPP1R14C	protein phosphatase 1, regulatory (inhibitor) subunit 14C
2.579	PRIC285	peroxisomal receptor A interacting complex 285
3.024	PRKAB1	protein kinase, AMP-activated, beta 1 non-catalytic subunit
2.752	PRKAB2	protein kinase, AMP-activated, beta 2 non-catalytic subunit
2.062	PRKX	protein kinase, X-linked
3.095	PROCR	protein C receptor, endothelial (EPCR)
2.043	PSMB9	proteasome subunit, beta type, 9
3.997	PSTPIP2	proline-serine-threonine phosphatase interacting protein 2
3.822	PTN	pleiotrophin
21.730	PTP4A1	protein tyrosine phosphatase type IVA, member 1
2.240	PTPN3	protein tyrosine phosphatase, non-receptor type 3
4.119	PVT1	Pvt1 oncogene (non-protein coding)
2.465	RAB1A	RAB1A, member RAS oncogene family
2.501	RAB20	RAB20, member RAS oncogene family
4.032	RAB27B	RAB27B, member RAS oncogene family
5.229	RAB38	RAB38, member RAS oncogene family
3.756	RALGDS	ral guanine nucleotide dissociation stimulator
2.087	RAP2B	RAP2B, member of RAS oncogene family
4.047	RAPGEF3	Rap guanine nucleotide exchange factor (GEF) 3
2.005	RELT	RELT tumor necrosis factor receptor
2.129	RETSAT	retinol saturase (all-trans-retinol 13,14-reductase)
2.045	RGAG4	retrotransposon gag domain containing 4
2.814	RGS20	regulator of G-protein signaling 20
2.268	RHBDF2	rhomboid 5 homolog 2 (Drosophila)
4.600	RIMBP3	RIMS binding protein 3
3.851	RNASEL	ribonuclease L (2',5'-oligoisoadenylate synthetase-dependent)
2.031	RND3	Rho family GTPase 3
3.419	RLIM	ring finger protein, LIM domain interacting
19.780	RNF144B	ring finger protein 144B
7.872	RNF19B	ring finger protein 19B

Table III. (part 10) Genes upregulated greater than 2-fold after p53 induction

Fold Change	Symbol	Entrez Gene Name
2.033	RORA	RAR-related orphan receptor A
6.745	RPS27L	ribosomal protein S27-like
4.786	RPS6KA1	ribosomal protein S6 kinase, 90kDa, polypeptide 1
19.100	RRAD	Ras-related associated with diabetes
3.138	RRM2B	ribonucleotide reductase M2 B (TP53 inducible)
8.536	RXRA	retinoid X receptor, alpha
2.041	S100A16	S100 calcium binding protein A16
5.968	SAMD9L	sterile alpha motif domain containing 9-like
2.705	SAT1	spermidine/spermine N1-acetyltransferase 1
4.059	SCD5	stearoyl-CoA desaturase 5
14.100	SCN2A	sodium channel, voltage-gated, type II, alpha subunit
10.010	SDC1	syndecan 1
3.097	SDC4	syndecan 4
2.144	SEL1L	sel-1 suppressor of lin-12-like (C. elegans)
2.036	SEMA3F	sema domain 3F
2.478	SEPT9	septin 9
2.705	SERINC5	serine incorporator 5
4.339	SERPINA1	serpin peptidase inhibitor, clade A
8.004	SESN1	sestrin 1
3.621	SESN2	sestrin 2
2.237	SETX	senataxin
2.432	SF3B14	splicing factor 3B, 14 kDa subunit
5.472	SFN	stratifin
3.647	SFTPF	surfactant associated 1 (pseudogene)
2.226	SFXN5	sideroflexin 5
2.018	SH3BP2	SH3-domain binding protein 2
3.820	SH3RF3	SH3 domain containing ring finger 3
3.301	SHROOM3	shroom family member 3
3.878	SIDT2	SID1 transmembrane family, member 2
11.420	SIPA1L2	signal-induced proliferation-associated 1 like 2
3.374	SLC25A21	solute carrier family 25 member 21
2.402	SLC25A30	solute carrier family 25, member 30
3.032	SLC25A45	solute carrier family 25, member 45
2.495	SLC30A1	solute carrier family 30 (zinc transporter), member 1
2.115	SLC35D1	solute carrier family 35 member D1
2.051	SLC40A1	solute carrier family 40 (iron-regulated transporter), member 1
3.851	SLC47A1	solute carrier family 47, member 1
3.322	SLC4A11	solute carrier family 4, sodium borate transporter, member 11
5.745	SLC9A2	solute carrier family 9 (sodium/hydrogen exchanger), member 2
2.219	SLC9A3R1	solute carrier family 9, member 3 regulator 1
2.115	SMAD3	SMAD family member 3
2.196	SMURF1	SMAD specific E3 ubiquitin protein ligase 1
3.174	SORBS1	sorbin and SH3 domain containing 1
2.428	SOX7	SRY (sex determining region Y)-box 7
2.221	SP100	SP100 nuclear antigen
2.387	SPATA7	spermatogenesis associated 7
3.014	CYTSB	cytospin B
2.758	SPINK5	serine peptidase inhibitor, Kazal type 5
3.321	SQSTM1	sequestosome 1
2.702	SRGAP2	SLIT-ROBO Rho GTPase activating protein 2
3.036	SSH1	slingshot homolog 1 (Drosophila)
2.969	SSH2	slingshot homolog 2 (Drosophila)

Table III. (part 11) Genes upregulated greater than 2-fold after p53 induction

Fold Change	Symbol	Entrez Gene Name
2.002	STAT1	signal transducer and activator of transcription 1, 91kDa
3.070	STAT3	signal transducer and activator of transcription 3
11.960	STOX2	storkhead box 2
2.360	STX6	syntaxin 6
2.582	SULT1E1	sulfotransferase family 1E, estrogen-preferring, member 1
9.588	SYNE1	spectrin repeat containing, nuclear envelope 1
2.370	SYT1	synaptotagmin I
8.935	SYTL1	synaptotagmin-like 1
2.274	TAF3	TAF3 RNA polymerase II, TATA box binding protein
2.851	TAP1	transporter 1, ATP-binding cassette, sub-family B
2.370	TAPBPL	TAP binding protein-like
2.178	TBC1D10A	TBC1 domain family, member 10A
4.480	TBC1D2	TBC1 domain family, member 2
2.484	TBC1D8	TBC1 domain family, member 8 (with GRAM domain)
2.025	TEF	thyrotrophic embryonic factor
3.413	TEP1	telomerase-associated protein 1
4.397	TGFA	transforming growth factor, alpha
7.555	TGFA	transforming growth factor, alpha
8.736	TGFBR1	transforming growth factor, beta receptor 1
3.287	TKT	transketolase
7.143	TLR3	toll-like receptor 3
2.053	TM2D1	TM2 domain containing 1
2.904	TM7SF2	transmembrane 7 superfamily member 2
2.049	TM7SF3	transmembrane 7 superfamily member 3
2.829	TMEM117	transmembrane protein 117
3.673	TMEM163	transmembrane protein 163
4.054	TMEM163	transmembrane protein 163
6.193	ANO4	anoctamin 4
5.215	TMEM40	transmembrane protein 40
2.162	TMEM63B	transmembrane protein 63B
2.944	TMEM71	transmembrane protein 71
3.111	TMOD1	tropomodulin 1
3.317	TMTC3	transmembrane and tetratricopeptide repeat containing 3
4.558	NEAT1	nuclear paraspeckle assembly transcript 1 (non-protein coding)
2.741	TNFAIP8	tumor necrosis factor, alpha-induced protein 8
2.878	TNFRSF10B	tumor necrosis factor receptor superfamily, member 10b
2.406	TNFRSF14	tumor necrosis factor receptor superfamily, member 14
2.635	TNFRSF25	tumor necrosis factor receptor superfamily, member 25
2.194	TNIP1	TNFAIP3 interacting protein 1
12.350	TP53I3	tumor protein p53 inducible protein 3
19.100	TP53INP1	tumor protein p53 inducible nuclear protein 1
2.196	TP53INP2	tumor protein p53 inducible nuclear protein 2
2.068	TRA2A	transformer 2 alpha homolog (Drosophila)
2.844	TRAF1	TNF receptor-associated factor 1
3.960	TRAF3IP2	TRAF3 interacting protein 2
4.865	TRAF4	TNF receptor-associated factor 4
3.068	TRIAP1	TP53 regulated inhibitor of apoptosis 1
3.893	TRIM22	tripartite motif-containing 22
3.133	TRIM3	tripartite motif-containing 3
2.502	TRIM32	tripartite motif-containing 32
2.208	TRIM38	tripartite motif-containing 38
2.151	TRIM8	tripartite motif-containing 8

Table III. (part 12) Genes upregulated greater than 2-fold after p53 induction

Fold Change	Symbol	Entrez Gene Name
2.949	TRIML2	tripartite motif family-like 2
2.417	TRIOBP	TRIO and F-actin binding protein
2.316	TRIP12	thyroid hormone receptor interactor 12
2.326	TSPAN1	tetraspanin 1
2.253	TSPAN31	tetraspanin 31
3.934	TSPAN9	tetraspanin 9
2.922	TTC18	tetratricopeptide repeat domain 18
2.457	TTYH3	tweety homolog 3 (Drosophila)
3.823	TUSC1	tumor suppressor candidate 1
2.537	UBASH3B	ubiquitin associated and SH3 domain containing, B
2.109	UBE2H	ubiquitin-conjugating enzyme E2H (UBC8 homolog, yeast)
2.424	UBE2J2	ubiquitin-conjugating enzyme E2, J2 (UBC6 homolog, yeast)
2.205	UBR3	ubiquitin protein ligase E3 component n-recognin 3 (putative)
2.039	UNKL	unkempt homolog (Drosophila)-like
2.155	UNQ1887	signal peptide peptidase 3
4.045	UQCC	ubiquinol-cytochrome c reductase complex chaperone
2.200	VAV2	vav 2 guanine nucleotide exchange factor
4.084	VCAN	versican
2.827	VDR	vitamin D (1,25- dihydroxyvitamin D3) receptor
2.574	VIPR1	vasoactive intestinal peptide receptor 1
2.210	VNN1	vanin 1
3.321	VPS13C	vacuolar protein sorting 13 homolog C (S. cerevisiae)
2.226	VPS13D	vacuolar protein sorting 13 homolog D (S. cerevisiae)
2.666	WASF3	WAS protein family, member 3
2.315	WDR1	WD repeat domain 1
2.189	WDR66	WD repeat domain 66
2.605	XCL2	chemokine (C motif) ligand 2
3.796	XPC	xeroderma pigmentosum, complementation group C
2.272	ZBED5	zinc finger, BED-type containing 5
2.077	ZBTB20	zinc finger and BTB domain containing 20
2.809	ZC3H12A	zinc finger CCCH-type containing 12A
3.620	ZFP36L2	zinc finger protein 36, C3H type-like 2
2.083	ZFP90	zinc finger protein 90 homolog (mouse)
2.425	ZFYVE1	zinc finger, FYVE domain containing 1
3.443	ZMAT3	zinc finger, matrin type 3
2.140	ZMYND8	zinc finger, MYND-type containing 8
2.190	ZNF195	zinc finger protein 195
2.997	ZNF37A	zinc finger protein 37A
2.593	ZNF385A	zinc finger protein 385A
2.156	ZNF451	zinc finger protein 451
2.079	ZNF488	zinc finger protein 488
2.345	ZNF493	zinc finger protein 493
2.573	ZNF493	zinc finger protein 493
4.077	ZNF506	zinc finger protein 506
4.752	ZNF540	zinc finger protein 540
3.527	ZNF564	zinc finger protein 564
2.877	ZNF654	zinc finger protein 654
2.271	ZNF667	zinc finger protein 667
3.260	ZNF702	zinc finger protein 702 (pseudogene)
2.338	ZNF708	zinc finger protein 708
3.843	ZNF79	zinc finger protein 79
3.573	ZNFX1	zinc finger, NFX1-type containing 1

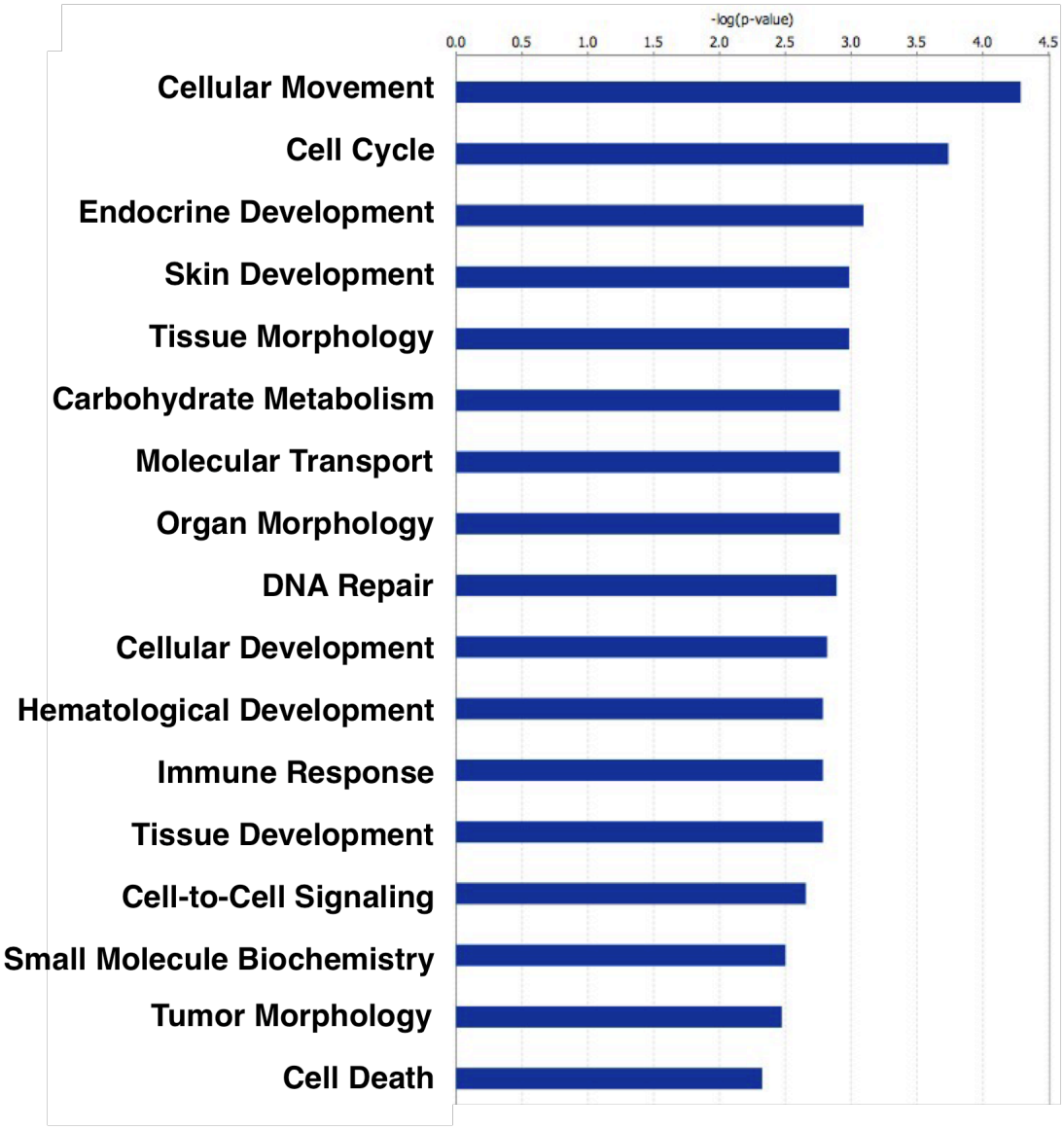

Figure 4. Gene Ontology analysis of putative p53 transcriptional targets The subset of genes generated by our selection criteria was analyzed through Ingenuity Software using Ingenuity Core Analysis to identify roles these genes play in signaling and metabolic pathways as well as cellular and disease processes. The top categories are presented and ordered from most to least significant.

These cells were exposed to ionizing radiation (8 Gy) and RNA was harvested 24 h later. We found that 82.5% of the putative transcriptional targets identified using our genomic analyses were in fact regulated in a p53-dependent manner (Figure 5).

Mathematical Models

A limiting factor of using microarray based data to analyze target gene expression is that the datasets often only include one time point. Clustering methods have attempted to resolve this issue by correlating similar gene expression profiles to suggest that a group of genes with similar transcript profiles over a timecourse are likely regulated by the same transcription factor. The dynamic mathematical model incorporates RNA production and degradation terms and prior biological knowledge, using a set of previously established target genes, and determines the activity of that transcription factor from microarray data (Barenco *et al.*, 2006). This algorithm ultimately results in a tool that allows for the calculation of confidence intervals for each potential transcriptional target (Barenco *et al.*, 2006).

To apply the dynamic mathematical algorithm, the MOLT4 human leukemia cell line was irradiated to activate endogenous p53 activity for gene expression analysis (Barenco *et al.*, 2006). A training set consisting of five well-known target genes including DDB2, p21, Sesn1, BIK, and TNFRSF10b was used to derive the p53 activity profile that drives the dynamic

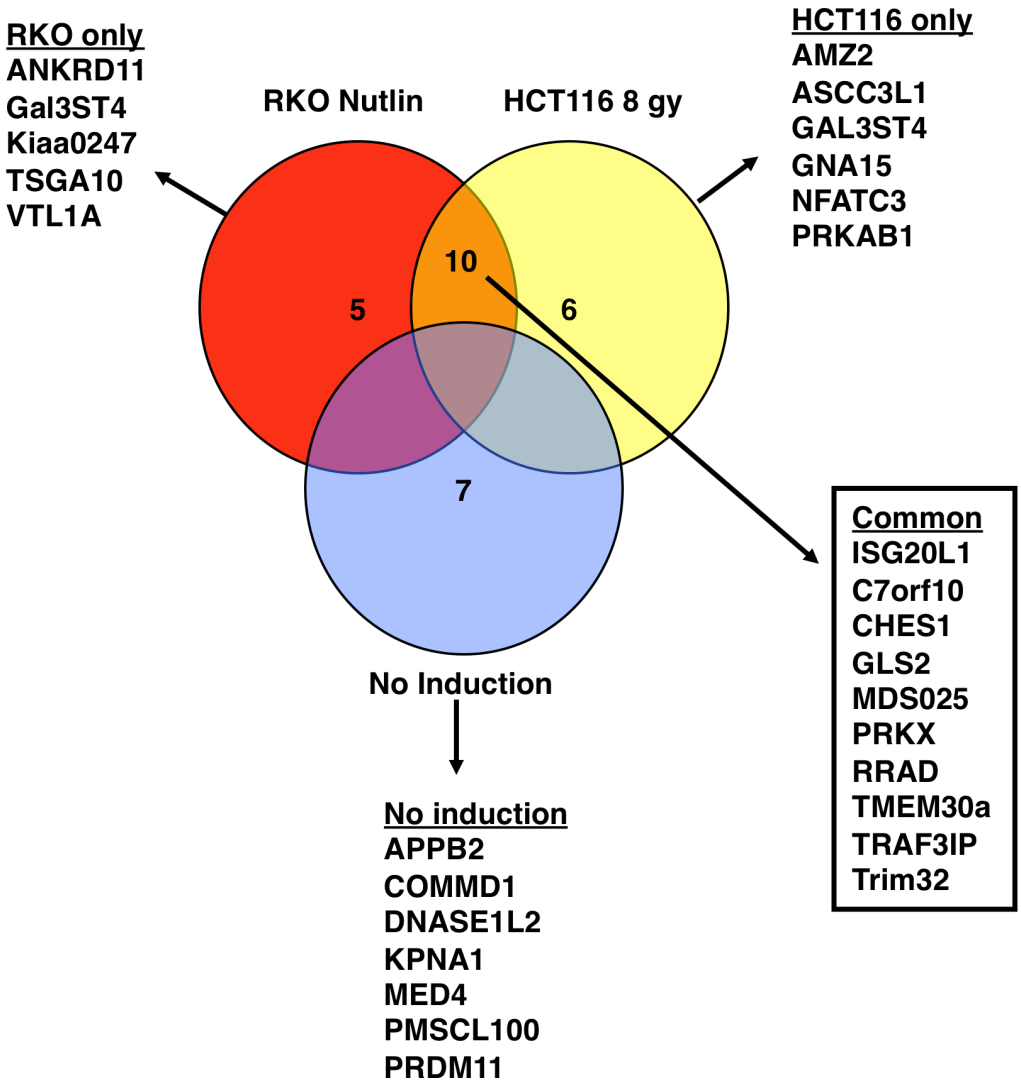

Figure 5. p53 transcriptional regulation of 40 putative target genes
Quantitative real-time PCR analysis was performed after RNA isolations from either RKO WT and E6 (p53 inactivated) cell lines treated with Nutlin (10 μM) or from the p53 isogenically matched HCT116 cells harvested 24 h after treatment with 8 γ ionizing radiation. We validated p53-dependent regulation of 82.5% of the putative transcriptional targets identified. Replicates were performed by Chris Pendleton

mathematical algorithm. Once applied to gene expression microarray data, a list of the top 50 genes transcriptionally regulated by p53 was published and ranked according to a sensitivity score. Additionally, to verify p53-dependent regulation gene expression microarray was performed on RNA harvested from MOLT4 cells in which p53 was knocked down by siRNA targeting. Of the p53 target genes predicted by the mathematical modeling algorithm, 90% were validated as being regulated in a p53-dependent manner based on their sensitivity score to siRNA targeting p53. Twenty-five of the top 50 putative p53 targets were unpublished at the time the algorithm was publicly released. However, since the generation of this ranked list in 2006, eight of the remaining 25 have since been published as verified p53 targets validating this dynamic mathematical modeling.

p53 Family Overlay

Work performed by our group shows that despite differences in cell lines and methodologies, comparison of p53 family ChIP and gene expression microarray datasets showed considerable overlap of putative transcriptional targets amongst the family members (Wei *et al.*, 2006; Yang *et al.*, 2006, Rosenbluth et al, personal communication). To begin a p53 family member comparison a comprehensive dataset for each p53 family member was selected. The p53 genome-wide, ChIP-PET screen described above (Wei *et al.*, 2006), a p63 genome-wide, ChIP-seq (Yang *et al.*, 2006) and a whole genome p73 ChIP dataset (Rosenbluth, personal communication) were chosen. Each dataset was

generated in a different cell line under different conditions. For p53, ChIP-PET methods used in HCT116 cells after treatment with 5-FU identified 1766 sites (Wei *et al.*, 2006). The p63 dataset was generated from a ME180 cervical carcinoma cell line with or without actinomycin D treatment and 5800 binding sites were found (Yang *et al.*, 2006). The p73 dataset was generated in the Rh30 cell line after treatment with rapamycin and found 7678 binding sites in control compared to 8165 binding sites of p73 after treatment (Rosenbluth, personal communication).

We further advanced the "p53-focused" collection of transcriptional targets with additional cross-comparisons using p63 and p73 ChIP and gene expression microarray analyses performed in our laboratory. Unlike the previous overlays where only ChIP results were described, we combined ChIP and gene expression analysis to identify putative targets that were bound and regulated by the family members. To further analyze with our set of putative p53 transcriptional targets, we used p73 and p63 gene expression analyses that were performed in our laboratory for comparison. Both ChIP and gene expression microarray analyses were performed with DNA and RNA, respectively, that was generated from primary cultures of human mammary (HMEC), skin (NHEK), and prostate epithelial cells (HPrEC) expressing nonsilencing or p63 siRNA. A similar approach was taken to identify novel targets of p73 by combining ChIP and gene expression microarray in H1299 ectopically expressing TAp73β as well as in the Rh30 cells where endogenous p73 activity was evaluated in cells grown in the

presence or absence of the mTOR inhibitor, rapamycin (Rosenbluth et al, personal communication).

A list of approximately 212 genes resulted from overlapping the three p53 family ChIP datasets described above with microarray gene expression datasets generated from p53-inducible model systems. Approximately 23% (48 genes) of these genes at the intersection of the ChIP and gene expression datasets have been validated and published previously as direct p53 transcriptional targets. Further, after overlaying these genes with the p63 and p73 genomic ChIP and gene expression datasets described above, we found that six genes were bound by all three family members; 17 genes were bound by p53 and p63; and an even greater number of 40 genes were bound by p53 and p73 (Figure 6). Of the 149 genes uniquely regulated by p53, 31 have been previously published and linked to p53 signaling.

Discussion

Using a combination of gene expression microarray analyses, ChIP, and mathematical modeling methods we identified putative p53 transcriptional targets for further functional characterization in the p53 signaling pathway. Our subset of p53 putative transcriptional targets has been further validated since its compilation in 2006. Our group and others have published many genes of functional biological significance from our list of p53 targets including RPS27L,

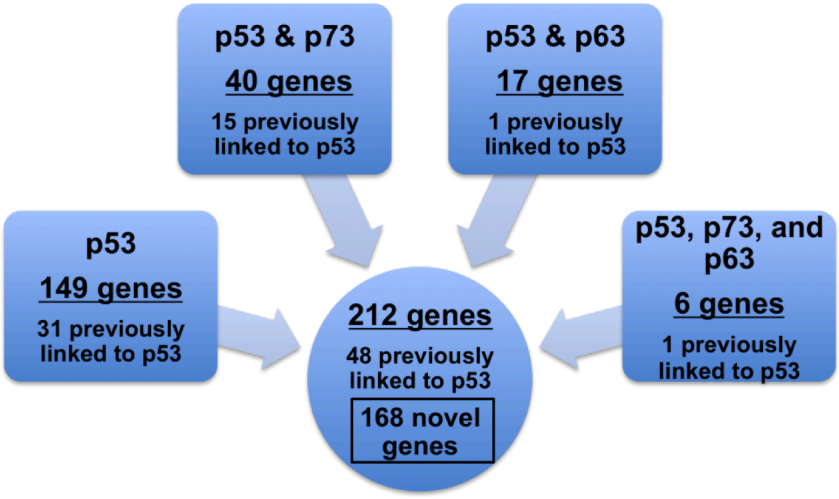

Figure 6. Overlay of putative p53 family transcriptional targets The overlay of putative p53 transcriptional targets identified as being common to a p53 genome-wide ChIP and gene expression analysis dataset yielded 212 putative target genes, 48 of which were previously published. This subset of p53 transcriptional targets was then compared with similar p63 and p73 datasets. ChIP and microarray analysis comparing control versus knockdown of p63 in three different normal cell lines including HMEC, NHEK, and human prostate epithelial cell line (HPrEC) {Barton et al, under review; Barbieri et al, 2006}. Similarly, ChIP and gene expression analysis for p73 was performed in H1299 ectopically expressing TAp73β as well as in the Rh30 cells where endogenous p73 was evaluated with and without the activating agent rapamycin (Rosenbluth et al, under review).

GLS2, PRKAB1, LIF, TOB1, PTP4A1/ PRL-1, COMMD1, ANKRD11, LASP1, STX6, and ISG20L1.

Endothelin-2 (EDN2) is one of only five putative p53 target genes, along with p21, that was identified in common with the ChIP-yeast, ChIP-PET, and inducible-p53 gene expression microarray datasets. Endothelin-1 and -3 are characterized as putative vasoactive peptides (Yanagisawa *et al.*, 1988) and chemoattractants during tumor angiogenesis and migration (Stiles *et al.*, 1997) as well as melanocyte development and melanoma (Eberle *et al.*, 1999). Previous work in our laboratory identified a strong p53-consensus binding site in EDN2 located within 2 kb of exon 1 and EDN2 was regulated in a p53-dependent manner (Hearnes *et al.*, 2005). In addition, we found that EDN2 can also be regulated by both p63 and p73, depending on cellular context. A significant increase in EDN2 levels occurred during epidermal differentiation (Kotake-Nara and Saida, 2006). In the lung cancer cell line H1299, that lacks expression of the p53 family members, ectopic TAp63γ expression led to an approximately 22-fold elevation of EDN2 as determined by qRT-PCR. Corroborating evidence that p63 contributes to EDN2 regulation was found in HMECs and human prostate epithelial cells (HPrECs) when suppression of p63, using an adenovirus targeting the DNA binding domain of p63, caused a 60% reduction in the expression levels of EDN2.

The unnamed protein KIAA0247 was identified as a putative p53 transcriptional target in each of the ChIP datasets mentioned above as well as

the p63 and p73 ChIP datasets generated in our laboratory. KIAA0247 was induced greater than 2-fold in our H1299 p53 inducible microarray gene expression dataset and ranked as one of the top 50 putative p53 targets by the mathematical algorithms. Induction of p73 expression in the Rh30 cell line treated or not with rapamycin, resulted in a greater than 15-fold increase in binding of p73 at the KIAA0247 consensus binding site (Rosenbluth et al., not yet published). This gene maps to chromosome 14q24.1 and has an open reading frame that encodes a putative 303 amino acid protein of a predicted molecular weight of 35 kDa. Functional domain analysis demonstrated the presence of one short consensus repeat domain (CCP/sushi/SCR region). The consensus repeat domain is commonly found in complement genes, often localizing to the cell surface, and involved in protein-protein interactions. In a few instances, the presence of this domain is necessary for apoptotic activation (e.g. IL-15R and Drs) (Tambe *et al.*, 2004; Wei *et al.*, 2001). Interestingly, KIAA0247 was identified as an induced gene in a p53-temperature sensitive model (Robinson *et al.*, 2003). The authors claimed that KIAA0247 has an AVPI-like motif. AVPI motifs, found in Smac/Diablo proteins, can compete for binding to the BIR3 domains of XIAPs thereby releasing bound caspases and inducing apoptosis (Sun *et al.*, 2007). The identification of KIAA0247 in an expression dataset where apoptosis was induced in a p53-dependent manner is further suggestive of its function in cell death (Robles *et al.*, 2001). Though the potential role of KIAA0247 in disease is not yet known, this gene has been found in both lung and

ovarian cancer gene expression signatures as a marker of prognosis and metastasis, respectively (Dressman *et al.*, 2007; Zhang *et al.*, 2007). It will be of interest to determine if KIAA0247 plays a role in cell death, and if the mechanism occurs as suggested by its AVPI motif, where KIAA0247 may bind XIAP thereby releasing caspase-9.

The gene ISG20L1/FLJ12484/AEN was identified in the ChIP-yeast selection method with a p53 consensus binding site located within one kb of the transcriptional start site (Hearnes *et al.*, 2005). This same p53 consensus site was identified in the ChIP-PET sequencing analysis with three overlapping PETs indicating increased likelihood of p53 binding (Wei *et al.*, 2006), and is the most highly ranked p53 consensus binding site found using the computer algorithm p53MH (Hoh *et al.*, 2002). ISG20L1 is transcriptionally upregulated across numerous cell types including lung, breast, hematopoietic, and colon cell lines after treatment with genotoxic stresses such as ionizing radiation, as well as after encountering the inflammatory stresses NO, H_2O_2, and hypoxia (Barenco *et al.*, 2006; Hearnes *et al.*, 2005; Staib *et al.*, 2005; Sun *et al.*, 2005; Wei *et al.*, 2006). The functional role of IGS20L1 downstream of the p53 family will be further explored in Chapter IV of this dissertation.

The identification of p53 transcriptional targets is central to further understanding of the functional signaling downstream of this tumor suppressor gene in both normal and disease states. We have used a number of criteria to create a subset of p53 putative transcriptional targets for further functional

characterization including presence in ChIP datasets, gene expression analyses, and ranking in p53 mathematical algorithms. Functional characterization of one of these target genes, ISG20L1, is presented in detail in Chapter IV of this dissertation.

CHAPTER IV

ISG20L1 IS A P53 FAMILY TARGET GENE THAT MODULATES GENOTOXIC STRESS-INDUCED AUTOPHAGY

Introduction

p53 can regulate autophagy in both a transcriptionally-dependent and -independent manner (Crighton *et al.*, 2006; Feng *et al.*, 2007). Autophagy is a mechanism used by cells to maintain metabolic homeostasis in the biological context of starvation (Komatsu *et al.*, 2005). During starvation, cells form double membrane autophagosomes that engulf cellular contents for degradation and these vesicles recycle the basic metabolic components for consumption (Levine, 2005). Although originally thought to be primarily induced to promote cell survival during starvation, autophagy also occurs after various forms of genotoxic stress and plays a role in cell death (Green and Chipuk, 2006; Kang *et al.*, 2007; Scott *et al.*, 2007; Shimizu *et al.*, 2004). p53 has a dual role in autophagy and the molecular mechanisms are only now being discerned (reviewed in (Green and Kroemer, 2009; Levine and Abrams, 2008)). Basal levels of cytoplasmic p53 repress autophagy in a transcriptionally-independent manner (Tasdemir *et al.*, 2008). Depletion of p53 or pharmacological inhibition using pifithrin-α causes induction of autophagy (Tasdemir *et al.*, 2008). The transcriptional dependent mechanisms of nuclear p53 are more widely described in connection of p53 and autophagy. Nuclear p53 stimulates autophagy through transactivation of target

genes such as Sestrins, TSC2, and DRAM (damage-regulated autophagy modulator) (reviewed in (Vousden and Ryan, 2009)). Under conditions of genotoxic stress such as ionizing radiation or camptothecin treatment, p53 upregulates the AMPK activators Sestrin1 and Sestrin2 that will ultimately induce autophagy through the inhibition of mTOR (Braunstein *et al.*, 2009; Budanov and Karin, 2008). Upregulated by various stress signals including DNA damage, DRAM is a transcriptional target of p53 that is lysosomal in location and required for p53-induced autophagy, although the mechanism by which DRAM regulates autophagy is currently unknown (Crighton *et al.*, 2006).

p63 and p73 are two p53 homologs that share similar structure and have both unique and coordinate roles during development and tumorigenesis (Murray-Zmijewski *et al.*, 2006). The signaling upstream of each p53 family member is dependent on cellular context and various regulatory mechanisms [reviewed in (Rosenbluth and Pietenpol, 2008)]. Recently, work from our laboratory has shown that in addition to the interplay of mTOR and p53, inhibition of mTOR activates p73 and results in p73-dependent modulation of genes involved in metabolism and autophagy (Rosenbluth and Pietenpol, 2008; Rosenbluth and Pietenpol, 2009). Though p73 also transcriptionally regulates the p53 target gene DRAM, p73-dependent autophagy does not require DRAM (Crighton *et al.*, 2007).

As presented in Chapter III, we have identified numerous, novel candidate p53 target genes by overlaying ChIP and gene expression datasets (Hearnes *et*

al., 2005; Schavolt and Pietenpol, 2007). Of interest was the discovery of ISG20L1, a gene that was named due to its significant similarity with ISG20L2, a nucleolar protein that functions in the processing of the 5.8S rRNA (Coute *et al.*, 2008). To determine the role that ISG20L1 plays in p53 family signaling, we generated an ISG20L1-specific antibody, analyzed ISG20L1 regulation by all three members of the p53 family, and functionally linked ISG20L1 to genotoxic stress-induced autophagy.

Results

ISG20L1 Antibody Production

The human ISG20L1 gene is 3.1 kb and evolutionarily conserved with 72% identity to *M. musculus*. We generated a rabbit polyclonal antibody to the human ISG20L1 protein (UniProt Q8WTP8) using a 15 amino acid sequence (HGSRGGAREAQDRRN) located at the C-terminus of the protein outside of the exonuclease III domain; database searching confirmed that this peptide is unique to ISG20L1. We performed Western analyses in conjunction with gene overexpression and knockdown assays, to determine that our newly developed antibody could specifically identify a protein of the predicted molecular weight (~37 kD). For overexpression analyses, protein lysates were prepared from H1299 cells engineered to ectopically express FLAG-tagged human ISG20L1. RNA knockdown experiments were performed in H460 cells by reverse transfecting siRNAs directed against ISG20L1 and subsequently treating with

ionizing radiation to upregulate endogenous ISG20L1 protein levels (Figure 7a). The antibody we produced had specificity for ISG20L1, the levels of which were significantly reduced after siRNA knockdown or enhanced with ectopic expression of ISG20L1, respectively (Figure 7a). These results are the first demonstration of detection and regulation of endogenous ISG20L1 protein.

Having confirmed antibody specificity, we analyzed the cellular localization of ISG20L1 in H1299 cells ectopically expressing a FLAG-tagged ISG20L1. Immunofluorescence analyses showed nuclear localization of ectopically expressed ISG20L1, similar to the staining pattern seen using a FLAG antibody (Figure 7b). Merging nuclear DAPI staining with ISG20L1-specific staining, showed ISG20L1 localizes to a region of the nucleus having decreased density identified as the nucleolus and higher magnification analyses confirm increased intensity at perinucleolar regions (Figure 7b). Although detectable by Western, we were unable to identify endogenous ISG20L1 using immunofluorescence.

p53 Family Regulation of ISG20L1

To analyze p53 regulation of ISG20L1 we used primary cultures of normal human keratinocytes (NHEKs), a model system with intact p53 signaling (Flatt *et al.*, 1998; Schavolt and Pietenpol, 2007). NHEKs were infected with control

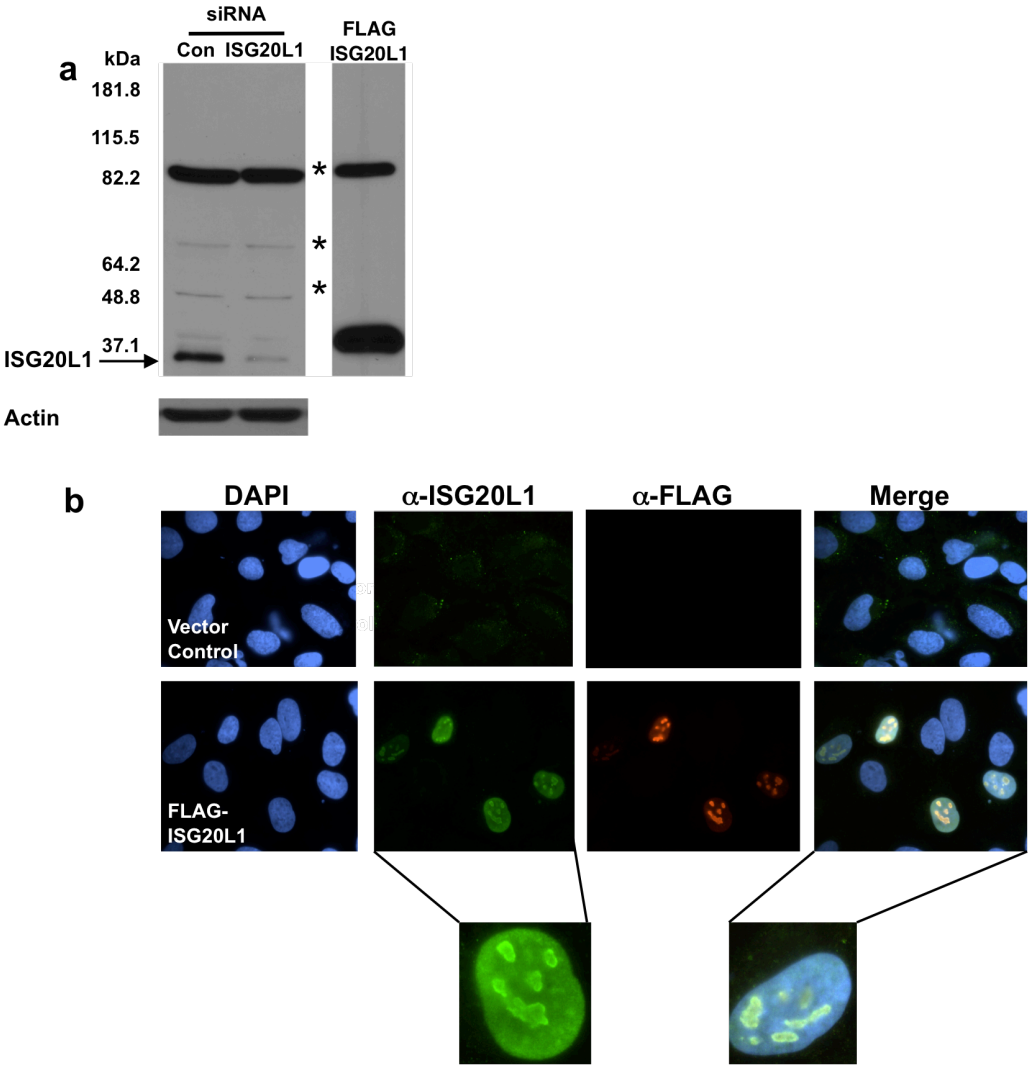

Figure 7. ISG20L1 antibody production and protein analysis
(a) Western analyses demonstrated the polyclonal antibody generated was able to detect endogenous ISG20L1. H460 cells were reverse transfected with Dharmacon siRNA control (Con) or Dharmacon ISG20L1 Ontarget Plus pool and grown for 72 h, at which point the cultures were treated with 8 Gy ionizing radiation and harvested 24 h after treatment (left panel). Ectopic expression of a FLAG-ISG20L1 detected by our ISG20L1 antibody serves as further positive control. Asterisks mark nonspecific bands and the arrow indicates ISG20L1. Western is representative of three independent experiments. **(b)** ISG20L1 is localized to the nucleolus and perinucleolar region. RKO cells were transfected with either empty vector (Vector Control) or FLAG-ISG20L1 and immunofluorescence analysis was performed 24 h later using a FLAG antibody or the ISG20L1 antibody and the nuclei co-stained with DAPI. Views of individual and merged stainings are shown. Insets are further magnification of individual cells to highlight the perinucleolar staining of ISG20L1. Immunofluorescence was performed on four independent transfections using ISG20L1 and FLAG antibodies.

shRNA or shRNA targeting p53 and exposed for 6 h to cisplatin to elevate p53 activity. Western analysis showed that both p53 and ISG20L1 protein levels were elevated after cisplatin treatment and this increase was primarily p53-dependent as the shRNA targeting p53 significantly decreased the cisplatin-induced elevation in p53 and ISG20L1 protein levels (Figure 8). We hypothesize that residual ISG20L1 expression was due to cisplatin-mediated elevation of TAp73 activity or protein as previously shown (Agami *et al.*, 1999; Gong *et al.*, 1999; Lapi *et al.*, 2006; Yuan *et al.*, 1999). However, p73 protein is difficult to detect in primary cultures of normal human keratinocytes, likely due to the low level of expression in normal cells (Schavolt and Pietenpol, 2007).

Given the residual expression of ISG20L1 in p53-depleted keratinocytes (Figure 8) and the overlapping binding and activity of p53 family members at many regulatory regions in the genome, we hypothesized that ISG20L1 is also regulated by p63 and p73. To test this hypothesis, we transfected 293FT cells with plasmids encoding the transcriptionally active isoforms of the p53 family (p53, TAp73β, and TAp63γ) as well as the transcriptional repressor ΔNp63α. These cells express low levels of TAp73, non-detectable p63, and wild-type p53 that is stabilized and inactivated by association with E1A and large T antigen (see pCEP4 control lane of Figure 9b). Twenty-four h after transfection, we isolated RNA and protein and analyzed ISG20L1 by qRT- PCR and Western, respectively. ISG20L1 levels were increased approximately 2-fold or more by

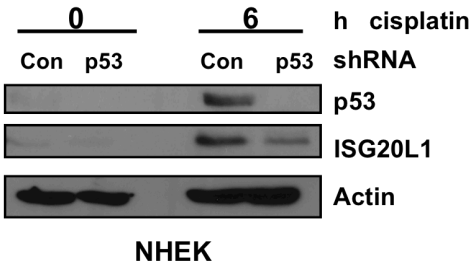

Figure 8. p53-dependent regulation of ISG20L1
NHEK cells were infected with shRNA lentiviral constructs expressing either shRNA to p53 or a scrambled shRNA (Con) and then treated with cisplatin (5 µg/mL) for 6 h. Protein lysates were prepared and analyzed for p53, ISG20L1, and actin. The Western blot is representative of three independent experiments. Christopher Barton performed replicates of this experiment.

p53, TAp73β, and TAp63γ while ΔNp63α expression decreased levels of ISG20L1 as seen at both the mRNA and protein level (Figure 9a and 9b).

Noting the elevation of ISG20L1 after TAp73 expression, we analyzed the ability of endogenous TAp73 to regulate ISG20L1 using the Rh30 rhabdomyosarcoma cell line. Rh30 cells do not express p63 and contain mutant p53, thereby allowing us to investigate the endogenous regulation of ISG20L1 solely by p73. We treated cells with paclitaxel or cisplatin, two agents known to increase p73 activity (Leong *et al.*, 2007; Oh *et al.*, 2008), and observed an elevation in TAp73 protein levels that were accompanied by an increase in ISG20L1 expression (Figure 10a). Elevation of ISG20L1 was TAp73-dependent as shRNA depletion of TAp73 eliminated ISG20L1 expression after treatment (Figure 10a, right panel). To verify p73-dependent regulation was not cell-type or damage specific, we infected MDA-MB-231, cells that are also lacking p63 and mutant for p53, with a shRNA lentivirus targeting p73 and treated with rapamycin, an agent known to elevate p73 activity in this cell line (Rosenbluth *et al.*, 2008). Rapamycin is an inhibitor of the TOR pathway that regulates cell growth and cell cycle progression based on nutrient-dependent signaling and thus rapamycin has similar effects as nutrient starvation (Peng *et al.*, 2002). ISG20L1 RNA levels were decreased ~50% by RNAi knockdown of p73 and rapamycin treatment resulted in a greater than 2-fold induction in ISG20L1 expression that was abrogated with p73 knockdown (Figure 10b). Thus, ISG20L1 can be modulated

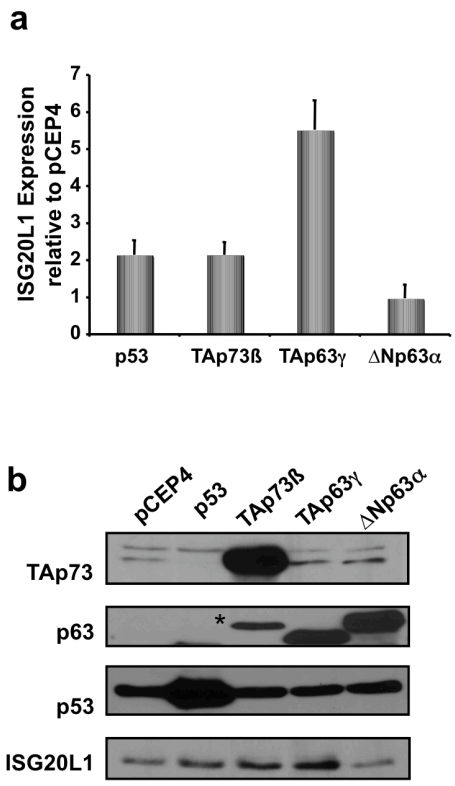

Figure 9. ISG20L1 is regulated by the p53 family

(a) 293FT cells were transfected with vector control (pCEP4) or the indicated p53 family members for 24 h and then analyzed by qRT-PCR for ISG20L1. Results represent 3 independent experiments and error bars show standard error. Experiment was performed by Clayton Marshall **(b)** Experiment was performed as in (a) and Western analysis performed. Results are representative of 3 independent experiments. *The p63 antibody used cross-reacts with p73 due to sequence similarity in the region containing the epitope recognized by the antibody.

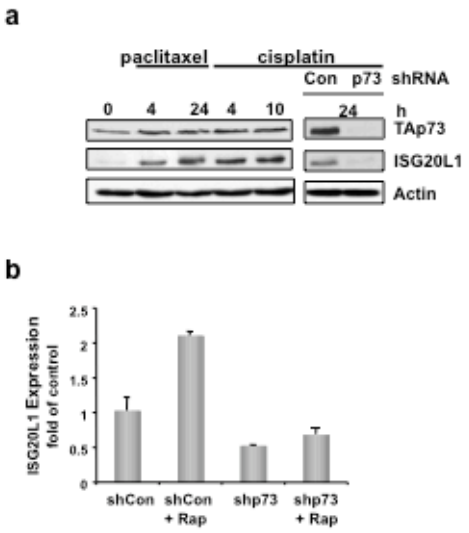

Figure 10. ISG20L1 is regulated by endogenous p73

(a) p73 regulates ISG20L1, seen in Rh30 cells treated with paclitaxel (5 nM) and cisplatin (5 µg/mL) for times indicated. Right panel, Rh30 cells were infected with a pSico vector that expresses control virus (Con) or shRNA targeting all isoforms of p73. Results are representative of 3 independent experiments. **(b)** MDA-MB-231 cells were infected as above. Forty-eight h later, cells were treated with rapamycin (40 nM) and RNA harvested for real-time analyses 24 h after treatment. Results represent 3 independent experiments and error bars show standard error. Experiment was performed by Jennifer Rosenbluth

by various forms of cell stress (genotoxic and metabolic), and in the absence of p53 its expression is dependent on other p53 family members.

Next we explored the ability of the p53 family members to bind the ISG20L1 promoter region. Previous findings suggest that the p53 family members have similar transcription factor binding domains, but p53 and p63 have different affinities due to slight differences in consensus site sequence composition and co-factor binding sites present in the promoter regions of regulated genes (Ortt and Sinha, 2006; Perez *et al.*, 2007; Shikama *et al.*, 1999; Zhu *et al.*, 1998). The p53 binding site discovered by our previous ChIP-based screen, CCACATGCCC-0-GGGCAAGCCC, was located approximately 450 bp upstream of the ISG20L1 transcriptional start site and matches the p53 canonical binding site at 18 of 20 base pairs, with no spacer in the palindrome (Hearnes *et al.*, 2005). To determine if p53 and p63 bind and regulate ISG20L1 at the same promoter region, we used human mammary epithelial cells (HMECs) that express p53 and p63 at levels sufficient for chromatin analyses (Perez *et al.*, 2007). HMECs were chemically crosslinked under control and cisplatin-treated conditions, the latter agent can regulate the p53 signaling axis (Fritsche *et al.*, 1993; Leong *et al.*, 2007). Chromatin was prepared and immunoprecipitated with antibodies to p53, p53-Ser15, p63, and a negative control antibody against a non-DNA binding protein (Venter *et al.*). Primers were used to amplify the region of the ISG20L1 gene previously reported to contain the p53 binding site (Hearnes *et al.*, 2005). Chromatin immunoprecipitation analysis (ChIP) showed increased

binding of p53 and p53-Ser15 after cisplatin treatment, and p63 bound the promoter region of ISG20L1 under both control and cisplatin treated conditions (Figure 11a). These data indicate that both family members cooperate to regulate ISG20L1 expression.

Given that HMECs do not express levels of p73 sufficient for chromatin analysis we performed p73 ChIP in the Rh30 cells to assess p73 binding levels at the ISG20L1 promoter in response to rapamycin treatment. After rapamycin treatment, p73 binding at the p53 consensus binding site in the ISG20L1 promoter increased ~15-fold as compared to a vehicle only-treated control (Figure 11b). Collectively, these data show that all three p53 family members can bind to the promoter region of ISG20L1 and regulate its gene expression.

ISG20L1 and Cell Death

Shortly after our discovery of ISG20L1 as a p53 target (Hearnes *et al.*, 2005), ISG20L1 was reported to have exonuclease function *in vitro* (Lee *et al.*, 2005) prompting us to determine if it played a role in DNA laddering during the execution phase of apoptosis. Using siRNA knockdown, we decreased ISG20L1 levels in RKO cells and treated with 5-fluorouracil (5-FU) to induce apoptosis. Neither knockdown of ISG20L1 nor 5-FU treatment after knockdown affected the onset or extent of apoptosis as measured by analyses of PARP and caspase-3 cleavage, sub-G1 content quantified by flow cytometry, and DNA laddering

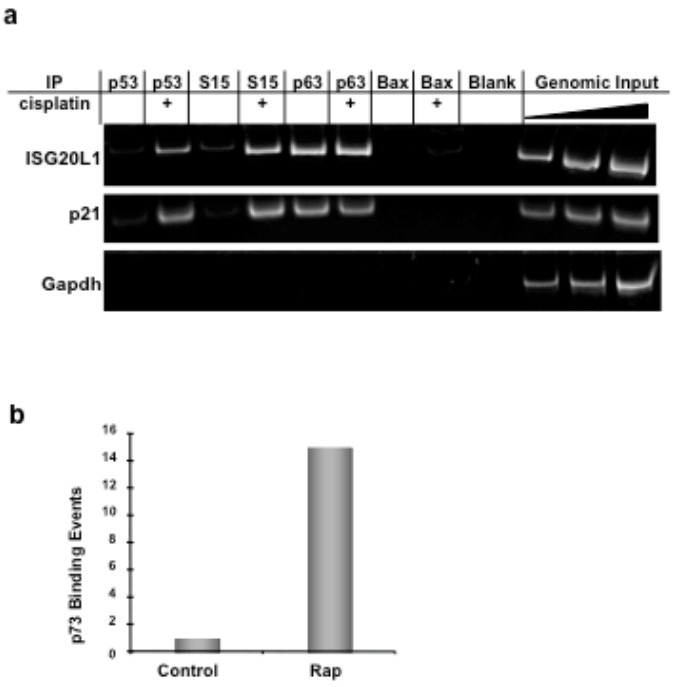

Figure 11. ISG20L1 is directly bound by the p53 family

(a) Antibodies specific to p53, p53-Ser15 (S15), p63, and Bax (negative control) were used for ChIP analysis of the ISG20L1 promoter under control and cisplatin-treated (24 h, 10 µg/mL) conditions in HMECs. The p53 binding site in the p21 promoter and a region containing no p53 binding site in the GAPDH promoter serve as positive and negative controls, respectively. Experiment is representative of duplicate independent templates. This experiment was performed by Deb Mays. **(b)** ChIP analysis of p73 binding to the ISG20L1 promoter in Rh30 cells treated with rapamycin (40 nM) for 24 h. This experiment was performed by Deb Mays and Jennifer Rosenbluth.

(Figure 12a and 12b). These data suggest that ISG20L1 does not play a role in the execution phase of apoptosis.

To determine if ISG20L1 plays a role in genotoxic stress-induced autophagy we analyzed the effect of ISG20L1 modulation (ectopic expression or knockdown) in RKO cells after etoposide, a treatment that induces autophagy. During autophagy an ubiquitin-like signaling cascade is initiated that results in cleavage of a protein essential for autophagy, microtubule associated-protein 1 light chain 3 (MAP1LC3) (reviewed in (Cecconi and Levine, 2008)). After cleavage and post-translational modification (lipidation), MAP1LC3 (LC3-II) associates with autophagosomal membranes (Kabeya *et al.*, 2000), and this modified form of LC3-II is used as a reliable molecular marker of autophagy (Klionsky *et al.*, 2008). We reverse transfected RKO cells with control or ISG20L1 siRNA and treated with etoposide. Etoposide treatment resulted in a considerable increase in both ISG20L1 and LC3-II protein levels (Figure 13a). Robust knockdown of ISG20L1 resulted in a significant reduction in LC3-II as measured by Western (Figure 13a, right panel) and an ~70% reduction in LC3 positive cells as measured by immunohistochemistry (IHC) using an antibody that detects endogenous, cleaved LC3 (Figure 13b and 13c). To assess if knockdown of ISG20L1 was modulating autophagy flux, we added protease inhibitors, E64d and pepstatin A, to inhibit lysosomal degradation and LC3-II turnover (Klionsky *et al.*, 2008). RKO cells were treated with etoposide and lysosomal inhibitors for 8 h, three days after reverse transfection with control or

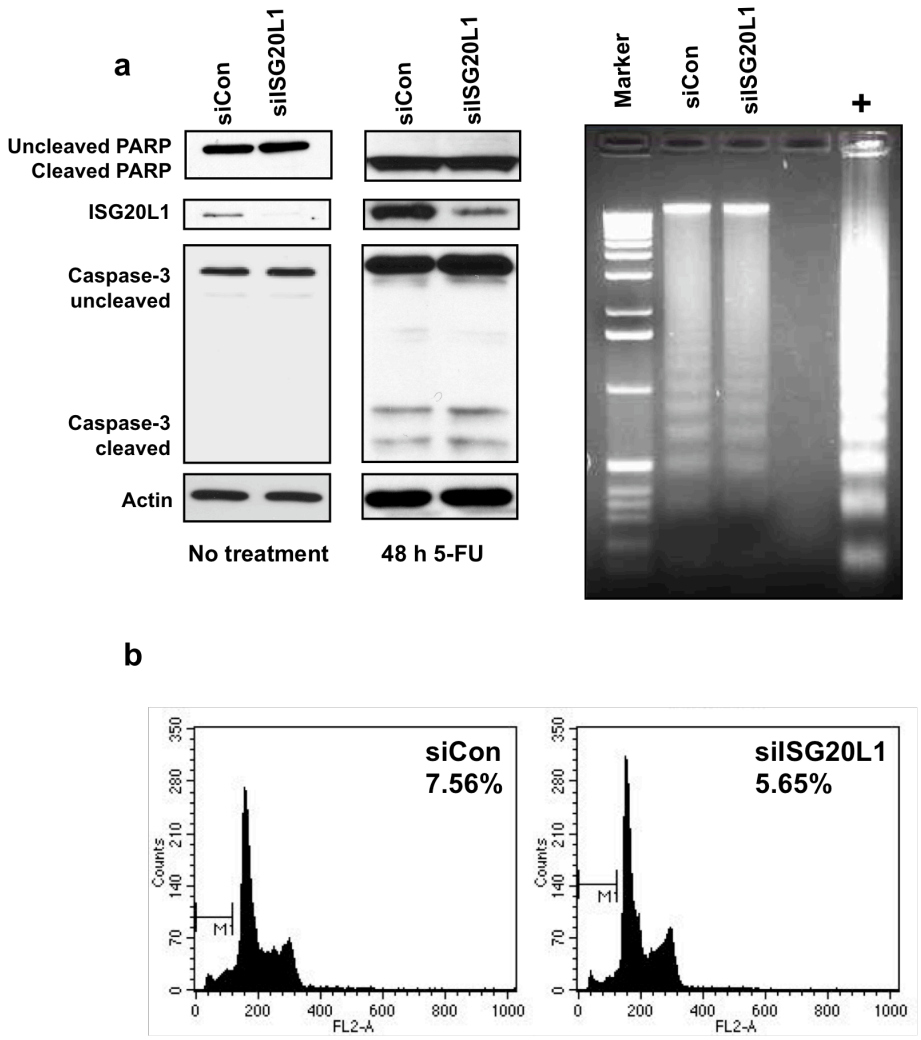

Figure 12. Knockdown of ISG20L1 does not affect 5-FU-induced apoptotic cell death

(a) RKO colon cancer cells were reverse transfected with control (siCon) or ISG20L1 targeting siRNA. Three days after transfection the cells were treated with 5-FU for 48 h and harvested for Western analysis. The Western blot (left and middle panel) is representative of three independent experiments and shows no change in caspase-3 or PARP cleavage after knockdown of ISG20L1 at either baseline 0 h, where there is low level, basal ISG20L1 expression or after 5-FU treatment. The right panel shows DNA laddering as observed on an ethidium bromide-stained gel, a characteristic marker of apoptosis, from the same samples as above treated with 5-FU. No difference in DNA laddering was evident (lanes are loaded evenly for DNA content). Positive control (+) was obtained from the Roche DNA laddering kit and represent U937 cells treated with camptothecin. Seema Sinha performed replicates of this experiment. **(b)** Flow cytometric analysis was performed on the samples described above at 48 h after 5-FU treatment and sub-G_1 percentage was calculated.

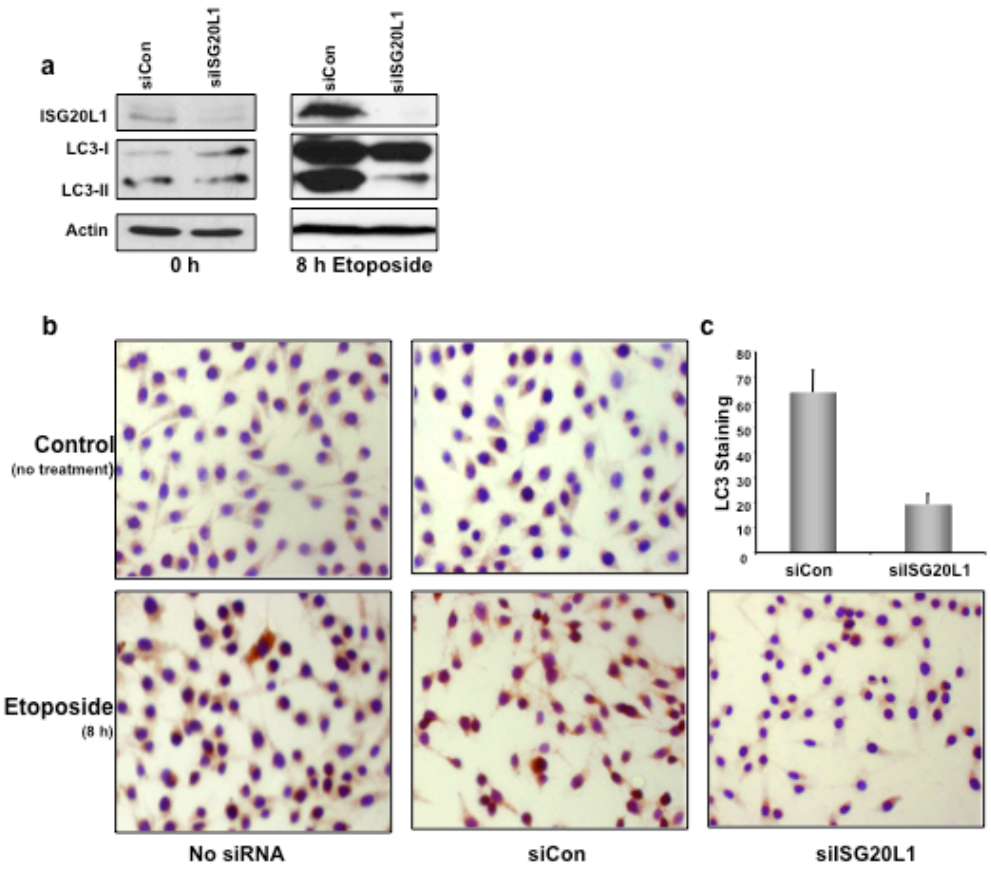

Figure 13. Knockdown of ISG20L1 decreases LC3-II

(a) RKO cells were reverse transfected with control or siISG20L1 and then treated with etoposide (20 μM) for 8 h before harvesting for Western analysis of ISG20L1, LC3, and actin. Western blot is representative of five independent experiments. **(b)** As performed in (b) knockdown of ISG20L1 suppresses autophagy as measured by IHC using an antibody specific to the cleaved form of LC3. IHC analysis of LC3 was performed in RKO cells induced to undergo autophagy after treatment with etoposide (20 μM). Controls include no siRNA and transfection of siRNA alone. **(c)** Results from (c) were quantified by counting number of cells staining positive for LC3 (dark brown) and dividing by the total number of cells (purple nuclear stain) to attain % LC3. Results are representative of 3 independent experiments and error bars represent standard deviation.

ISG20L1 siRNA. Under these conditions, knockdown of ISG20L1 decreased LC3-II levels and thus autophagic flux (Figure 14a). We investigated if ectopic expression of ISG20L1 affected autophagy and transfected RKO cells with vector control (pCEP4) or pCEP4 expressing ISG20L1. RKO cells ectopically expressing ISG20L1 showed an increase in LC3-II by Western analysis (Figure 14b).

To verify these results were not cell type-, damage-, or assay-specific U2OS cells were transfected with control siRNA or three unique siRNAs that target ISG20L1 with varying degrees of knockdown. After treatment with 5-FU, LC3-II levels decreased in a dose-dependent manner relative to levels of ISG20L1 knockdown (Figure 15). We further determined that knockdown of ISG20L1 in U2OS cells treated with 5-FU does not alter cell cycle distribution (Figure 16).

Autophagy was first studied and quantified using electron microscopic (EM) detection of autophagosomes (Klionsky *et al.*, 2008; Mizushima, 2004; Mizushima *et al.*). To verify that the modulation of LC3-II observed in 5-FU treated U2OS cells was a reliable marker of autophagy, we performed EM on parallel cultures of U2OS cells expressing either control siRNA or the siISG20L1-1 and representative electron micrographs are shown (Figure 17). Morphometric analysis (Swanlund *et al.*; Yla-Anttila *et al.*, 2009) showed an approximately 6-fold decrease in the percentage of autophagic vacuole volume fraction after

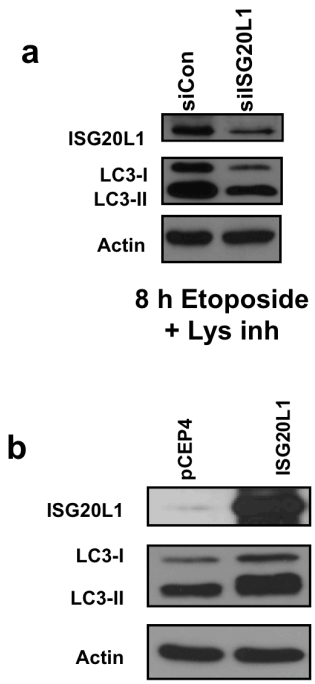

Figure 14. ISG20L1 expression modulates autophagy
(a) To measure autophagy flux, RKO cells were reverse transfected with control or siISG20L1 and treated with etoposide (20 μM) and lysosomal inhibitors (10 μg/mL E64d and pepstatin A) for 8 h before harvesting for Western analysis of ISG20L1, LC3, and actin. Results are representative of four independent experiments. **(b)** RKO cells were transfected with control, pCEP4, or ISG20L1 for 24 h before harvesting for Western analysis of ISG20L1, LC3, and actin. The Western blot is representative of four independent experiments.

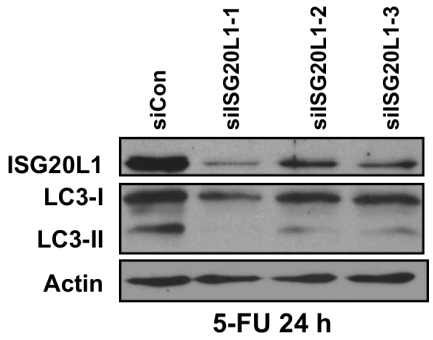

Figure 15. Autophagy levels decrease in a dose-dependent manner relative to levels of ISG20L1

U2OS cells were reverse transfected with three unique Dharmacon siRNAs targeting ISG20L1 and treated for 24 h (0.13 mM 5-FU) to induce autophagy as seen in the siControl lane by the modification of LC3-I to LC3-II. Levels of achieved knockdown of ISG20L1 correlate with the decrease in LC3-II. Western blot analysis is representative of four independent experiments.

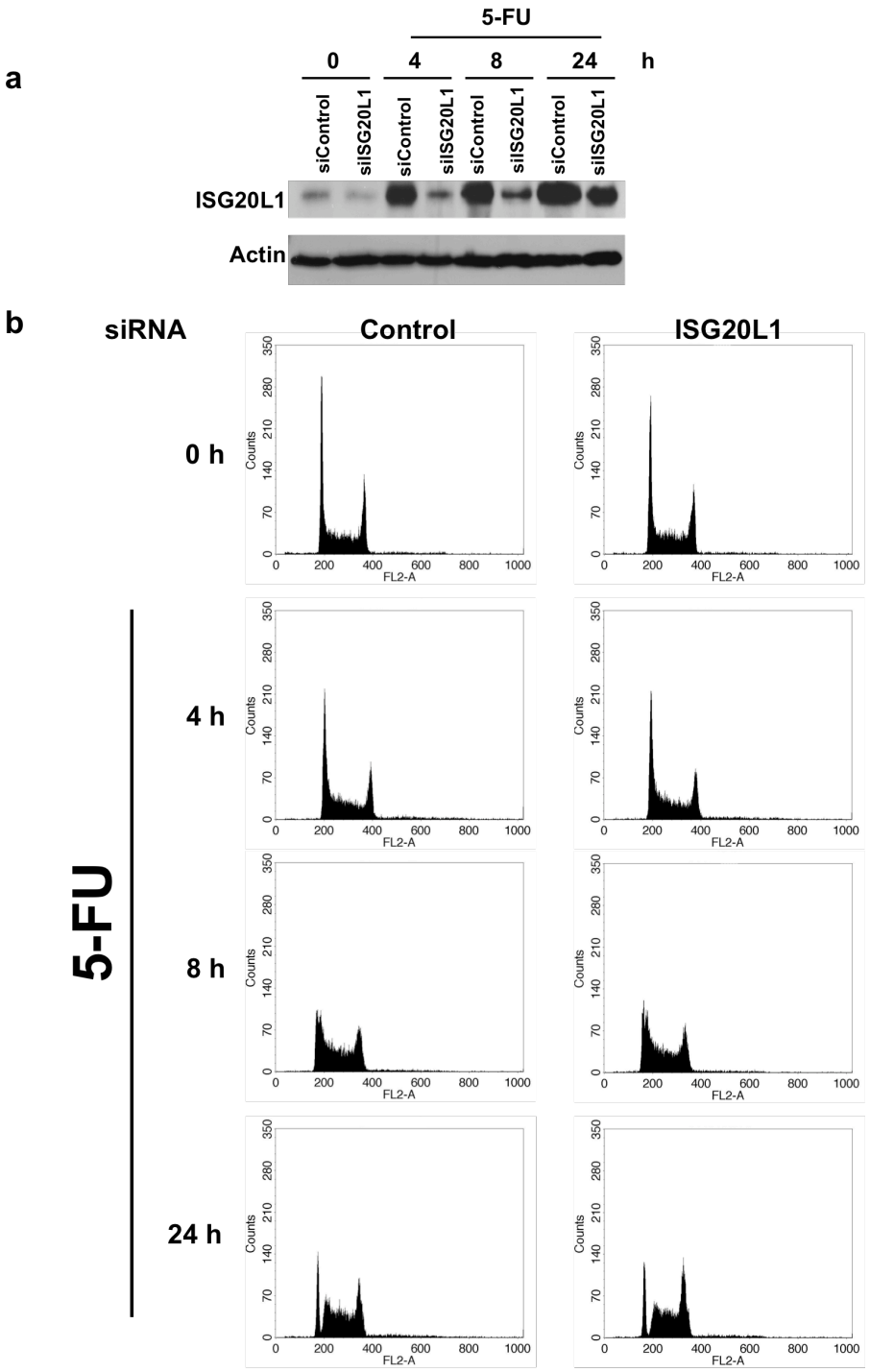

Figure 16. Knockdown of ISG20L1 does not alter cell-cycle progression
(a) U2OS cells were reverse transfected with nonsilencing control or siRNA targeting ISG20L1 and three days later treated or not with 5-FU over the indicated timecourse. Western analyses was performed to measure ISG20L1 and actin. **(b)** Flow cytometry was performed for each condition over the timecourse performed in (a) and a representative example of three independent experiments is shown.

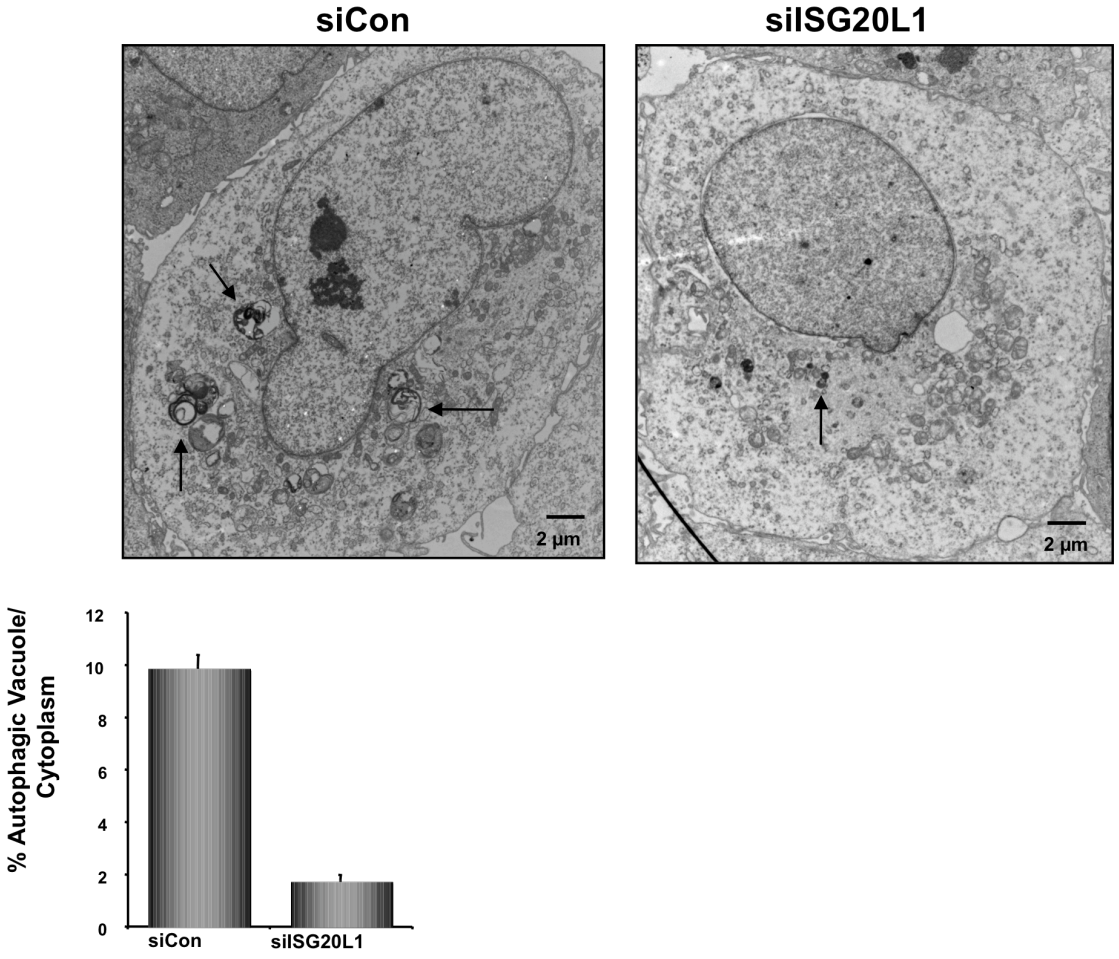

Figure 17. Knockdown of ISG20L1 decreases autophagic vacuole volume
U2OS cells were reverse transfected with control or siRNA targeting ISG20L1 and 3 days later treated for 24 h with 5-FU. Electron microscopy was performed and representative images can be seen (top panels) Arrowheads indicate autophagosomes or autophagolysosomes. Morphometric analyses was performed on electron micrographs and the percentage of autophagic vacuoles per cytoplasmic volume is shown. Results represent the mean and standard error, $p<.0001$, $n=25$ (right panel). This experiment was performed in duplicate.

knockdown of ISG20L1 (Figure 17, $p<0.0001$, n = 25 cells, duplicate experiments).

As described in the previous section, after autophagy induction, lipidated LC3-II is associated with autophagosomal membranes, resulting in the formation of punctate foci that can be quantified by fluorescence microscopy (Kabeya *et al.*, 2000; Klionsky *et al.*, 2008). To assess autophagy flux in the U2OS cell system, we used a LC3 (mRFP-GFP-LC3) vector that generates a LC3 fusion protein tagged at the 5' end with red fluorescent protein (RFP) and green fluorescent protein (GFP). Expression of mRFP-GFP-LC3 allows the distinction between early autophagic organelles (dual RFP+GFP+ puncta) and mature, acidified autolysosomes (RFP+ GFP- puncta) as the GFP signal is quenched in acidic compartments (Kimura *et al.*, 2007 2008; Klionsky *et al.*, 2008). U2OS cells stably expressing mRFP-GFP-LC3 were transfected with control or ISG20L1 expressing vectors and treated with 5-FU for 24 h. Those cells ectopically expressing ISG20L1 had a greater number of total LC3 foci and a 2.6-fold increase in the percentage of (RFP+GFP-) LC3 puncta per cell representing an increase in maturing autophagosomes (Figure 18, $p<0.001$, n = 50 cells; yellow arrows represent early autophagosomes that are $RFP^{+}GFP^{+}$, white arrows indicate late autolysosomal foci that are $RFP^{+}GFP^{-}$). These data show that ISG20L1 affects autophagy flux through autophagosome formation and maturation into autolysosomes.

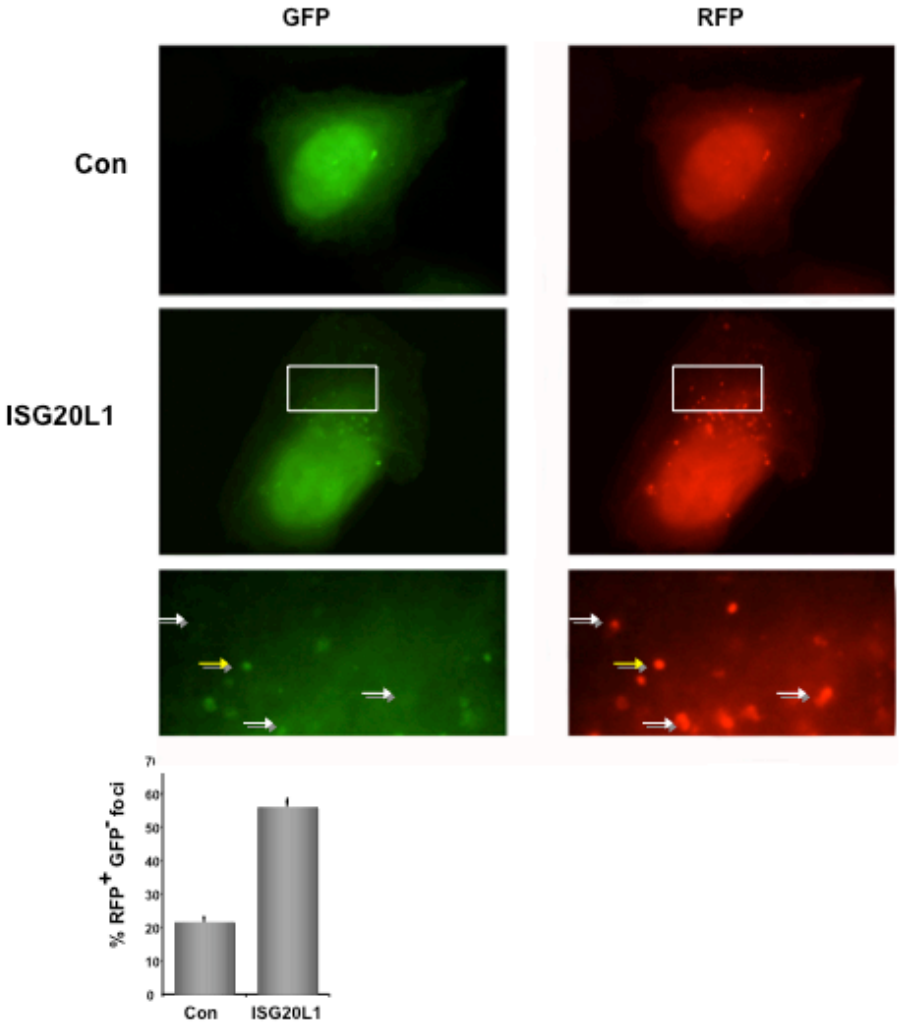

Figure 18. Exogenous ISG20L1 expression increases autophagy flux
Vector control and ISG20L1 were transfected in U2OS cells stably expressing the tandemly tagged mRFP-GFP-LC3 (tLC3) and then treated for 24 h with 5-FU. Representative panels show GFP alone and RFP alone for control and ISG20L1 as well as magnification of the area outlined by the white box of ISG20L1. White arrows highlight RFP+GFP- only foci representative of autolysosomes (late stage autophagy, $RFP^{+}GFP^{-}$); and yellow arrows indicate early autophagosomes where both GFP and RFP are fluorescing. Quantitation was performed and results are the mean and standard error of $RFP^{+}GFP^{-}$ foci expressed as a percentage of total foci ($p<.001$, $n=50$).

To extend and translate our mechanistic findings to the biologically relevant endpoint of cell growth, we analyzed the effect of ISG20L1 expression using colony formation assays. We transfected RKO, H1299, HCT116 cells as well as ATG5$^{+/+}$ and ATG5$^{-/-}$ mouse embryonic fibroblasts (MEFs) with control or ISG20L1 expression vectors, selected the cells in hygromycin for 10 days, and measured clonogenic growth. ATG5$^{-/-}$ MEFs were derived from an *ATG5*-null mouse model system and shown to be autophagy defective (Kuma *et al.*, 2004).

A representative result from one of the tumor-derived cell lines (HCT116) is presented in Figure 19. Cells ectopically expressing ISG20L1 had a 48% reduction in colony formation as compared to those cultures expressing an empty vector control. Parallel flow cytometric analyses were performed at 48, 72, and 96 h after transfection and no differences were observed in sub-G_1 DNA content or Annexin V staining, between control and ISG20L1 expressing cells (Figure 20 and 21). Use of the *ATG5*$^{+/+}$ and *ATG5*$^{-/-}$ MEFs enabled us to determine if the decreased clonogenic survival after expression of ISG20L1 was dependent on ATG5-induced autophagic processes. As observed in the human cell lines, ectopic expression of ISG20L1 in the *ATG5*$^{+/+}$ MEFs decreased colony number by ~77% compared to control. Importantly, this ISG20L1-induced decrease in colony number was partially rescued in *ATG5*$^{-/-}$ cells (over 2-fold increase; Figure 22). Collectively, these data are consistent with a function for ISG20L1 in genotoxic stress-induced autophagy and decreased cell survival.

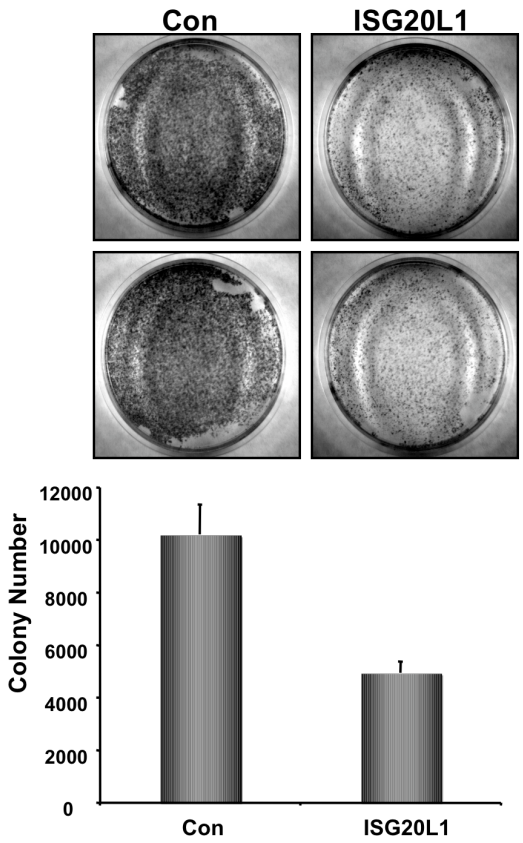

Figure 19. ISG20L1 decreases clonogenic survival
HCT116 cells were transfected with pCEP4 vector control or ISG20L1, selected in hygromycin B, and the number of colonies formed after selection counted using Biorad Quantity One software, shown in the lower panel. Duplicates of each transfection are shown. Similar results were observed in cultures of RKO and H1299 cells (data not shown). Results represent the mean and standard error.

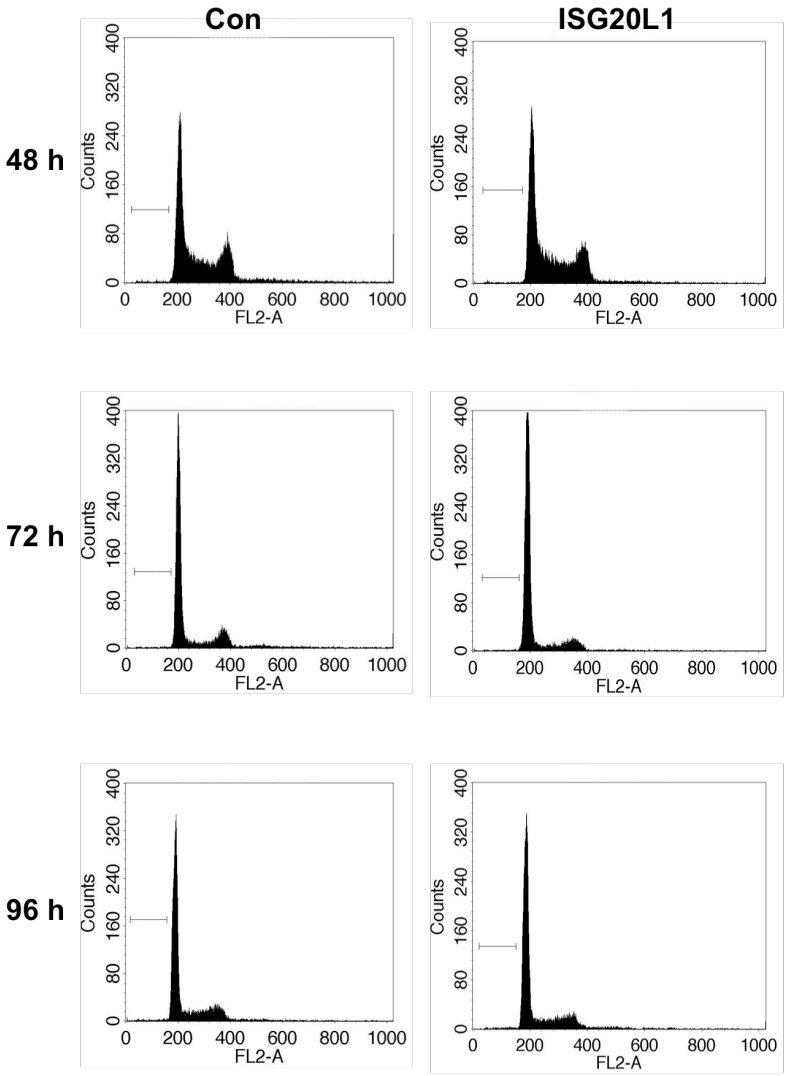

Figure 20. Decrease in clonogenic survival after ectopic ISG20L1 expression is not accompanied by increase in apoptosis.

Flow cytometry was performed over a timecourse with H1299 cells ectopically expressing either vector control or ISG20L1. A representative example of three separate experiments is shown.

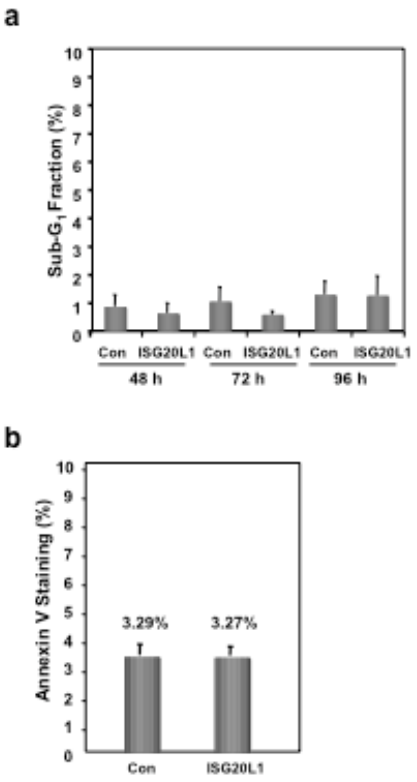

Figure 21. Ectopic ISG20L1 expression does not alter markers of apoptosis
(a) The sub-G_1 percentage was analyzed for those samples described in part Fig 20. **(c)** To further assess apoptosis, Annexin-V staining and flow cytometry were performed on H1299 cells 48 h after transfection with vector control or ISG20L1 and percent of cells stained for Annexin-V under both experimental conditions shown from three experiments, error bars represent standard deviation.

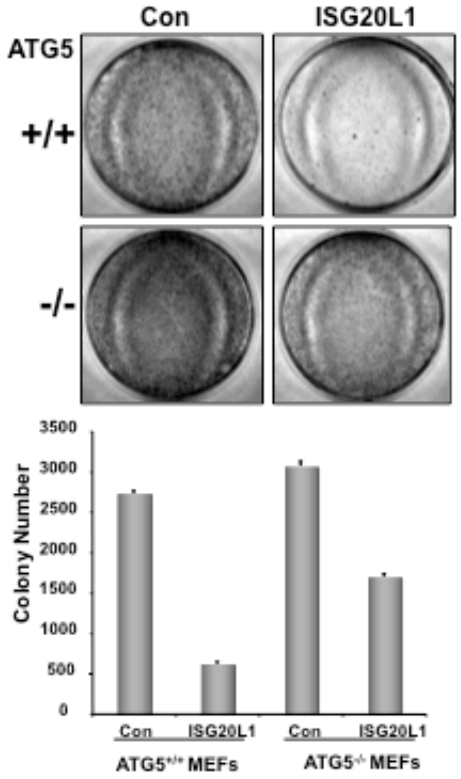

Figure 22. Decrease in clonogenic survival after ISG20L1 is partially rescued in autophagy deficient cells

ATG5$^{+/+}$ and ATG$^{-/-}$ MEFs were transfected with vector control (pCEP4) and ISG20L1; selected in hygromycin B; and the number of colonies formed after selection were counted using BioRad Quantity One software. Representative pictures are shown (upper panels) for each plasmid in both autophagy proficient (ATG5$^{+/+}$) and deficient (ATG$^{-/-}$) MEFs. Colony number quantified in the lower panel represent mean and standard error of each transfection for both ATG5$^{+/+}$ and ATG$^{-/-}$ MEFs performed in triplicate.

Discussion

Several studies provide evidence for a role of p53 in autophagy, a process first recognized as important in cell survival and now thought to function in tumor suppression (Crighton *et al.*, 2006; Feng *et al.*, 2005; Yue *et al.*, 2003). We strengthen this link between the p53 signaling axis and genotoxic-stress induced autophagy by identifying ISG20L1 as a transcriptional target of all three p53 family members. Using a newly generated antibody, we show that ISG20L1 levels increase in a p53- and TAp73-dependent manner after various forms of stress. In addition to p53, the family members p63 and p73 can bind and directly regulate ISG20L1 expression. Ectopic expression of ISG20L1 decreased cell survival without induction of apoptosis as determined by flow cytometric analyses of sub-G_1 DNA content or Annexin V staining, and the decreased clonogenic survival was partly rescued in an autophagy deficient background (*ATG5*$^{-/-}$ MEFs). ISG20L1 was not involved in modulating 5-FU-mediated apoptosis, as suppression of ISG20L1 in RKO cells did not alter the incidence or extent of apoptosis as measured by PARP and caspase-3 cleavage, sub-G1 content, and DNA laddering. In contrast, siRNA knockdown of ISG20L1 decreased genotoxic stress-induced autophagy as measured by electron microscopy, biochemical, and immunohistochemical analyses of LC3-II. Thus, we identified ISG20L1 as a p53-family dependent, genotoxic stress-induced modulator of autophagy.

The nucleolus is the cellular site of rRNA synthesis and processing as well as ribosomal assembly (Scheer and Hock, 1999). One of the first connections of

p53 to nucleolar signaling was the observation that a dominant-negative form of the nucleolar protein Bop1 could induce p53-dependent cell cycle arrest (Pestov *et al.*, 2001). Recent publications have linked nucleolar proteins to arbitrating cellular response to stress, including autophagy (David-Pfeuty, 1999; Olson, 2004; Rubbi and Milner, 2003). For example, nucleolar ARF can inhibit the production of the immature 12S rRNA intermediate, interact with the 5.8S rRNA (Sugimoto *et al.*, 2003), and activate autophagy in p53-positive cells (Abida and Gu, 2008).

Our data validates previous findings of ISG20L1 nucleolar localization (Kawase *et al.*, 2008; Lee *et al.*, 2005). ISG20L2, a family member of ISG20L1, also localizes to the nucleolus and is involved in the processing of 12S rRNA to the mature 5.8S rRNA, part of the large ribosomal subunit (Coute *et al.*, 2008). *In vitro* assays have shown that the exonuclease III domain of ISG20L1 is required to degrade single- and double- stranded DNA and RNA (Kawase *et al.*, 2008; Lee *et al.*, 2005). Collectively, the recent findings that ISG20L1 can degrade RNA, our data and others showing nucleolar localization of ISG20L1, and our linkage of ISG20L1 to autophagy suggests it will be important to examine the role of ISG20L1 in rRNA processing and ribosomal assembly during cellular response to stress (Kawase *et al.*, 2008; Kraft *et al.*, 2008; Lee *et al.*, 2005).

There is growing evidence for the interplay between autophagy and the p53 family. As mentioned above, p19ARF and the short mitochondrial form (smARF) are able to induce autophagy in both p53-dependent and –independent

manners (Abida and Gu, 2008). A number of genes involved in autophagy are directly regulated by p53 including the mTOR inhibitors, TSC1 and PTEN, Sestrin1 and Sestrin2, and the damage-regulated autophagy modulator (Venter *et al.*) (Crighton *et al.*, 2006; Feng *et al.*, 2005). Additionally, inhibition of mTOR by p53 is associated with autophagy and occurs through DNA damaged-induced signaling involving AMPK and TSC1/2 (Feng *et al.*, 2005). p73 transcriptional activity has also been linked to autophagy as p73 is bound to a number of genes involved in metabolism and autophagy (Crighton *et al.*, 2007; Rosenbluth and Pietenpol, 2009). Our results show that ISG20L1 is contributing to cellular demise by modulating the process of autophagy that is commonly associated with type II cell death (Bursch *et al.*, 2008; Eisenberg-Lerner *et al.*, 2009).

The identification of ISG20L1 as a p53 family target and discovery that modulation of this target can regulate autophagic processes further strengthens the connection between p53 signaling and autophagy. Given the keen interest in targeting autophagy as an anticancer therapeutic approach in tumor cells that are defective in apoptosis, investigation of genes and signaling pathways involved in cell death associated with autophagy is critical.

CHAPTER V

SUMMARY AND FUTURE DIRECTIONS

p53 is the most frequently mutated gene in human cancer (Baker *et al.*, 1989; Daujat *et al.*, 2001; Momand *et al.*, 2000; Nigro *et al.*, 1989). As a transcription factor, p53 regulates a multitude of genes involved in cell cycle progression (el-Deiry *et al.*, 1994), genomic stability (Tanaka *et al.*, 2000), cellular senescence (Shay *et al.,* 1991), apoptosis (Oda *et al.*, 2000b), angiogenesis (Ravi *et al.*, 2000), cell migration (Gadea *et al.*, 2002), and autophagy (Crighton *et al.*, 2006). The transcriptional activity of p53 is required for its tumor-suppressor ability (Pietenpol *et al.*, 1994). The goal of this dissertation was to identify novel p53 family transcriptional targets and determine their functions in biologically-relevant processes downstream of the p53 family signaling axis.

Identification and characterization of p53 family target genes

Our experience has shown the false discovery rate to be high when only using a single assay (i.e. ChIP or microarray analysis) to identify p53-bound or regulated genes. Given this observation, along with the public availability of a vast array of p53 datasets, we overlaid numerous genomic datasets from both ChIP and gene expression assays to identify a subset of high-confidence putative p53 target genes. The generation of our gene list is described in Chapter III of

this dissertation, and includes a number of previously published p53 target genes, such as p21 and MDM2.

We utilized a number of criteria to create a panel of putative p53 transcriptional targets. To identify those genes that were directly bound and regulated by p53, we analyzed three unique ChIP datasets that provide ~1,600 predicted p53 binding sites (Hearnes *et al.*, 2005; Smeenk *et al.*, 2008; Wei *et al.*, 2006). Since presence of a p53 binding site in a gene does not always equate to transcriptional regulation, we also performed gene expression microarray analyses on RNA isolated from an inducible p53 cell model system that undergoes p53 mediated arrest. When compared to the p53 null-parental cell line, induction of p53 resulted in upregulation of 624 genes two-fold or greater. Additionally, we used a gene expression dataset generated previously in our laboratory from primary human keratinocytes engineered to ectopically express p53 (Schavolt and Pietenpol, 2007). After combining ChIP and gene expression data, the last tool used in the identification of new p53 transcriptional targets was a mathematical algorithm that ranks the probability of a gene being a putative transcriptional target based on gene expression data (Barenco *et al.*, 2006).

Since the generation of our putative p53 target gene collection, 10 genes have been published by our laboratory and others. For example, we identified the ribosomal gene RPS27L as a novel p53 target gene. During our characterization of RPS27L, another laboratory published it as a p53 target gene that regulates apoptosis (He and Sun, 2007; Li *et al.*, 2007). Gene ontology

analyses show that a number of the identified p53 target genes function in multiple pathways governed by p53, such as cell cycle regulation, DNA repair, and cell death. In addition, other genes in our subset are identified as being involved in processes novel to p53 signaling including cell-to-cell signaling, cell morphology, and cellular metabolism. Given this, we anticipate that our future analyses will not only discover target genes that function in canonical p53 signaling pathways, but may ultimately reveal completely novel signaling mechanisms regulated by p53 itself.

Early studies aimed at identifying p53-regulated genes often involved analyzing a single gene, in a single p53-regulated process, such as apoptosis. Though these studies provided an enormous wealth of information with regards to p53 function, the "single-gene-single-assay" approach can often be laborious and time-consuming. The advancement in genomic technologies makes possible the study of multiple genes in a high-throughput manner, using assays based on gene depletion and/or exogenous expression. With my panel of numerous putative p53 target genes and new genomic and molecularly-based technologies, our future plans for this project include a high throughput siRNA loss-of-function screen to identify the contribution of these genes to biological processes regulated by p53. A high throughput analysis of genes will allow for more rapid characterization of novel target genes associated with p53-regulated cellular functions, such as cell cycle arrest, apoptosis, and autophagy, to name a few.

Loss-of-function screens are now routinely used to identify genes and pathways, that when targeted, sensitize tumor cells to various drugs. The majority of siRNA screens existing in the literature, test for a single biological endpoint or are investigating the identification of genes involved in a single pathway. For example, a recent study by a Vanderbilt graduate student, Dr. Courtney Lovejoy, involved a loss of function screen using siRNA in human cells to identify genes that when downregulated lead to a DNA damage response as measured by the DNA damage marker H2AX-phosphorylation (Lovejoy *et al.*, 2009). This screen identified 73 novel genes that when silenced activated the DNA damage response pathway. p53 is involved in numerous cellular pathways and these loss-of-function screens now afford us the opportunity to study the complexity of p53 signaling by characterizing novel target gene functions in a high-throughput manner using assays that cover a wide range of biological endpoints including DNA repair, apoptosis, cell survival, migration, and autophagy.

The subset of p53 family target genes described in detail in Chapter III are currently being assayed in siRNA loss-of-function screens. We have Dharmacon OnTarget pools of siRNA that consist of four individual siRNAs all targeting the same gene. A total of 164 genes are being assayed in a microtiter plate format. The biological assays that will be performed were chosen either due to prior linkage of p53 signaling to the biological endpoint being assayed or based on gene ontology analysis. The biological assays are measuring (i) changes in cell

number (Alamar blue, Invitrogen); (ii) apoptosis (Caspase-Glo 3/7 assay, Promega); (iii) DNA damage and repair (KAP1 immunofluorescence); (iv) autophagy (Monodansylcadaverine cell kit, Cayman Chemicals); and (v) migration (Oris Pro Cell Migration Assays, Platypus Technologies). Positive hits will be screened in secondary validation assays using two individual siRNA from Qiagen. For example a positive hit from the KAP1 DNA damage screen will be tested for H2AX-phosphorylation, and a positive hit in the migration screen will be tested in larger format using a scratch assay. For those genes identified as overlapping with the other p53 family members, p63 or p73, we may add additional screens with biologically relevant end assays such as keratinocyte or human mesenchymal stem cell differentiation.

To determine p53-dependence, nonsilencing or siRNA targeting p53 will be used in combination with siRNAs targeting the genes under investigation to determine if biological effects of target gene knockdown are p53-dependent. Appropriate controls will be used to perform our loss-of-function screen. Controls include four individual nonsilencing siRNAs that allow normalization across the plates. Positive controls will be included that are appropriate to the biological endpoint being examined, for example siRNA targeting caspase-3 will be used for the cell death, Caspase-GLO 3/7 assay. We are performing these functional screens in primary human mammary epithelial cells (HMECs). These cells were selected based on the p53 family member expression status where HMECs express all of the family members. The transfection conditions have been

optimized for maximum efficiency of siRNA uptake. The siRNA screen is performed by reverse transfecting the HMECs using a preoptimized cell number with siRNA oligos targeting the genes of interest. Each functional experiment is performed in triplicate to allow for statistical analysis. Three days after reverse transfection, each cell line is treated with the IC_{50} of cisplatin, a DNA intercalator, known to activate the various members of the p53 family (Fomenkov *et al.*, 2004; Toh *et al.*, 2004). The duration of treatment depends upon the biological endpoint being assayed.

With the number of putative transcriptional targets growing, we can no longer characterize all these genes on an individual basis. A more high-throughput siRNA screening method is the only practical approach for initial characterization to inform us which target genes should receive more in depth and detailed investigation for the role played downstream of the p53 family signaling pathway.

Unanswered Questions in the p53 field

In addition to regulating mRNA expression, p53 also regulates the expression of noncoding RNA. Noncoding RNAs (ncRNAs) include miRNAs that are short 22 nucleotide long ribonucleic acid molecules and act as post-transcriptional regulators by binding to 3'-untranslated regions of the mRNA transcript thus targeting it for degradation (Bartel, 2009).

Preliminary studies have begun to uncover the interplay of the p53 family and miRNAs. ChIP analyses of p53 binding have shown perfect matches for the p53 consensus site and binding at genomic loci that are not located near coding regions invoking the question of p53 function at these locations (Hearnes *et al.*, 2005; Wei *et al.*, 2006). A number of publications have suggested a connection between the miRNA-34 family (miRNA-34a, -34b, -34c) and p53. The miRNA-34 family is induced after DNA damage in a p53-dependent manner (Bommer *et al.*, 2007; Chang *et al.*, 2007; Corney *et al.*, 2007; Tazawa *et al.*, 2007). p53 consensus binding sites were found in the two transcripts encoding miRNA-34a and miRNA-34b/c (Wei *et al.*, 2006). Ectopic expression of miRNA-34 family induced similar results of G1 cell cycle arrest, inhibition of proliferation, and decreased clonogenic cell survival (Bommer *et al.*, 2007; Tazawa *et al.*, 2007). Recently, work performed in our laboratory has also found a direct connection between p73 and miRNA. p73 binds 116 miRNAs and expression levels of 142 miRNAs changed greater than 50% after p73 knockdown (Rosenbluth et al, personal communication).

Given the connections between the p53 family and direct regulation of miRNAs, a number of important questions remain in this field. As transcription factors, p53 family members have previously been assayed for their ability to regulate target gene expression and now it will be important to investigate if regulation of transcriptional targets occurs directly by p53 or through secondary effects after induction of the miRNA-34 family. It will be necessary to further

analyze miRNA-34 alterations in cancer and how restoration of miRNA-34 function could potentially be used as an anti-cancer therapeutic. Additionally, it will be important to discover other miRNAs controlled by the p53 family. Since the connection between miRNA-34 and p53, only two other miRNA-145 and miRNA-192 have published evidence for p53-dependent regulation (Sachdeva *et al.*, 2009; Song *et al.*, 2008). MicroRNA expression arrays obtained from three different models including an inducible p53 cell line, a p53 isogenic cell line HCT116 treated with DNA-damaging agents, and a conditional p53 model suggest that many miRNAs are both up- and down-regulated in a p53-dependent manner (Chang *et al.*, 2007; Tarasov *et al.*, 2007). Future research is required to characterize these miRNA and their subsequent targets downstream of p53 signaling. Experiments that would yield light on this topic would be a comparison of gene expression arrays after knocking down p53, miRNA-34, or p53 and miRNA-34 to determine the necessity of miRNAs in p53 transcriptional activities. This type of experiment would show if miRNA-34 expression can downregulate a specific subset of p53-regulated genes and if p53 requires miRNA for transcriptional regulation of certain target genes.

p53 and autophagy: paradoxical signaling

Numerous transcriptional targets of p53 function in cell cycle arrest or apoptosis. As we discover more novel target genes, new roles for p53 in various biological processes are being described, including p53 in the regulation of

autophagy. Autophagy is a recycling process of cellular catabolism that allows a cell to breakdown cytoplasmic components for reuse by the cell. Initially, autophagy was discovered after induction by starvation where electron microscopy captured the formation of the characteristic double membrane autophagosomes that enveloped portions of the cell's cytoplasm (De Duve and Wattiaux, 1966). These autophagosomes proceed to fuse with lysosomal compartments of the cell where degradative enzymes such as cathepsins degrade the macromolecules contained within the autophagolysosome (Berg *et al.*, 1998). Since the discovery of this process in 1966, autophagy has been implicated in a number of different normal and disease states. The importance of autophagy has also been seen in the development of higher eukaryotes where mice lacking the essential autophagy component Beclin1 die during embryogenesis and ATG5- or ATG7-null mice die perinatally (Kuma *et al.*, 2004; Yue *et al.*, 2003). A number of disease states and pathologies are also attributed to the process of autophagy including neurodegenerative diseases (Huntington's, Alzheimer's, Parkinson's); antiviral and antimicrobial immunity; and cancer.

p53 activated under DNA-damage and metabolic stress conditions is also a known regulator of autophagy (Crighton *et al.*, 2006; Feng *et al.*, 2005; Tasdemir *et al.*, 2008). p53 can both positively and negatively regulate autophagy in a transcriptionally-dependent and –independent manner respectively. Inhibition of autophagy is suggested to occur by low levels of cytoplasmic transcriptionally-independent functions of p53. The more widely

described role of p53 in autophagy is through the transcription-dependent induction of autophagic activity following cellular stress. p53 can regulate the upstream activators of AMPK, Sestrin1 and Sestrin2, after genotoxic and oxidative stress, to induce autophagy (Budanov and Karin, 2008). Outside of the mTOR pathway, p53 has been shown to regulate several transcriptional targets that modulate autophagy including DAPK-1, DRAM, and the target gene discussed in Chapter IV of this dissertation, ISG20L1. The damage-regulated autophagy modulator (DRAM) is regulated by both p53 and p73; however was only found necessary for p53 induced autophagy that resulted in cell death (Crighton *et al.*, 2007). DRAM is lysosomal in location, induces markers of autophagy, and decreases cell survival but the mechanism by which it functions in autophagy has not been deciphered (Crighton *et al.*, 2006).

Dissertation research, described in Chapter IV, identified a novel p53 family transcriptional target, ISG20L1, that is involved in genotoxic stress-induced autophagy (Eby *et al.*). Using a newly generated antibody, we found that ISG20L1 levels increase in a p53- and TAp73-dependent manner after various forms of stress. In addition to p53, the family members p63 and p73 can bind and directly regulate ISG20L1 expression. Ectopic expression of ISG20L1 decreased cell survival without induction of apoptosis as determined by flow cytometric analyses of sub-G_1 DNA content or Annexin V staining. Decreased clonogenic survival was partly rescued in an autophagy deficient cell line ($ATG5^{-/-}$ MEFs). ISG20L1 was not involved in modulating 5-FU-mediated apoptosis, as

suppression of ISG20L1 in RKO cells did not alter the incidence or extent of apoptosis as measured by PARP and caspase-3 cleavage, sub-G1 content, or DNA laddering. In contrast, siRNA knockdown of ISG20L1 decreased genotoxic stress-induced autophagy as measured by electron microscopy, as well as biochemical, and immunohistochemical analyses of the autophagy marker LC3-II. Thus, we identified ISG20L1 as a p53-family dependent, genotoxic stress-induced modulator of autophagy.

Further investigation will be necessary to determine the molecular mechanism of ISG20L1 in the modulation of autophagy. The family member IGS20L2 was recently shown to have exoribonuclease activity that is necessary for processing of the 12S rRNA into the mature 5.8S rRNA form (Coute *et al.*, 2008). Preliminary data shows that IGS20L1 has 3'-5' exonuclease activity and is perinucleolar in localization, where rRNA maturation occurs (Lee *et al.*, 2005). Other proteins involved in autophagy have been shown to play a role in nucleolar structure and processing of rRNA. For example, $p19^{ARF}$-null MEFs have a greater number of nucleoli and increased processing of immature rRNA compared to wild-type controls (Apicelli *et al.*, 2008). ARF, as described previously, can alter autophagy through p53-dependent and –independent mechanisms (Abida and Gu, 2008; Reef *et al.*, 2006). Additionally, the mTOR pathway that regulates autophagy, plays a large role in sensing nutrient availability and adjusting the synthesis of ribosomal components (Mayer and Grummt, 2006). Thus we are interested in determining if ISG20L1 plays a role in

rRNA processing and if that mechanism alters autophagy. Planned experiments would determine if knockdown of ISG20L1 alters processing of rRNA from the pre-rRNA to mature forms of rRNA (12s- 5.8s rRNA) using Northern methods or quantitative real-time PCR primers specific to the various cleavage forms.

Future research to identify additional novel p53 family transcriptional targets involved in autophagy will be performed through our ongoing siRNA functional screen to characterize p53 target genes as discussed above. Our laboratory and others have linked both p53 and p73 to autophagic processes (Eby *et al.*; Rosenbluth and Pietenpol, 2009). The field of autophagy will need to further investigate what seems to be a contradictory role of p53 in both the suppression and activation of autophagy. It could be hypothesized that these opposing roles of p53 are merely protein-level and context dependent as low levels of cytoplasmic p53 inhibits whereas nuclear, transcriptionally active p53 activates autophagy. This dual nature of p53 activity, as well as our laboratory findings that p73 is connected to the process of autophagy, invokes the question of the importance of autophagy as a p53 family tumor suppressive mechanism.

Many questions remain in the field of autophagy regarding its ability to provide either oncogenic survival mechanisms or tumor suppressive methods in the process of tumorigenesis. Evidence shows that under hypoxic conditions autophagy can promote tumor cell survival *in* vivo (Degenhardt *et al.*, 2006). Cells that have developed defects in apoptosis have also been shown to live for weeks under conditions of nutrient withdrawal (Lum *et al.*, 2005). At the same

time, loss of autophagy gene expression occurs in human tumors and corresponding mouse models results in increased incidence of tumor formation, thus suggesting a strong tumor suppressive role for the process of autophagy. Monoallelic loss of *Beclin1* is common in breast, ovarian, and prostate cancer as well as monoallelic deletions of *UVRAG* in colon cancer (Goi *et al.*, 2003). Though the exact mechanism of tumor suppression is not known, autophagy has been suggested to suppress tumorigenesis through cell death mechanisms (Chen and Karantza-Wadsworth, 2009). Various models for the role of autophagy in cell death exist and include autophagy as the primary inducer of cell death; autophagy induction prior to/ or at the time of apoptosis activation; and lastly that apoptotic induction actually inhibits autophagic mechanisms (Qian *et al.*, 2007; Yu *et al.*, 2006). When both apoptosis and autophagy pathways are inhibited, cell death by necrosis was evident but activation of only one of these pathways decreased levels of necrosis (Kunchithapautham and Rohrer, 2007). Thus it remains unclear if autophagy alone is sufficient to complete cell death or if it requires cross-talk with other cell death machinery.

Further characterization of the events leading to cell death requires additional *in vitro* experiments to shed light on the crosstalk between autophagy and apoptosis. Measuring multiple markers of apoptosis and autophagy in a panel of cell lines after starvation or genotoxic stress-induced cell death will result in valuable data regarding the timing and communication between these two pathways. Further, using siRNA or specific inhibitors to suppress either

autophagy or apoptosis will yield information on their individual roles as they contribute to cell death. As more whole tumor genomes become available, it will be interesting to determine the frequency of alterations seen in the autophagic pathway. In a recent seminar at Vanderbilt University, Dr. Beth Levine showed the first evidence of tumor regression in a mouse xenograft model using a small molecule that interrupts the Bcl-2 and Beclin1 complex allowing Beclin1 to induce autophagy. Further investigation to discover if this small molecule causes autophagic induced pathways associated with cell death and of course determination if this small molecule can have a therapeutic benefit alone or in combination with other anticancer therapies in humans will need to be studied. To determine if autophagy is sufficient for cell death, novel methods for the assessment of autophagy will be critical in investigating the anticancer therapeutic potential of autophagy.

Concluding Remarks

As we identify p53-dependent target genes involved in a diversity of cellular processes, we continue to discover novel functions for p53 signaling. During the course of my dissertation research, I overlaid a number of genomic datasets and employed a mathematical ranking algorithm to identify a collection of putative p53 transcriptional targets. I further characterized the role of one of these targets, ISG20L1, as a p53 family regulated target gene that modulates autophagy. My research has laid the groundwork to apply high-throughput

siRNA technology in a way that has not been done before to simultaneously characterize these putative p53 target genes in multiple biological assays.

Connections between the p53 family and autophagy are relatively new and ISG20L1 is one of only a handful of direct targets linking these pathways. A pressing question in the fields of p53 and autophagy that requires further investigation is the role of autophagy in cell death. To target autophagy for anticancer therapeutic purposes, it will be necessary to characterize the role of autophagy in tumor suppression and cell death. With the completion of the siRNA functional screens, we hope to uncover and explore additional pathways and novel roles of p53 and its family members.

REFERENCES

Abida WM, Gu W (2008). p53-Dependent and p53-independent activation of autophagy by ARF. *Cancer Res* **68:** 352-7.

Agami R, Blandino G, Oren M, Shaul Y (1999). Interaction of c-Abl and p73alpha and their collaboration to induce apoptosis. *Nature* **399:** 809-13.

Alcorta DA, Xiong Y, Phelps D, Hannon G, Beach D, Barrett JC (1996). Involvement of the cyclin-dependent kinase inhibitor p16 (INK4a) in replicative senescence of normal human fibroblasts. *Proc Natl Acad Sci U S A* **93:** 13742-7.

Apicelli AJ, Maggi LB, Jr., Hirbe AC, Miceli AP, Olanich ME, Schulte-Winkeler CL *et al* (2008). A non-tumor suppressor role for basal p19ARF in maintaining nucleolar structure and function. *Mol Cell Biol* **28:** 1068-80.

Baeuerle PA, Baltimore D (1988). I kappa B: a specific inhibitor of the NF-kappa B transcription factor. *Science* **242:** 540-6.

Baker SJ, Fearon ER, Nigro JM, Hamilton SR, Preisinger AC, Jessup JM *et al* (1989). Chromosome 17 deletions and p53 gene mutations in colorectal carcinomas. *Science* **244:** 217-21.

Baptiste N, Friedlander P, Chen X, Prives C (2002). The proline-rich domain of p53 is required for cooperation with anti-neoplastic agents to promote apoptosis of tumor cells. *Oncogene* **21:** 9-21.

Barbieri CE, Pietenpol JA (2005). p53 family members: similar biochemistry, different biology. *Cancer Biol Ther* **4:** 419-20.

Barenco M, Tomescu D, Brewer D, Callard R, Stark J, Hubank M (2006). Ranked prediction of p53 targets using hidden variable dynamic modeling. *Genome Biol* **7:** R25.

Bartel DP (2009). MicroRNAs: target recognition and regulatory functions. *Cell* **136:** 215-33.

Bayle JH, Elenbaas B, Levine AJ (1995). The carboxyl-terminal domain of the p53 protein regulates sequence-specific DNA binding through its nonspecific nucleic acid-binding activity. *Proc Natl Acad Sci U S A* **92:** 5729-33.

Beau I, Esclatine A, Codogno P (2008). Lost to translation: when autophagy targets mature ribosomes. *Trends Cell Biol* **18:** 311-4.

Bell DW, Varley JM, Szydlo TE, Kang DH, Wahrer DC, Shannon KE *et al* (1999). Heterozygous germ line hCHK2 mutations in Li-Fraumeni syndrome. *Science* **286:** 2528-31.

Berg TO, Fengsrud M, Stromhaug PE, Berg T, Seglen PO (1998). Isolation and characterization of rat liver amphisomes. Evidence for fusion of autophagosomes with both early and late endosomes. *J Biol Chem* **273:** 21883-92.

Bernales S, McDonald KL, Walter P (2006). Autophagy counterbalances endoplasmic reticulum expansion during the unfolded protein response. *PLoS Biol* **4:** e423.

Birch JM, Alston RD, McNally RJ, Evans DG, Kelsey AM, Harris M *et al* (2001). Relative frequency and morphology of cancers in carriers of germline TP53 mutations. *Oncogene* **20:** 4621-8.

Bischoff JR, Kirn DH, Williams A, Heise C, Horn S, Muna M *et al* (1996). An adenovirus mutant that replicates selectively in p53-deficient human tumor cells. *Science* **274:** 373-6.

Bommer GT, Gerin I, Feng Y, Kaczorowski AJ, Kuick R, Love RE *et al* (2007). p53-mediated activation of miRNA34 candidate tumor-suppressor genes. *Curr Biol* **17:** 1298-307.

Braunstein S, Badura ML, Xi Q, Formenti SC, Schneider RJ (2009). Regulation of protein synthesis by ionizing radiation. *Mol Cell Biol* **29:** 5645-56.

Bredesen DE (2000). Apoptosis: overview and signal transduction pathways. *J Neurotrauma* **17:** 801-10.

Brunner HG, Hamel BC, Bokhoven Hv H (2002). P63 gene mutations and human developmental syndromes. *Am J Med Genet* **112:** 284-90.

Budanov AV, Karin M (2008). p53 target genes sestrin1 and sestrin2 connect genotoxic stress and mTOR signaling. *Cell* **134:** 451-60.

Bunz F, Dutriaux A, Lengauer C, Waldman T, Zhou S, Brown JP *et al* (1998). Requirement for p53 and p21 to sustain G2 arrest after DNA damage. *Science* **282:** 1497-501.

Burns TF, Bernhard EJ, El-Deiry WS (2001). Tissue specific expression of p53 target genes suggests a key role for KILLER/DR5 in p53-dependent apoptosis in vivo. *Oncogene* **20:** 4601-12.

Bursch W, Karwan A, Mayer M, Dornetshuber J, Frohwein U, Schulte-Hermann R *et al* (2008). Cell death and autophagy: cytokines, drugs, and nutritional factors. *Toxicology* **254:** 147-57.

Buschmann T, Fuchs SY, Lee CG, Pan ZQ, Ronai Z (2000). SUMO-1 modification of Mdm2 prevents its self-ubiquitination and increases Mdm2 ability to ubiquitinate p53. *Cell* **101:** 753-62.

Buschmann T, Potapova O, Bar-Shira A, Ivanov VN, Fuchs SY, Henderson S *et al* (2001). Jun NH2-terminal kinase phosphorylation of p53 on Thr-81 is important for p53 stabilization and transcriptional activities in response to stress. *Mol Cell Biol* **21:** 2743-54.

Caron de Fromentel C, Soussi T (1992). TP53 tumor suppressor gene: a model for investigating human mutagenesis. *Genes Chromosomes Cancer* **4:** 1-15.

Cawley S, Bekiranov S, Ng HH, Kapranov P, Sekinger EA, Kampa D *et al* (2004). Unbiased mapping of transcription factor binding sites along human chromosomes 21 and 22 points to widespread regulation of noncoding RNAs. *Cell* **116:** 499-509.

Cecconi F, Levine B (2008). The role of autophagy in mammalian development: cell makeover rather than cell death. *Dev Cell* **15:** 344-57.

Celli J, Duijf P, Hamel BC, Bamshad M, Kramer B, Smits AP *et al* (1999). Heterozygous germline mutations in the p53 homolog p63 are the cause of EEC syndrome. *Cell* **99:** 143-53.

Chan TA, Hermeking H, Lengauer C, Kinzler KW, Vogelstein B (1999). 14-3-3Sigma is required to prevent mitotic catastrophe after DNA damage. *Nature* **401:** 616-20.

Chang TC, Wentzel EA, Kent OA, Ramachandran K, Mullendore M, Lee KH *et al* (2007). Transactivation of miR-34a by p53 broadly influences gene expression and promotes apoptosis. *Mol Cell* **26:** 745-52.

Chen J, Sadowski I (2005). Identification of the mismatch repair genes PMS2 and MLH1 as p53 target genes by using serial analysis of binding elements. *Proc Natl Acad Sci U S A* **102:** 4813-8.

Chen N, Karantza-Wadsworth V (2009). Role and regulation of autophagy in cancer. *Biochim Biophys Acta* **1793:** 1516-23.

Cheng Q, Chen L, Li Z, Lane WS, Chen J (2009). ATM activates p53 by regulating MDM2 oligomerization and E3 processivity. *Embo J* **28:** 3857-67.

Chipuk JE, Kuwana T, Bouchier-Hayes L, Droin NM, Newmeyer DD, Schuler M *et al* (2004). Direct activation of Bax by p53 mediates mitochondrial membrane permeabilization and apoptosis. *Science* **303:** 1010-4.

Cho Y, Gorina S, Jeffrey PD, Pavletich NP (1994). Crystal structure of a p53 tumor suppressor-DNA complex: understanding tumorigenic mutations. *Science* **265:** 346-55.

Corney DC, Flesken-Nikitin A, Godwin AK, Wang W, Nikitin AY (2007). MicroRNA-34b and MicroRNA-34c are targets of p53 and cooperate in control of cell proliferation and adhesion-independent growth. *Cancer Res* **67:** 8433-8.

Coute Y, Kindbeiter K, Belin S, Dieckmann R, Duret L, Bezin L *et al* (2008). ISG20L2, a novel vertebrate nucleolar exoribonuclease involved in ribosome biogenesis. *Mol Cell Proteomics* **7:** 546-59.

Crighton D, O'Prey J, Bell HS, Ryan KM (2007). p73 regulates DRAM-independent autophagy that does not contribute to programmed cell death. *Cell Death Differ* **14:** 1071-9.

Crighton D, Wilkinson S, O'Prey J, Syed N, Smith P, Harrison PR *et al* (2006). DRAM, a p53-induced modulator of autophagy, is critical for apoptosis. *Cell* **126:** 121-34.

d'Adda di Fagagna F, Reaper PM, Clay-Farrace L, Fiegler H, Carr P, Von Zglinicki T *et al* (2003). A DNA damage checkpoint response in telomere-initiated senescence. *Nature* **426:** 194-8.

Dameron KM, Volpert OV, Tainsky MA, Bouck N (1994). The p53 tumor suppressor gene inhibits angiogenesis by stimulating the production of thrombospondin. *Cold Spring Harb Symp Quant Biol* **59:** 483-9.

Daujat S, Neel H, Piette J (2001). MDM2: life without p53. *Trends Genet* **17:** 459-64.

David-Pfeuty T (1999). Potent inhibitors of cyclin-dependent kinase 2 induce nuclear accumulation of wild-type p53 and nucleolar fragmentation in human untransformed and tumor-derived cells. *Oncogene* **18:** 7409-22.

Davison TS, Vagner C, Kaghad M, Ayed A, Caput D, Arrowsmith CH (1999). p73 and p63 are homotetramers capable of weak heterotypic interactions with each other but not with p53. *J Biol Chem* **274:** 18709-14.

De Duve C, Wattiaux R (1966). Functions of lysosomes. *Annu Rev Physiol* **28:** 435-92.

De Laurenzi V, Costanzo A, Barcaroli D, Terrinoni A, Falco M, Annicchiarico-Petruzzelli M *et al* (1998). Two new p73 splice variants, gamma and delta, with different transcriptional activity. *J Exp Med* **188:** 1763-8.

Debbas M, White E (1993). Wild-type p53 mediates apoptosis by E1A, which is inhibited by E1B. *Genes Dev* **7:** 546-54.

Degenhardt K, Mathew R, Beaudoin B, Bray K, Anderson D, Chen G *et al* (2006). Autophagy promotes tumor cell survival and restricts necrosis, inflammation, and tumorigenesis. *Cancer Cell* **10:** 51-64.

Derry WB, Putzke AP, Rothman JH (2001). Caenorhabditis elegans p53: role in apoptosis, meiosis, and stress resistance. *Science* **294:** 591-5.

Di Micco R, Fumagalli M, Cicalese A, Piccinin S, Gasparini P, Luise C *et al* (2006). Oncogene-induced senescence is a DNA damage response triggered by DNA hyper-replication. *Nature* **444:** 638-42.

Dimri GP, Lee X, Basile G, Acosta M, Scott G, Roskelley C *et al* (1995). A biomarker that identifies senescent human cells in culture and in aging skin in vivo. *Proc Natl Acad Sci U S A* **92:** 9363-7.

Donehower LA, Harvey M, Slagle BL, McArthur MJ, Montgomery CA, Jr., Butel JS *et al* (1992). Mice deficient for p53 are developmentally normal but susceptible to spontaneous tumours. *Nature* **356:** 215-21.

Dornan D, Wertz I, Shimizu H, Arnott D, Frantz GD, Dowd P *et al* (2004). The ubiquitin ligase COP1 is a critical negative regulator of p53. *Nature* **429:** 86-92.

Dressman HK, Berchuck A, Chan G, Zhai J, Bild A, Sayer R *et al* (2007). An integrated genomic-based approach to individualized treatment of patients with advanced-stage ovarian cancer. *J Clin Oncol* **25:** 517-25.

Duan J, Nilsson L (2006). Effect of Zn2+ on DNA recognition and stability of the p53 DNA-binding domain. *Biochemistry* **45:** 7483-92.

Eberle J, Weitmann S, Thieck O, Pech H, Paul M, Orfanos CE (1999). Downregulation of endothelin B receptor in human melanoma cell lines parallel to differentiation genes. *J Invest Dermatol* **112:** 925-32.

Eby KG, Rosenbluth JM, Mays DJ, Marshall CB, Barton CE, Sinha S *et al* ISG20L1 is a p53 family target gene that modulates genotoxic stress-induced autophagy. *Mol Cancer* **9:** 95.

Eisenberg-Lerner A, Bialik S, Simon HU, Kimchi A (2009). Life and death partners: apoptosis, autophagy and the cross-talk between them. *Cell Death Differ* **16:** 966-75.

el-Deiry WS, Harper JW, O'Connor PM, Velculescu VE, Canman CE, Jackman J *et al* (1994). WAF1/CIP1 is induced in p53-mediated G1 arrest and apoptosis. *Cancer Res* **54:** 1169-74.

el-Deiry WS, Kern SE, Pietenpol JA, Kinzler KW, Vogelstein B (1992). Definition of a consensus binding site for p53. *Nat Genet* **1:** 45-9.

el-Deiry WS, Tokino T, Velculescu VE, Levy DB, Parsons R, Trent JM *et al* (1993). WAF1, a potential mediator of p53 tumor suppression. *Cell* **75:** 817-25.

Eliyahu D, Michalovitz D, Eliyahu S, Pinhasi-Kimhi O, Oren M (1989). Wild-type p53 can inhibit oncogene-mediated focus formation. *Proc Natl Acad Sci U S A* **86:** 8763-7.

Etienne-Manneville S, Hall A (2003). Cdc42 regulates GSK-3beta and adenomatous polyposis coli to control cell polarity. *Nature* **421:** 753-6.

Fakharzadeh SS, Trusko SP, George DL (1991). Tumorigenic potential associated with enhanced expression of a gene that is amplified in a mouse tumor cell line. *Embo J* **10:** 1565-9.

Farre JC, Manjithaya R, Mathewson RD, Subramani S (2008). PpAtg30 tags peroxisomes for turnover by selective autophagy. *Dev Cell* **14:** 365-76.

Feng Z, Hu W, de Stanchina E, Teresky AK, Jin S, Lowe S *et al* (2007). The regulation of AMPK beta1, TSC2, and PTEN expression by p53: stress, cell and tissue specificity, and the role of these gene products in modulating the IGF-1-AKT-mTOR pathways. *Cancer Res* **67:** 3043-53.

Feng Z, Zhang H, Levine AJ, Jin S (2005). The coordinate regulation of the p53 and mTOR pathways in cells. *Proc Natl Acad Sci U S A* **102:** 8204-9.

Fields S, Jang SK (1990). Presence of a potent transcription activating sequence in the p53 protein. *Science* **249:** 1046-9.

Finlay CA, Hinds PW, Levine AJ (1989). The p53 proto-oncogene can act as a suppressor of transformation. *Cell* **57:** 1083-93.

Flaman JM, Robert V, Lenglet S, Moreau V, Iggo R, Frebourg T (1998). Identification of human p53 mutations with differential effects on the bax and p21 promoters using functional assays in yeast. *Oncogene* **16:** 1369-72.

Flatt PM, Price JO, Shaw A, Pietenpol JA (1998). Differential cell cycle checkpoint response in normal human keratinocytes and fibroblasts. *Cell Growth Differ* **9:** 535-43.

Flatt PM, Tang LJ, Scatena CD, Szak ST, Pietenpol JA (2000). p53 regulation of G(2) checkpoint is retinoblastoma protein dependent. *Mol Cell Biol* **20:** 4210-23.

Flores ER, Sengupta S, Miller JB, Newman JJ, Bronson R, Crowley D *et al* (2005). Tumor predisposition in mice mutant for p63 and p73: evidence for broader tumor suppressor functions for the p53 family. *Cancer Cell* **7:** 363-73.

Flores ER, Tsai KY, Crowley D, Sengupta S, Yang A, McKeon F *et al* (2002). p63 and p73 are required for p53-dependent apoptosis in response to DNA damage. *Nature* **416:** 560-4.

Fomenkov A, Zangen R, Huang YP, Osada M, Guo Z, Fomenkov T *et al* (2004). RACK1 and stratifin target DeltaNp63alpha for a proteasome degradation in head and neck squamous cell carcinoma cells upon DNA damage. *Cell Cycle* **3:** 1285-95.

Freedman DA, Epstein CB, Roth JC, Levine AJ (1997). A genetic approach to mapping the p53 binding site in the MDM2 protein. *Mol Med* **3:** 248-59.

Fritsche M, Haessler C, Brandner G (1993). Induction of nuclear accumulation of the tumor-suppressor protein p53 by DNA-damaging agents. *Oncogene* **8:** 307-18.

Fukazawa T, Fujiwara T, Morimoto Y, Shao J, Nishizaki M, Kadowaki Y *et al* (1999). Differential involvement of the CD95 (Fas/APO-1) receptor/ligand system on apoptosis induced by the wild-type p53 gene transfer in human cancer cells. *Oncogene* **18:** 2189-99.

Gadea G, Lapasset L, Gauthier-Rouviere C, Roux P (2002). Regulation of Cdc42-mediated morphological effects: a novel function for p53. *Embo J* **21:** 2373-82.

Gadea G, Roger L, Anguille C, de Toledo M, Gire V, Roux P (2004). TNFalpha induces sequential activation of Cdc42- and p38/p53-dependent pathways that antagonistically regulate filopodia formation. *J Cell Sci* **117:** 6355-64.

Gaiddon C, Lokshin M, Ahn J, Zhang T, Prives C (2001). A subset of tumor-derived mutant forms of p53 down-regulate p63 and p73 through a direct interaction with the p53 core domain. *Mol Cell Biol* **21:** 1874-87.

Georges AB, Benayoun BA, Caburet S, Veitia RA Generic binding sites, generic DNA-binding domains: where does specific promoter recognition come from? *Faseb J* **24:** 346-56.

Ghosh A, Stewart D, Matlashewski G (2004). Regulation of human p53 activity and cell localization by alternative splicing. *Mol Cell Biol* **24:** 7987-97.

Goi T, Kawasaki M, Yamazaki T, Koneri K, Katayama K, Hirose K *et al* (2003). Ascending colon cancer with hepatic metastasis and cholecystolithiasis in a patient with situs inversus totalis without any expression of UVRAG mRNA: report of a case. *Surg Today* **33:** 702-6.

Gong JG, Costanzo A, Yang HQ, Melino G, Kaelin WG, Jr., Levrero M *et al* (1999). The tyrosine kinase c-Abl regulates p73 in apoptotic response to cisplatin-induced DNA damage. *Nature* **399:** 806-9.

Gozuacik D, Kimchi A (2006). DAPk protein family and cancer. *Autophagy* **2:** 74-9.

Graeber TG, Peterson JF, Tsai M, Monica K, Fornace AJ, Jr., Giaccia AJ (1994). Hypoxia induces accumulation of p53 protein, but activation of a G1-phase checkpoint by low-oxygen conditions is independent of p53 status. *Mol Cell Biol* **14:** 6264-77.

Green DR, Chipuk JE (2006). p53 and metabolism: Inside the TIGAR. *Cell* **126:** 30-2.

Green DR, Kroemer G (2009). Cytoplasmic functions of the tumour suppressor p53. *Nature* **458:** 1127-30.

Gressner O, Schilling T, Lorenz K, Schulze Schleithoff E, Koch A, Schulze-Bergkamen H *et al* (2005). TAp63alpha induces apoptosis by activating signaling via death receptors and mitochondria. *Embo J* **24:** 2458-71.

Gu W, Roeder RG (1997). Activation of p53 sequence-specific DNA binding by acetylation of the p53 C-terminal domain. *Cell* **90:** 595-606.

Gu Y, Turck CW, Morgan DO (1993). Inhibition of CDK2 activity in vivo by an associated 20K regulatory subunit. *Nature* **366:** 707-10.

Gutierrez MG, Master SS, Singh SB, Taylor GA, Colombo MI, Deretic V (2004). Autophagy is a defense mechanism inhibiting BCG and Mycobacterium tuberculosis survival in infected macrophages. *Cell* **119:** 753-66.

Harper JW, Elledge SJ, Keyomarsi K, Dynlacht B, Tsai LH, Zhang P *et al* (1995). Inhibition of cyclin-dependent kinases by p21. *Mol Biol Cell* **6:** 387-400.

Harrison B, Kraus M, Burch L, Stevens C, Craig A, Gordon-Weeks P *et al* (2008). DAPK-1 binding to a linear peptide motif in MAP1B stimulates autophagy and membrane blebbing. *J Biol Chem* **283:** 9999-10014.

He H, Sun Y (2007). Ribosomal protein S27L is a direct p53 target that regulates apoptosis. *Oncogene* **26:** 2707-16.

Hearnes JM, Mays DJ, Schavolt KL, Tang L, Jiang X, Pietenpol JA (2005). Chromatin immunoprecipitation-based screen to identify functional genomic binding sites for sequence-specific transactivators. *Mol Cell Biol* **25:** 10148-58.

Heise C, Ganly I, Kim YT, Sampson-Johannes A, Brown R, Kirn D (2000). Efficacy of a replication-selective adenovirus against ovarian carcinomatosis is dependent on tumor burden, viral replication and p53 status. *Gene Ther* **7:** 1925-9.

Hinds P, Finlay C, Levine AJ (1989). Mutation is required to activate the p53 gene for cooperation with the ras oncogene and transformation. *J Virol* **63:** 739-46.

Ho JS, Ma W, Mao DY, Benchimol S (2005). p53-Dependent transcriptional repression of c-myc is required for G1 cell cycle arrest. *Mol Cell Biol* **25:** 7423-31.

Hoh J, Jin S, Parrado T, Edington J, Levine AJ, Ott J (2002). The p53MH algorithm and its application in detecting p53-responsive genes. *Proc Natl Acad Sci U S A* **99:** 8467-72.

Hollstein MC, Peri L, Mandard AM, Welsh JA, Montesano R, Metcalf RA *et al* (1991). Genetic analysis of human esophageal tumors from two high incidence geographic areas: frequent p53 base substitutions and absence of ras mutations. *Cancer Res* **51:** 4102-6.

Honda R, Tanaka H, Yasuda H (1997). Oncoprotein MDM2 is a ubiquitin ligase E3 for tumor suppressor p53. *FEBS Lett* **420:** 25-7.

Honda R, Yasuda H (1999). Association of p19(ARF) with Mdm2 inhibits ubiquitin ligase activity of Mdm2 for tumor suppressor p53. *Embo J* **18:** 22-7.

Hsu FF, Lin TY, Chen JY, Shieh SY p53-Mediated transactivation of LIMK2b links actin dynamics to cell cycle checkpoint control. *Oncogene*.

Hwang BJ, Ford JM, Hanawalt PC, Chu G (1999). Expression of the p48 xeroderma pigmentosum gene is p53-dependent and is involved in global genomic repair. *Proc Natl Acad Sci U S A* **96:** 424-8.

Ianakiev P, Kilpatrick MW, Toudjarska I, Basel D, Beighton P, Tsipouras P (2000). Split-hand/split-foot malformation is caused by mutations in the p63 gene on 3q27. *Am J Hum Genet* **67:** 59-66.

Imamura K, Ogura T, Kishimoto A, Kaminishi M, Esumi H (2001). Cell cycle regulation via p53 phosphorylation by a 5'-AMP activated protein kinase activator, 5-aminoimidazole- 4-carboxamide-1-beta-D-ribofuranoside, in a human hepatocellular carcinoma cell line. *Biochem Biophys Res Commun* **287:** 562-7.

Issaeva N, Bozko P, Enge M, Protopopova M, Verhoef LG, Masucci M *et al* (2004). Small molecule RITA binds to p53, blocks p53-HDM-2 interaction and activates p53 function in tumors. *Nat Med* **10:** 1321-8.

Jackson JG, Pereira-Smith OM (2006). p53 is preferentially recruited to the promoters of growth arrest genes p21 and GADD45 during replicative senescence of normal human fibroblasts. *Cancer Res* **66:** 8356-60.

Jeffers JR, Parganas E, Lee Y, Yang C, Wang J, Brennan J *et al* (2003). Puma is an essential mediator of p53-dependent and -independent apoptotic pathways. *Cancer Cell* **4:** 321-8.

Johnson DS, Mortazavi A, Myers RM, Wold B (2007). Genome-wide mapping of in vivo protein-DNA interactions. *Science* **316:** 1497-502.

Jongmans W, Artuso M, Vuillaume M, Bresil H, Jackson SP, Hall J (1996). The role of Ataxia telangiectasia and the DNA-dependent protein kinase in the p53-mediated cellular response to ionising radiation. *Oncogene* **13:** 1133-8.

Kabeya Y, Mizushima N, Ueno T, Yamamoto A, Kirisako T, Noda T *et al* (2000). LC3, a mammalian homologue of yeast Apg8p, is localized in autophagosome membranes after processing. *Embo J* **19:** 5720-8.

Kang C, You YJ, Avery L (2007). Dual roles of autophagy in the survival of Caenorhabditis elegans during starvation. *Genes Dev* **21:** 2161-71.

Kang SH, Vieira K, Bungert J (2002). Combining chromatin immunoprecipitation and DNA footprinting: a novel method to analyze protein-DNA interactions in vivo. *Nucleic Acids Res* **30:** e44.

Karlseder J, Smogorzewska A, de Lange T (2002). Senescence induced by altered telomere state, not telomere loss. *Science* **295:** 2446-9.

Kartasheva NN, Contente A, Lenz-Stoppler C, Roth J, Dobbelstein M (2002). p53 induces the expression of its antagonist p73 Delta N, establishing an autoregulatory feedback loop. *Oncogene* **21:** 4715-27.

Kastan MB, Onyekwere O, Sidransky D, Vogelstein B, Craig RW (1991). Participation of p53 protein in the cellular response to DNA damage. *Cancer Res* **51:** 6304-11.

Katayama M, Kawaguchi T, Berger MS, Pieper RO (2007). DNA damaging agent-induced autophagy produces a cytoprotective adenosine triphosphate surge in malignant glioma cells. *Cell Death Differ* **14:** 548-58.

Katoh I, Aisaki KI, Kurata SI, Ikawa S, Ikawa Y (2000). p51A (TAp63gamma), a p53 homolog, accumulates in response to DNA damage for cell regulation. *Oncogene* **19:** 3126-30.

Kaushik S, Massey AC, Cuervo AM (2006). Lysosome membrane lipid microdomains: novel regulators of chaperone-mediated autophagy. *Embo J* **25:** 3921-33.

Kawase T, Ichikawa H, Ohta T, Nozaki N, Tashiro F, Ohki R *et al* (2008). p53 target gene AEN is a nuclear exonuclease required for p53-dependent apoptosis. *Oncogene* **27:** 3797-810.

Kerr JF, Wyllie AH, Currie AR (1972). Apoptosis: a basic biological phenomenon with wide-ranging implications in tissue kinetics. *Br J Cancer* **26:** 239-57.

Kessis TD, Slebos RJ, Nelson WG, Kastan MB, Plunkett BS, Han SM *et al* (1993). Human papillomavirus 16 E6 expression disrupts the p53-mediated cellular response to DNA damage. *Proc Natl Acad Sci U S A* **90:** 3988-92.

Khuri FR, Nemunaitis J, Ganly I, Arseneau J, Tannock IF, Romel L *et al* (2000). a controlled trial of intratumoral ONYX-015, a selectively-replicating adenovirus, in combination with cisplatin and 5-fluorouracil in patients with recurrent head and neck cancer. *Nat Med* **6:** 879-85.

Kimura S, Noda T, Yoshimori T (2007). Dissection of the autophagosome maturation process by a novel reporter protein, tandem fluorescent-tagged LC3. *Autophagy* **3:** 452-60.

Kingma PS, Osheroff N (1997). Spontaneous DNA damage stimulates topoisomerase II-mediated DNA cleavage. *J Biol Chem* **272:** 7488-93.

Klionsky DJ, Abeliovich H, Agostinis P, Agrawal DK, Aliev G, Askew DS *et al* (2008). Guidelines for the use and interpretation of assays for monitoring autophagy in higher eukaryotes. *Autophagy* **4:** 151-75.

Knudson AG, Jr. (1971). Mutation and cancer: statistical study of retinoblastoma. *Proc Natl Acad Sci U S A* **68:** 820-3.

Komatsu M, Waguri S, Ueno T, Iwata J, Murata S, Tanida I *et al* (2005). Impairment of starvation-induced and constitutive autophagy in Atg7-deficient mice. *J Cell Biol* **169:** 425-34.

Kotake-Nara E, Saida K (2006). Endothelin-2/vasoactive intestinal contractor: regulation of expression via reactive oxygen species induced by CoCl2, and Biological activities including neurite outgrowth in PC12 cells. *ScientificWorldJournal* **6:** 176-86.

Kraft C, Deplazes A, Sohrmann M, Peter M (2008). Mature ribosomes are selectively degraded upon starvation by an autophagy pathway requiring the Ubp3p/Bre5p ubiquitin protease. *Nat Cell Biol* **10:** 602-10.

Kuma A, Hatano M, Matsui M, Yamamoto A, Nakaya H, Yoshimori T *et al* (2004). The role of autophagy during the early neonatal starvation period. *Nature* **432:** 1032-6.

Kunchithapautham K, Rohrer B (2007). Apoptosis and autophagy in photoreceptors exposed to oxidative stress. *Autophagy* **3:** 433-41.

Lane DP, Crawford LV (1979). T antigen is bound to a host protein in SV40-transformed cells. *Nature* **278:** 261-3.

Lapi E, Iovino A, Fontemaggi G, Soliera AR, Iacovelli S, Sacchi A *et al* (2006). S100A2 gene is a direct transcriptional target of p53 homologues during keratinocyte differentiation. *Oncogene* **25:** 3628-37.

Lee JH, Koh YA, Cho CK, Lee SJ, Lee YS, Bae S (2005). Identification of a novel ionizing radiation-induced nuclease, AEN, and its functional characterization in apoptosis. *Biochem Biophys Res Commun* **337:** 39-47.

Lee JM, Bernstein A (1995). Apoptosis, cancer and the p53 tumour suppressor gene. *Cancer Metastasis Rev* **14:** 149-61.

Lees-Miller SP, Sakaguchi K, Ullrich SJ, Appella E, Anderson CW (1992). Human DNA-activated protein kinase phosphorylates serines 15 and 37 in the amino-terminal transactivation domain of human p53. *Mol Cell Biol* **12:** 5041-9.

Leng RP, Lin Y, Ma W, Wu H, Lemmers B, Chung S *et al* (2003). Pirh2, a p53-induced ubiquitin-protein ligase, promotes p53 degradation. *Cell* **112:** 779-91.

Leong CO, Vidnovic N, DeYoung MP, Sgroi D, Ellisen LW (2007). The p63/p73 network mediates chemosensitivity to cisplatin in a biologically defined subset of primary breast cancers. *J Clin Invest* **117:** 1370-80.

Leu JI, Dumont P, Hafey M, Murphy ME, George DL (2004). Mitochondrial p53 activates Bak and causes disruption of a Bak-Mcl1 complex. *Nat Cell Biol* **6:** 443-50.

Levine AJ (1989). The p53 tumor suppressor gene and gene product. *Princess Takamatsu Symp* **20:** 221-30.

Levine B (2005). Eating oneself and uninvited guests: autophagy-related pathways in cellular defense. *Cell* **120:** 159-62.

Levine B, Abrams J (2008). p53: The Janus of autophagy? *Nat Cell Biol* **10:** 637-9.

Li J, Tan J, Zhuang L, Banerjee B, Yang X, Chau JF *et al* (2007). Ribosomal protein S27-like, a p53-inducible modulator of cell fate in response to genotoxic stress. *Cancer Res* **67:** 11317-26.

Li M, Brooks CL, Wu-Baer F, Chen D, Baer R, Gu W (2003a). Mono- versus polyubiquitination: differential control of p53 fate by Mdm2. *Science* **302:** 1972-5.

Li Y, Raffo AJ, Drew L, Mao Y, Tran A, Petrylak DP *et al* (2003b). Fas-mediated apoptosis is dependent on wild-type p53 status in human cancer cells expressing a temperature-sensitive p53 mutant alanine-143. *Cancer Res* **63:** 1527-33.

Liang J, Shao SH, Xu ZX, Hennessy B, Ding Z, Larrea M *et al* (2007). The energy sensing LKB1-AMPK pathway regulates p27(kip1) phosphorylation mediating the decision to enter autophagy or apoptosis. *Nat Cell Biol* **9:** 218-24.

Liang XH, Jackson S, Seaman M, Brown K, Kempkes B, Hibshoosh H *et al* (1999). Induction of autophagy and inhibition of tumorigenesis by beclin 1. *Nature* **402:** 672-6.

Lin YL, Sengupta S, Gurdziel K, Bell GW, Jacks T, Flores ER (2009). p63 and p73 transcriptionally regulate genes involved in DNA repair. *PLoS Genet* **5:** e1000680.

Linzer DI, Levine AJ (1979). Characterization of a 54K dalton cellular SV40 tumor antigen present in SV40-transformed cells and uninfected embryonal carcinoma cells. *Cell* **17:** 43-52.

Liu L, Scolnick DM, Trievel RC, Zhang HB, Marmorstein R, Halazonetis TD *et al* (1999). p53 sites acetylated in vitro by PCAF and p300 are acetylated in vivo in response to DNA damage. *Mol Cell Biol* **19:** 1202-9.

Liu Y, Cox SR, Morita T, Kourembanas S (1995). Hypoxia regulates vascular endothelial growth factor gene expression in endothelial cells. Identification of a 5' enhancer. *Circ Res* **77:** 638-43.

Lovejoy CA, Xu X, Bansbach CE, Glick GG, Zhao R, Ye F *et al* (2009). Functional genomic screens identify CINP as a genome maintenance protein. *Proc Natl Acad Sci U S A* **106:** 19304-9.

Lum JJ, Bauer DE, Kong M, Harris MH, Li C, Lindsten T *et al* (2005). Growth factor regulation of autophagy and cell survival in the absence of apoptosis. *Cell* **120:** 237-48.

Ma B, Levine AJ (2007). Probing potential binding modes of the p53 tetramer to DNA based on the symmetries encoded in p53 response elements. *Nucleic Acids Res* **35:** 7733-47.

Malkin D, Li FP, Strong LC, Fraumeni JF, Jr., Nelson CE, Kim DH *et al* (1990). Germ line p53 mutations in a familial syndrome of breast cancer, sarcomas, and other neoplasms. *Science* **250:** 1233-8.

Martoriati A, Doumont G, Alcalay M, Bellefroid E, Pelicci PG, Marine JC (2005). dapk1, encoding an activator of a p19ARF-p53-mediated apoptotic checkpoint, is a transcription target of p53. *Oncogene* **24:** 1461-6.

Mayer C, Grummt I (2006). Ribosome biogenesis and cell growth: mTOR coordinates transcription by all three classes of nuclear RNA polymerases. *Oncogene* **25:** 6384-91.

Medema RH, Klompmaker R, Smits VA, Rijksen G (1998). p21waf1 can block cells at two points in the cell cycle, but does not interfere with processive DNA-replication or stress-activated kinases. *Oncogene* **16:** 431-41.

Mills AA, Zheng B, Wang XJ, Vogel H, Roop DR, Bradley A (1999). p63 is a p53 homologue required for limb and epidermal morphogenesis. *Nature* **398:** 708-13.

Milner J, Medcalf EA (1991). Cotranslation of activated mutant p53 with wild type drives the wild-type p53 protein into the mutant conformation. *Cell* **65:** 765-74.

Mitchell PJ, Tjian R (1989). Transcriptional regulation in mammalian cells by sequence-specific DNA binding proteins. *Science* **245:** 371-8.

Mizushima N (2004). Methods for monitoring autophagy. *Int J Biochem Cell Biol* **36:** 2491-502.

Mizushima N, Yamamoto A, Hatano M, Kobayashi Y, Kabeya Y, Suzuki K *et al* (2001). Dissection of autophagosome formation using Apg5-deficient mouse embryonic stem cells. *J Cell Biol* **152:** 657-68.

Mizushima N, Yoshimori T, Levine B Methods in mammalian autophagy research. *Cell* **140:** 313-26.

Momand J, Wu HH, Dasgupta G (2000). MDM2--master regulator of the p53 tumor suppressor protein. *Gene* **242:** 15-29.

Momand J, Zambetti GP, Olson DC, George D, Levine AJ (1992). The mdm-2 oncogene product forms a complex with the p53 protein and inhibits p53-mediated transactivation. *Cell* **69:** 1237-45.

Morselli E, Tasdemir E, Maiuri MC, Galluzzi L, Kepp O, Criollo A *et al* (2008). Mutant p53 protein localized in the cytoplasm inhibits autophagy. *Cell Cycle* **7:** 3056-61.

Muller-Tiemann BF, Halazonetis TD, Elting JJ (1998). Identification of an additional negative regulatory region for p53 sequence-specific DNA binding. *Proc Natl Acad Sci U S A* **95:** 6079-84.

Munoz-Gamez JA, Rodriguez-Vargas JM, Quiles-Perez R, Aguilar-Quesada R, Martin-Oliva D, de Murcia G *et al* (2009). PARP-1 is involved in autophagy induced by DNA damage. *Autophagy* **5:** 61-74.

Murray-Zmijewski F, Lane DP, Bourdon JC (2006). p53/p63/p73 isoforms: an orchestra of isoforms to harmonise cell differentiation and response to stress. *Cell Death Differ* **13:** 962-72.

Nakamura S, Roth JA, Mukhopadhyay T (2000). Multiple lysine mutations in the C-terminal domain of p53 interfere with MDM2-dependent protein degradation and ubiquitination. *Mol Cell Biol* **20:** 9391-8.

Nakano K, Vousden KH (2001). PUMA, a novel proapoptotic gene, is induced by p53. *Mol Cell* **7:** 683-94.

Nicholls CD, McLure KG, Shields MA, Lee PW (2002). Biogenesis of p53 involves cotranslational dimerization of monomers and posttranslational dimerization of dimers. Implications on the dominant negative effect. *J Biol Chem* **277:** 12937-45.

Nigro JM, Baker SJ, Preisinger AC, Jessup JM, Hostetter R, Cleary K *et al* (1989). Mutations in the p53 gene occur in diverse human tumour types. *Nature* **342:** 705-8.

Oda E, Ohki R, Murasawa H, Nemoto J, Shibue T, Yamashita T *et al* (2000a). Noxa, a BH3-only member of the Bcl-2 family and candidate mediator of p53-induced apoptosis. *Science* **288:** 1053-8.

Oda K, Arakawa H, Tanaka T, Matsuda K, Tanikawa C, Mori T *et al* (2000b). p53AIP1, a potential mediator of p53-dependent apoptosis, and its regulation by Ser-46-phosphorylated p53. *Cell* **102:** 849-62.

Oh YK, Lee HJ, Jeong MH, Rhee M, Mo JW, Song EH *et al* (2008). Role of activating transcription factor 3 on TAp73 stability and apoptosis in paclitaxel-treated cervical cancer cells. *Mol Cancer Res* **6:** 1232-49.

Okada Y, Osada M, Kurata S, Sato S, Aisaki K, Kageyama Y *et al* (2002). p53 gene family p51(p63)-encoded, secondary transactivator p51B(TAp63alpha) occurs without forming an immunoprecipitable complex with MDM2, but responds to genotoxic stress by accumulation. *Exp Cell Res* **276:** 194-200.

Olins AL, Olins DE (1974). Spheroid chromatin units (v bodies). *Science* **183:** 330-2.

Olson MO (2004). Sensing cellular stress: another new function for the nucleolus? *Sci STKE* **2004:** pe10.

Ortt K, Sinha S (2006). Derivation of the consensus DNA-binding sequence for p63 reveals unique requirements that are distinct from p53. *FEBS Lett* **580:** 4544-50.

Osada M, Park HL, Nagakawa Y, Yamashita K, Fomenkov A, Kim MS *et al* (2005). Differential recognition of response elements determines target gene specificity for p53 and p63. *Mol Cell Biol* **25:** 6077-89.

Pal S, Datta K, Mukhopadhyay D (2001). Central role of p53 on regulation of vascular permeability factor/vascular endothelial growth factor (VPF/VEGF) expression in mammary carcinoma. *Cancer Res* **61:** 6952-7.

Palmero EI, Achatz MI, Ashton-Prolla P, Olivier M, Hainaut P Tumor protein 53 mutations and inherited cancer: beyond Li-Fraumeni syndrome. *Curr Opin Oncol* **22:** 64-9.

Pavletich NP, Chambers KA, Pabo CO (1993). The DNA-binding domain of p53 contains the four conserved regions and the major mutation hot spots. *Genes Dev* **7:** 2556-64.

Peng T, Golub TR, Sabatini DM (2002). The immunosuppressant rapamycin mimics a starvation-like signal distinct from amino acid and glucose deprivation. *Mol Cell Biol* **22:** 5575-84.

Perez CA, Ott J, Mays DJ, Pietenpol JA (2007). p63 consensus DNA-binding site: identification, analysis and application into a p63MH algorithm. *Oncogene* **26:** 7363-70.

Perou CM, Sorlie T, Eisen MB, van de Rijn M, Jeffrey SS, Rees CA *et al* (2000). Molecular portraits of human breast tumours. *Nature* **406:** 747-52.

Pestov DG, Strezoska Z, Lau LF (2001). Evidence of p53-dependent cross-talk between ribosome biogenesis and the cell cycle: effects of nucleolar protein Bop1 on G(1)/S transition. *Mol Cell Biol* **21:** 4246-55.

Petiot A, Ogier-Denis E, Blommaart EF, Meijer AJ, Codogno P (2000). Distinct classes of phosphatidylinositol 3'-kinases are involved in signaling pathways that control macroautophagy in HT-29 cells. *J Biol Chem* **275:** 992-8.

Petitjean A, Achatz MI, Borresen-Dale AL, Hainaut P, Olivier M (2007). TP53 mutations in human cancers: functional selection and impact on cancer prognosis and outcomes. *Oncogene* **26:** 2157-65.

Pietenpol JA, Tokino T, Thiagalingam S, el-Deiry WS, Kinzler KW, Vogelstein B (1994). Sequence-specific transcriptional activation is essential for growth suppression by p53. *Proc Natl Acad Sci U S A* **91:** 1998-2002.

Pimkina J, Humbey O, Zilfou JT, Jarnik M, Murphy ME (2009). ARF induces autophagy by virtue of interaction with Bcl-xl. *J Biol Chem* **284:** 2803-10.

Ptashne M, Gann A (1998). Imposing specificity by localization: mechanism and evolvability. *Curr Biol* **8:** R897.

Qian W, Liu J, Jin J, Ni W, Xu W (2007). Arsenic trioxide induces not only apoptosis but also autophagic cell death in leukemia cell lines via up-regulation of Beclin-1. *Leuk Res* **31:** 329-39.

Qian Y, Zhang J, Yan B, Chen X (2008). DEC1, a basic helix-loop-helix transcription factor and a novel target gene of the p53 family, mediates p53-dependent premature senescence. *J Biol Chem* **283:** 2896-905.

Qu X, Yu J, Bhagat G, Furuya N, Hibshoosh H, Troxel A *et al* (2003). Promotion of tumorigenesis by heterozygous disruption of the beclin 1 autophagy gene. *J Clin Invest* **112:** 1809-20.

Rathmell WK, Kaufmann WK, Hurt JC, Byrd LL, Chu G (1997). DNA-dependent protein kinase is not required for accumulation of p53 or cell cycle arrest after DNA damage. *Cancer Res* **57:** 68-74.

Ravi R, Mookerjee B, Bhujwalla ZM, Sutter CH, Artemov D, Zeng Q *et al* (2000). Regulation of tumor angiogenesis by p53-induced degradation of hypoxia-inducible factor 1alpha. *Genes Dev* **14:** 34-44.

Reef S, Zalckvar E, Shifman O, Bialik S, Sabanay H, Oren M *et al* (2006). A short mitochondrial form of p19ARF induces autophagy and caspase-independent cell death. *Mol Cell* **22:** 463-75.

Reisman D, Elkind NB, Roy B, Beamon J, Rotter V (1993). c-Myc trans-activates the p53 promoter through a required downstream CACGTG motif. *Cell Growth Differ* **4:** 57-65.

Rippe K, von Hippel PH, Langowski J (1995). Action at a distance: DNA-looping and initiation of transcription. *Trends Biochem Sci* **20:** 500-6.

Robinson M, Jiang P, Cui J, Li J, Wang Y, Swaroop M *et al* (2003). Global genechip profiling to identify genes responsive to p53-induced growth arrest and apoptosis in human lung carcinoma cells. *Cancer Biol Ther* **2:** 406-15.

Robles AI, Bemmels NA, Foraker AB, Harris CC (2001). APAF-1 is a transcriptional target of p53 in DNA damage-induced apoptosis. *Cancer Res* **61:** 6660-4.

Rodriguez MS, Desterro JM, Lain S, Lane DP, Hay RT (2000). Multiple C-terminal lysine residues target p53 for ubiquitin-proteasome-mediated degradation. *Mol Cell Biol* **20:** 8458-67.

Rosenbluth JM, Johnson K, Tang L, Triplett T, Pietenpol JA (2009). Evaluation of p63 and p73 antibodies for cross-reactivity. *Cell Cycle* **8:** 3702-6.

Rosenbluth JM, Mays DJ, Pino MF, Tang LJ, Pietenpol JA (2008). A gene signature-based approach identifies mTOR as a regulator of p73. *Mol Cell Biol* **28:** 5951-64.

Rosenbluth JM, Pietenpol JA (2008). The jury is in: p73 is a tumor suppressor after all. *Genes Dev* **22:** 2591-5.

Rosenbluth JM, Pietenpol JA (2009). mTOR regulates autophagy-associated genes downstream of p73. *Autophagy* **5:** 114-6.

Rozen S, Skaletsky H (2000). Primer3 on the WWW for general users and for biologist programmers. *Methods Mol Biol* **132:** 365-86.

Rubbi CP, Milner J (2003). Disruption of the nucleolus mediates stabilization of p53 in response to DNA damage and other stresses. *Embo J* **22:** 6068-77.

Rustgi AK (2007). The genetics of hereditary colon cancer. *Genes Dev* **21:** 2525-38.

Sachdeva M, Zhu S, Wu F, Wu H, Walia V, Kumar S *et al* (2009). p53 represses c-Myc through induction of the tumor suppressor miR-145. *Proc Natl Acad Sci U S A* **106:** 3207-12.

Sahai E, Marshall CJ (2003). Differing modes of tumour cell invasion have distinct requirements for Rho/ROCK signalling and extracellular proteolysis. *Nat Cell Biol* **5:** 711-9.

Samuels-Lev Y, O'Connor DJ, Bergamaschi D, Trigiante G, Hsieh JK, Zhong S *et al* (2001). ASPP proteins specifically stimulate the apoptotic function of p53. *Mol Cell* **8:** 781-94.

Sandri MI, Isaacs RJ, Ongkeko WM, Harris AL, Hickson ID, Broggini M *et al* (1996). p53 regulates the minimal promoter of the human topoisomerase IIalpha gene. *Nucleic Acids Res* **24:** 4464-70.

Schavolt KL, Pietenpol JA (2007). p53 and Delta Np63 alpha differentially bind and regulate target genes involved in cell cycle arrest, DNA repair and apoptosis. *Oncogene* **26:** 6125-32.

Scheer U, Hock R (1999). Structure and function of the nucleolus. *Curr Opin Cell Biol* **11:** 385-90.

Schena M, Shalon D, Davis RW, Brown PO (1995). Quantitative monitoring of gene expression patterns with a complementary DNA microarray. *Science* **270:** 467-70.

Scherer SJ, Maier SM, Seifert M, Hanselmann RG, Zang KD, Muller-Hermelink HK *et al* (2000). p53 and c-Jun functionally synergize in the regulation of the DNA repair gene hMSH2 in response to UV. *J Biol Chem* **275:** 37469-73.

Scott RC, Juhasz G, Neufeld TP (2007). Direct induction of autophagy by Atg1 inhibits cell growth and induces apoptotic cell death. *Curr Biol* **17:** 1-11.

Shay JW, Pereira-Smith OM, Wright WE (1991). A role for both RB and p53 in the regulation of human cellular senescence. *Exp Cell Res* **196:** 33-9.

Shen Y, Li DD, Wang LL, Deng R, Zhu XF (2008). Decreased expression of autophagy-related proteins in malignant epithelial ovarian cancer. *Autophagy* **4:** 1067-8.

Sherif ZA, Nakai S, Pirollo KF, Rait A, Chang EH (2001). Downmodulation of bFGF-binding protein expression following restoration of p53 function. *Cancer Gene Ther* **8:** 771-82.

Shikama N, Lee CW, France S, Delavaine L, Lyon J, Krstic-Demonacos M *et al* (1999). A novel cofactor for p300 that regulates the p53 response. *Mol Cell* **4:** 365-76.

Shimizu S, Kanaseki T, Mizushima N, Mizuta T, Arakawa-Kobayashi S, Thompson CB *et al* (2004). Role of Bcl-2 family proteins in a non-apoptotic programmed cell death dependent on autophagy genes. *Nat Cell Biol* **6:** 1221-8.

Smeenk L, van Heeringen SJ, Koeppel M, van Driel MA, Bartels SJ, Akkers RC *et al* (2008). Characterization of genome-wide p53-binding sites upon stress response. *Nucleic Acids Res* **36:** 3639-54.

Sniezek JC, Matheny KE, Westfall MD, Pietenpol JA (2004). Dominant negative p63 isoform expression in head and neck squamous cell carcinoma. *Laryngoscope* **114:** 2063-72.

Song B, Wang Y, Kudo K, Gavin EJ, Xi Y, Ju J (2008). miR-192 Regulates dihydrofolate reductase and cellular proliferation through the p53-microRNA circuit. *Clin Cancer Res* **14:** 8080-6.

Staib F, Robles AI, Varticovski L, Wang XW, Zeeberg BR, Sirotin M *et al* (2005). The p53 tumor suppressor network is a key responder to microenvironmental components of chronic inflammatory stress. *Cancer Res* **65:** 10255-64.

Stewart ZA, Pietenpol JA (1999). Cell cycle checkpoints as therapeutic targets. *J Mammary Gland Biol Neoplasia* **4:** 389-400.

Stewart ZA, Tang LJ, Pietenpol JA (2001). Increased p53 phosphorylation after microtubule disruption is mediated in a microtubule inhibitor- and cell-specific manner. *Oncogene* **20:** 113-24.

Stiewe T, Theseling CC, Putzer BM (2002). Transactivation-deficient Delta TA-p73 inhibits p53 by direct competition for DNA binding: implications for tumorigenesis. *J Biol Chem* **277:** 14177-85.

Stiles JD, Ostrow PT, Balos LL, Greenberg SJ, Plunkett R, Grand W *et al* (1997). Correlation of endothelin-1 and transforming growth factor beta 1 with malignancy and vascularity in human gliomas. *J Neuropathol Exp Neurol* **56:** 435-9.

Stommel JM, Marchenko ND, Jimenez GS, Moll UM, Hope TJ, Wahl GM (1999). A leucine-rich nuclear export signal in the p53 tetramerization domain: regulation of subcellular localization and p53 activity by NES masking. *Embo J* **18:** 1660-72.

Stoyanova T, Roy N, Kopanja D, Raychaudhuri P, Bagchi S (2009). DDB2 (damaged-DNA binding protein 2) in nucleotide excision repair and DNA damage response. *Cell Cycle* **8:** 4067-71.

Strano S, Fontemaggi G, Costanzo A, Rizzo MG, Monti O, Baccarini A *et al* (2002). Physical interaction with human tumor-derived p53 mutants inhibits p63 activities. *J Biol Chem* **277:** 18817-26.

Sturzbecher HW, Brain R, Addison C, Rudge K, Remm M, Grimaldi M *et al* (1992). A C-terminal alpha-helix plus basic region motif is the major structural determinant of p53 tetramerization. *Oncogene* **7:** 1513-23.

Subbaramaiah K, Altorki N, Chung WJ, Mestre JR, Sampat A, Dannenberg AJ (1999). Inhibition of cyclooxygenase-2 gene expression by p53. *J Biol Chem* **274:** 10911-5.

Sugimoto M, Kuo ML, Roussel MF, Sherr CJ (2003). Nucleolar Arf tumor suppressor inhibits ribosomal RNA processing. *Mol Cell* **11:** 415-24.

Sun H, Nikolovska-Coleska Z, Lu J, Meagher JL, Yang CY, Qiu S *et al* (2007). Design, synthesis, and characterization of a potent, nonpeptide, cell-permeable, bivalent Smac mimetic that concurrently targets both the BIR2 and BIR3 domains in XIAP. *J Am Chem Soc* **129:** 15279-94.

Sun Y, Tran BN, Worley LA, Delston RB, Harbour JW (2005). Functional analysis of the p53 pathway in response to ionizing radiation in uveal melanoma. *Invest Ophthalmol Vis Sci* **46:** 1561-4.

Swanlund JM, Kregel KC, Oberley TD Investigating autophagy: Quantitative morphometric analysis using electron microscopy. *Autophagy* **6**.

Szak ST, Mays D, Pietenpol JA (2001). Kinetics of p53 binding to promoter sites in vivo. *Mol Cell Biol* **21:** 3375-86.

Takai H, Smogorzewska A, de Lange T (2003). DNA damage foci at dysfunctional telomeres. *Curr Biol* **13:** 1549-56.

Tambe Y, Isono T, Haraguchi S, Yoshioka-Yamashita A, Yutsudo M, Inoue H (2004). A novel apoptotic pathway induced by the drs tumor suppressor gene. *Oncogene* **23:** 2977-87.

Tanaka H, Arakawa H, Yamaguchi T, Shiraishi K, Fukuda S, Matsui K *et al* (2000). A ribonucleotide reductase gene involved in a p53-dependent cell-cycle checkpoint for DNA damage. *Nature* **404:** 42-9.

Tanaka T, Ohkubo S, Tatsuno I, Prives C (2007). hCAS/CSE1L associates with chromatin and regulates expression of select p53 target genes. *Cell* **130:** 638-50.

Tarasov V, Jung P, Verdoodt B, Lodygin D, Epanchintsev A, Menssen A *et al* (2007). Differential regulation of microRNAs by p53 revealed by massively parallel sequencing: miR-34a is a p53 target that induces apoptosis and G1-arrest. *Cell Cycle* **6:** 1586-93.

Tasdemir E, Maiuri MC, Galluzzi L, Vitale I, Djavaheri-Mergny M, D'Amelio M *et al* (2008). Regulation of autophagy by cytoplasmic p53. *Nat Cell Biol* **10:** 676-87.

Tazawa H, Tsuchiya N, Izumiya M, Nakagama H (2007). Tumor-suppressive miR-34a induces senescence-like growth arrest through modulation of the E2F pathway in human colon cancer cells. *Proc Natl Acad Sci U S A* **104:** 15472-7.

Teodoro JG, Parker AE, Zhu X, Green MR (2006). p53-mediated inhibition of angiogenesis through up-regulation of a collagen prolyl hydroxylase. *Science* **313:** 968-71.

Thompson PM, Seifried BA, Kyemba SK, Jensen SJ, Guo C, Maris JM *et al* (2001). Loss of heterozygosity for chromosome 14q in neuroblastoma. *Med Pediatr Oncol* **36:** 28-31.

Timpson P, Jones GE, Frame MC, Brunton VG (2001). Coordination of cell polarization and migration by the Rho family GTPases requires Src tyrosine kinase activity. *Curr Biol* **11:** 1836-46.

Toh WH, Siddique MM, Boominathan L, Lin KW, Sabapathy K (2004). c-Jun regulates the stability and activity of the p53 homologue, p73. *J Biol Chem* **279:** 44713-22.

Tokino T, Thiagalingam S, el-Deiry WS, Waldman T, Kinzler KW, Vogelstein B (1994). p53 tagged sites from human genomic DNA. *Hum Mol Genet* **3:** 1537-42.

Tomasini R, Tsuchihara K, Wilhelm M, Fujitani M, Rufini A, Cheung CC *et al* (2008). TAp73 knockout shows genomic instability with infertility and tumor suppressor functions. *Genes Dev* **22:** 2677-91.

Tsukada M, Ohsumi Y (1993). Isolation and characterization of autophagy-defective mutants of Saccharomyces cerevisiae. *FEBS Lett* **333:** 169-74.

Ueba T, Nosaka T, Takahashi JA, Shibata F, Florkiewicz RZ, Vogelstein B *et al* (1994). Transcriptional regulation of basic fibroblast growth factor gene by p53 in

human glioblastoma and hepatocellular carcinoma cells. *Proc Natl Acad Sci U S A* **91:** 9009-13.

Vassilev LT, Vu BT, Graves B, Carvajal D, Podlaski F, Filipovic Z *et al* (2004). In vivo activation of the p53 pathway by small-molecule antagonists of MDM2. *Science* **303:** 844-8.

Vazquez A, Bond EE, Levine AJ, Bond GL (2008). The genetics of the p53 pathway, apoptosis and cancer therapy. *Nat Rev Drug Discov* **7:** 979-87.

Venter JC, Adams MD, Myers EW, Li PW, Mural RJ, Sutton GG *et al* (2001). The sequence of the human genome. *Science* **291:** 1304-51.

Vousden KH, Ryan KM (2009). p53 and metabolism. *Nat Rev Cancer* **9:** 691-700.

Wang P, Reed M, Wang Y, Mayr G, Stenger JE, Anderson ME *et al* (1994). p53 domains: structure, oligomerization, and transformation. *Mol Cell Biol* **14:** 5182-91.

Wang XQ, Ongkeko WM, Lau AW, Leung KM, Poon RY (2001). A possible role of p73 on the modulation of p53 level through MDM2. *Cancer Res* **61:** 1598-603.

Watcharasit P, Bijur GN, Zmijewski JW, Song L, Zmijewska A, Chen X *et al* (2002). Direct, activating interaction between glycogen synthase kinase-3beta and p53 after DNA damage. *Proc Natl Acad Sci U S A* **99:** 7951-5.

Wei CL, Wu Q, Vega VB, Chiu KP, Ng P, Zhang T *et al* (2006). A global map of p53 transcription-factor binding sites in the human genome. *Cell* **124:** 207-19.

Wei X, Orchardson M, Gracie JA, Leung BP, Gao B, Guan H *et al* (2001). The Sushi domain of soluble IL-15 receptor alpha is essential for binding IL-15 and inhibiting inflammatory and allogenic responses in vitro and in vivo. *J Immunol* **167:** 277-82.

Weinberg RL, Freund SM, Veprintsev DB, Bycroft M, Fersht AR (2004). Regulation of DNA binding of p53 by its C-terminal domain. *J Mol Biol* **342:** 801-11.

Wilhelm MT, Rufini A, Wetzel MK, Tsuchihara K, Inoue S, Tomasini R *et al* Isoform-specific p73 knockout mice reveal a novel role for {Delta}Np73 in the DNA damage response pathway. *Genes Dev* **24:** 549-60.

Xie Z, Klionsky DJ (2007). Autophagosome formation: core machinery and adaptations. *Nat Cell Biol* **9:** 1102-9.

Xu J, Morris GF (1999). p53-mediated regulation of proliferating cell nuclear antigen expression in cells exposed to ionizing radiation. *Mol Cell Biol* **19:** 12-20.

Yamaguchi K, Wu L, Caballero OL, Hibi K, Trink B, Resto V *et al* (2000). Frequent gain of the p40/p51/p63 gene locus in primary head and neck squamous cell carcinoma. *Int J Cancer* **86:** 684-9.

Yanagisawa M, Kurihara H, Kimura S, Tomobe Y, Kobayashi M, Mitsui Y *et al* (1988). A novel potent vasoconstrictor peptide produced by vascular endothelial cells. *Nature* **332:** 411-5.

Yang A, Kaghad M, Wang Y, Gillett E, Fleming MD, Dotsch V *et al* (1998). p63, a p53 homolog at 3q27-29, encodes multiple products with transactivating, death-inducing, and dominant-negative activities. *Mol Cell* **2:** 305-16.

Yang A, Schweitzer R, Sun D, Kaghad M, Walker N, Bronson RT *et al* (1999). p63 is essential for regenerative proliferation in limb, craniofacial and epithelial development. *Nature* **398:** 714-8.

Yang A, Walker N, Bronson R, Kaghad M, Oosterwegel M, Bonnin J *et al* (2000). p73-deficient mice have neurological, pheromonal and inflammatory defects but lack spontaneous tumours. *Nature* **404:** 99-103.

Yang A, Zhu Z, Kapranov P, McKeon F, Church GM, Gingeras TR *et al* (2006). Relationships between p63 binding, DNA sequence, transcription activity, and biological function in human cells. *Mol Cell* **24:** 593-602.

Yang J, Ahmed A, Poon E, Perusinghe N, de Haven Brandon A, Box G *et al* (2009). Small-molecule activation of p53 blocks hypoxia-inducible factor 1alpha and vascular endothelial growth factor expression in vivo and leads to tumor cell apoptosis in normoxia and hypoxia. *Mol Cell Biol* **29:** 2243-53.

Yla-Anttila P, Vihinen H, Jokitalo E, Eskelinen EL (2009). Monitoring autophagy by electron microscopy in Mammalian cells. *Methods Enzymol* **452:** 143-64.

Yorimitsu T, Nair U, Yang Z, Klionsky DJ (2006). Endoplasmic reticulum stress triggers autophagy. *J Biol Chem* **281:** 30299-304.

Yu L, Wan F, Dutta S, Welsh S, Liu Z, Freundt E *et al* (2006). Autophagic programmed cell death by selective catalase degradation. *Proc Natl Acad Sci U S A* **103:** 4952-7.

Yuan ZM, Shioya H, Ishiko T, Sun X, Gu J, Huang YY *et al* (1999). p73 is regulated by tyrosine kinase c-Abl in the apoptotic response to DNA damage. *Nature* **399:** 814-7.

Yue Z, Jin S, Yang C, Levine AJ, Heintz N (2003). Beclin 1, an autophagy gene essential for early embryonic development, is a haploinsufficient tumor suppressor. *Proc Natl Acad Sci U S A* **100:** 15077-82.

Zalckvar E, Berissi H, Eisenstein M, Kimchi A (2009). Phosphorylation of Beclin 1 by DAP-kinase promotes autophagy by weakening its interactions with Bcl-2 and Bcl-XL. *Autophagy* **5:** 720-2.

Zeng X, Chen L, Jost CA, Maya R, Keller D, Wang X *et al* (1999). MDM2 suppresses p73 function without promoting p73 degradation. *Mol Cell Biol* **19:** 3257-66.

Zhan Q, Antinore MJ, Wang XW, Carrier F, Smith ML, Harris CC *et al* (1999). Association with Cdc2 and inhibition of Cdc2/Cyclin B1 kinase activity by the p53-regulated protein Gadd45. *Oncogene* **18:** 2892-900.

Zhan Q, Carrier F, Fornace AJ, Jr. (1993). Induction of cellular p53 activity by DNA-damaging agents and growth arrest. *Mol Cell Biol* **13:** 4242-50.

Zhang XY, Zhang KT, Tian F, Xia Y, Wu YQ, Liu XJ (2007). Integrative analysis and validation of robust gene signature in lung cancer. *Biochem Biophys Res Commun* **358:** 710-5.

Zhu J, Jiang J, Zhou W, Chen X (1998). The potential tumor suppressor p73 differentially regulates cellular p53 target genes. *Cancer Res* **58:** 5061-5.